Doctoral Thesis

SUPERCRITICAL WATER GASIFICATION CHARACTERISTICS OF AMINO ACIDS

(アミノ酸の超臨界水ガス化特性)

Thachanan Samanmulya

Mechanical Science and Engineering

Graduate School of Engineering

Hiroshima University, JAPAN

September 2014

ABSTRACT

Wet biomass, organic waste or sewage, contains so high moisture content that the heat of vaporization of water exceeds the heat of combustion of the biomass, the conventional dry gasification is not satisfied anymore. One of possible method is the steam reforming of biomass. The major problem in gasification by steam reforming is the formation of tars and char as the biomass does not react directly with steam at atmosphere pressure.

Supercritical water gasification (SCWG) process is as one of the promising alternatives, taking an advantage of the high moisture content by using the water as a reaction medium. The free radical condition of the supercritical water, moreover, promotes the gasification reaction. Supercritical water has some very usual properties, which are different from those of liquid or gas. Many organic compounds cannot be dissolved in normal water. But supercritical water behaves like an organic solvent. Organic materials can be dissolved in it. Supercritical water in particular has the ability to dissolve materials not normally soluble in liquid water or steam. These properties make supercritical water a very promising reaction medium for the conversion of biomass to value-added products. At supercritical conditions beyond the critical point of water (374 ^{o}C and 22.1 MPa), water is an effective solvent for organic components and gases, and also plays an important role of an H^{+}/OH^{-} ions as acid/base catalyst due to its unique solvent properties (e.g. density, dielectric constant and ion product). Thus, SCWG can convert wet biomasses into fuel gases, such as hydrogen and small hydrocarbon gases (e.g., CH_4, C_2H_4, and C_2H_6).

Although SCWG results in fewer amounts of the tarry materials than that from the dry gasification due to the enhanced organic solubility in the supercritical water conditions, these by-products (tarry material) acts as the inhibitor for the complete gasification.

The prediction of gasification rate in supercritical water is still difficult, and it is a big

problem in reactor design. The investigation of reaction mechanism of biomass in SCWG process is helpful to insight into what reaction taking place during the heating up period of this process. To determine the reaction mechanism of biomass in SCWG process, the utilization of model compound is effective. Amino acids have been chosen to be a model compound of protein. Because the behavior of the proteins is important, especially for food waste and sewage from household, but have not yet to be clearly determined.

To achieve high gasification efficiency, an activated carbon catalyst is known to be effective. However, it was recently reported that the effectiveness of this catalyst differs from feedstock to feedstock. It has been found to be effective for glucose- and cellulose-containing feedstocks, but quite limited for fermentation residue. It is therefore extremely important to find out for which biomass materials the activated carbon catalyst is effective; however, there has so far been no report on a systematic investigation to achieve this. In particular, its effectiveness for the gasification of compounds with heteroatoms, such as proteins, is of interest. Glycine is the simplest amino acid, and can be a good model compound of proteins. The purpose of the first study is to assess the effectiveness of activated carbon for the supercritical water gasification of glycine.

Glycine gasification was performed using the tubular flow reactor which was made of SS316 steel tubing (i.d., 2.17 mm; o.d., 3.18 mm) with a length of 12 m. Activated carbon from coconut shell (PDX-1, Kuraray Co., Ltd.) with median particle size of 29 μm was used in this work and its concentration was fixed at 0.5 wt%. Feedstock containing the activated carbon catalyst was fed into the reactor by a piston pump (Toyo Koatsu Co.). The reaction pressure was maintained at 25 MPa and the desired temperature was reached before the addition of the feedstock. The residence time was changed in the range of 63 to 188 s by adjusting the feedstock flow rate. The gas generation rate was determined by measuring the time for effluent

gas to fill a vial of known volume. The gaseous product was analyzed using gas chromatography (GC). CO_2 and CO were detected by GC with a thermal conductivity detector (GC-TCD) with He as the carrier gas. CH_4, C_2H_4, and C_2H_6 were detected using GC with a flame ionization detector (GC-FID) with He as the carrier gas. H_2 was detected by GC-TCD with N_2 as the carrier gas. The liquid product was analyzed by a total organic carbon (TOC) analyzer to quantify the amounts of carbon in the liquid product (non-purgeable organic carbon, NPOC) and in the dissolved gas product (inorganic carbon, IC).

Glycine gasification had performed to determine the effect of feedstock concentration, the effect of residence time, and the effect of reaction temperature with a comparison of with and without activated carbon as a catalyst. When the feedstock concentration was high, carbon gasification efficiency became lower. At a sufficiently low concentration of 1 wt%, the carbon gasification reaction followed the first order reaction rate. Its reaction rate constant was well expressed by the Arrhenius equation with a pre-exponential factor of 2.73×10^4 s^{-1} and an activation energy of 106.9 kJ mol^{-1}. The product gas was composed of H_2, CO_2, CO, CH_4, and a small amount of C_2H_6 and C_2H_4. The effect of operation parameters on its composition agreed with the thermodynamic predictions. The activated carbon catalyst was found to be ineffective for glycine gasification.

As the gasification rate of glycine have already measured, the determination of gasification of other amino acids and comparison of their gasification rates would be interesting. Alanine was chosen to be the next target because they are two similar compounds that differ by only one functional group, it might give some insight into the effect of the functional group on decomposition rate in supercritical water. Then, the purpose of the second study is to compare the gasification rate of glycine and alanine, which are different by hydrogen and methyl as a functional group. The effect of the methyl group would be elucidated. The effect of feedstock

concentration and the effect of reaction temperature were also determined.

Alanine gasification was conducted in the same apparatus as previous of glycine gasification. The same range of reaction temperature had been used, 500 to 650 ^{o}C, but the concentration of alanine were 1.0, 2.0, and 3.0 wt%. The gasification efficiency of alanine is not affected by the feedstock concentration employed here, which is likely to first order behavior. But glycine, the gasification efficiency decreased with increasing concentration. This is expected of tarry material production occur at high concentrations. It is known that the order of the reaction for tarry material production is higher than unity for the case of glucose from our previous research team's work. The same can be expected for amino acids. To determine the gasification characteristics, the effect of tarry material production should be omitted. It is not possible to completely get rid of it, but judging from the effect of residence time, 1.0 wt% was found to be sufficiently dilute so that the gasification characteristics is expressed as a first order reaction with a small error as we had reported in the first work. In case of alanine, the effect of tarry material production is negligible, and we can safely assume first order kinetics. Maybe the methyl group has the ability to suppress tarry material production. However, amino groups can produce ammonia or amine molecules, which were observed as ammonium ion in our liquid samples, the alkalinity of the liquid should also increase while increased feedstock concentration. This alkali might have functioned as the catalyst for the water gas shift reaction. Alkali stabilizes the carbon dioxide, and enhanced water gas shift reaction is expected.

Increasing reaction temperature, gasification efficiency of alanine trends to increase sharply as was observed by our previous of glycine and agrees with the results of glucose that was conducted by Xu et al (1996). As the experimental data of the carbon gasification efficiency, the gasification rates of glycine and alanine are identical. Then, the pre-exponential factor and an activation energy of glycine had been corrected to 7.37×10^{5} s^{-1} and 131 kJ mol^{-1}

respectively as same as alanine. This fact implies that the methyl group in alanine does not have a significant effect on carbon gasification efficiency. One of the possibilities is that the carboxyl group, which is common to both glycine and alanine, is reacting first. Since the carbon atom is not strongly electrophilic or nucleophilic, the methyl group will not affect the reactivity of the carboxyl group. This mechanism can explain why the methyl group does not affect the carbon gasification rate. Gas composition of glycine and alanine have been compared. The methane gas would have been produced from the methyl group of alanine that is shown in a higher fraction. Another clear difference between glycine and alanine is that water gas shift reaction proceeds to a greater extent for glycine.

As the gasification of glycine and alanine are identical. It is interesting that if other amino acids are also gasified with the same, we will be able to safely apply this gasification rate to other amino acids and likely proteins as well. Thus, valine and leucine are chosen to be candidate of amino acids which are in the same aliphatic classification with glycine and alanine. The difference by functional groups of valine and leucine, which are propyl and butyl, would give some insight effect on gasification characteristics. However, structure of compounds may effect on gasification. Then, proline was also chosen to show the gasification of amino acids which is cyclic structure. So, valine, leucine and proline gasification characteristics are the third target.

All above mention amino acids was performed in the same apparatus and the same supercritical water gasification conditions as previous work. Surprisingly, and to our disappointment, the gasification rate of valine is much lower than that of glycine and alanine. Valine was decomposed and produced isopropyl radicals in supercritical water conditions. This radical are much different than glycine and alanine which are hydrogen and methyl that can react rapidly with others radicals or molecules. Isopropyl radicals are quite stable which are

called the secondary radicals. In additional, the reaction of isopropyl radicals with each other generates 2,3-dimethylbutane, which is a liquid-phase product. The formation of this bulky molecule could lead to the production of polymers because radicals of higher carbon numbers are more stable than smaller radicals and are relatively easily produced. This may the reason why the gasification of valine is low. Its reaction rate constant was well expressed by the Arrhenius equation with a pre-exponential factor of 6.97×10^{1} s^{-1} and an activation energy of 70 kJ mol^{-1}.

Leucine contains isobutyl as a functional group and releases it in supercritical water conditions. Isobutyl radicals from leucine decomposition are primary radicals that it can react with water to produce isopropyl alcohol and methyl radical can be removed from it to react and generate methane. As isobutyl radicals were defined to be primary radicals as hydrogen of glycine and methyl of alanine, accordingly, their gasification rates are similar but an activation energy of leucine is a bit higher which is 135 kJ mol^{-1}.

Gasification rate of proline is higher than valine and determined a pre-exponential factor of 1.96×10^{2} s^{-1} and an activation energy of 73 kJ mol^{-1}. The radical produced from proline is primary and will decompose easily. This explains why its gasification rate is almost equal to those of glycine and alanine. However, gasification of proline is less sensitive to reaction temperature than that of glycine, alanine, and leucine. This may be due to stabilization of the transition state of the carboxyl radical−producing reaction by the ring structure.

Finally, we had made a purposed reaction network of the 5 amino acids that can be well clarified those of decomposition and radicals production. These reaction network may explain why the gasification rate is same for glycine, alanine, and leucine ,and different for valine and proline. The reaction rate constant of each 5 amino acids was well expressed by the

Arrhenius equation with a sufficiently low concentration of 1 wt%.

THESIS STRUCTURE

Chapter 1: Introduction Biomass and Biomass Utilization is introduced in this chapter to show an alternative about using of renewable energy. Then, the interest and innovation process, the supercritical water gasification is introduce to explain why it is suitable and effective for the conversion of biomass to energy.

Chapter 2: Literature review The related research works in supercritical water gasification, biomass (real), and biomass model compounds are reviewed and discussed in particular to point out the significant of using model compounds to elucidate the reaction mechanism and study the characteristics of protein content biomass.

Chapter 3: Aim and objectives The motivation will be explained in this chapter to show how this work is inspired and also indicating the aim and objectives of this work.

Chapter 4: Experimental method The whole chapter 4 presents the description of experimental method which is applied in this work. Feedstock materials, experimental procedures, experimental conditions, product analytical methods for gas phase product and liquid phase product are explained in detail.

Chapter 5: Supercritical water gasification of amino acid: a parametric study The experimental of glycine solution feedstock were conducted under supercritical water conditions. The conditions were varied the parametric of supercritical water gasification which are feedstock concentration, reaction temperature, residence time, and a presence of activated carbon catalyst (0.5 wt%). The experimental results were discussed based on the carbon gasification efficiency that refers to amount of carbon contained in feedstock change to amount of carbon contained

in gas product. An Arrhenius equation was sufficient able to explain the reaction temperature dependence on the glycine gasification rate.

Chapter 6: Effect of methyl functional group on supercritical water gasification of amino acid Alanine was chosen to study in this chapter. 1.0 wt% of alanine solution was gasified under supercritical water condition. By comparison of glycine and alanine, the methyl functional group, which is only different for both of them, would be clarified.

Chapter 7: Gasification Characteristics of aliphatic amino acids in supercritical water conditions After glycine and alanine were compared, the amino acids in the same class as them, which are valine and leucine, were conducted under supercritical water gasification conditions to determine the gasification characteristics. Based on gas composition product that have been qualified, the proposed reaction mechanism of those amino acids decomposition and gasification are elucidated.

Chapter 8: Effect of molecule structure on supercritical water gasification of amino acid Proline, the cyclic structure compound, was applied for this study and carried out with the same conditions of supercritical water gasification to show the gasification characteristics. The decomposition and gasification mechanism of proline is also proposed base on the gas composition product that has been observed after it gasified.

Chapter 9: Conclusion and recommendation for future work This last chapter presents the conclusion remarks and shows the contributions for the future work on the field of biomass gasification, especially for biomass protein content, to develop the supercritical water gasification technology. At last, the potential future work on biomass protein content and so on is recommended.

Dedicate to the memory of my father, Dumronkchai Samanmulya (1953 - 2012) who inspired my doctoral study. I miss him every day, but I am glad to know he saw this process through its completion, offering the support to make it possible, as well as plenty of kind encouragement.

This PhD belongs to him by all means.

ACKNOWLEDGEMENTS

First, I would like to acknowledge the Ministry of Education, Culture, Sports, Science and Technology of Japan (Monbukagakusho) for the financial support throughout my doctoral study. I am really very grateful for the support.

I would like to express my deep gratitude to my supervisor, Prof. Yukihiko Matsumura for his guidance and fortitude in the past three years of my doctoral study. I appreciate his advising technique which made me more confident and independent on my research. Thank you so much for all your kind support, Sensei.

I am thankful to Assoc. Prof. Shuhei Inoue, Assist. Prof. Machi Kanna, and Assist. Prof. Takashi Yanagida, who are always give me the support for my study and everyday life.

I am deeply grateful to Assoc. Prof. Tawatchai Charinpanitkul for all his kind support from Chulalongkorn University, Thailand. With his encouragement, it makes me believe “I CAN DO IT”.

I would like to thank all members in Thermal Engineering Laboratory and including Thai friends in Hiroshima University for cheering, discussing, accompanying and helping me in any situation during my study.

Last but not least, I would like express my thanks to my beloved family, SAMANMULYA, who always there and encourage me. Without any doubt, my PhD belongs to them.

TABLE OF CONTENTS

LIST OF TABLES

LIST OF FIGURES

GLOSSARY

A	Pre-exponential factor
E_a	Activation energy [J/mol, kJ/mol]
$[H^+]$	H^+ concentration
k	Reaction rate constant
k_0	Pre-exponential factor [s^{-1}]
K_w	Dissociation constant of water/ Ion product [$(mol/kg)^2$]
n_{C0}	initial amount of carbon [mol],
n_{Cg}	amount of gasified carbon [mol],
$[OH^-]$	OH^- concentration
P	Reaction pressure [MPa], or the room pressure on the day of experiment [hPa]
R	Ideal gas constant [0.08206 $L \cdot atm \cdot K^{-1} \cdot mol^{-1}$]
t	time or residence time [s]
T	Reaction temperature, or the room temperature on the day of experiment [K, □C]
$\Delta V^{\pm}$	Volume of activation equation 2.2

V_{total}	volume of injected gas, GC analysis
V_{air}	volume of air
V_{CO}	volume of carbon monoxide gas
V_{CO2}	volume of carbon dioxide gas
$V_{methane}$	volume of methane gas
$V_{ethylene}$	volume of ethylene gas
V_{ethane}	volume of ethane gas
$V_{product\ gas}$	volume of mixed product gases after minus volume of air
$V_{1\ mol\ of\ product\ gas}$	volume of mixed product gases in 1 mol

Greek letters

ε	Dielectric constant of water [dimensionless]
ρ	Water density [kg/m^3]
ρ_c	Critical density of water (322 kg/m^3)

Abbreviations

5-HMF	5-Hydroxymethyl-2-furfural
CGE	Carbon Gasification Efficiency
FID	Flame Ionization Detector
GC	Gas Chromatography
GC-FID	Gas Chromatography with a Flame Ionization Detector
GC-TCD	Gas Chromatography with a Thermal Conductivity Detector
HCW	Hot compressed water
HNEI	Hawaii Natural Energy Institute
IC	Inorganic Carbon
JSME	Japan Society Mechanical Engineering
NPOC	Non-Purgeable Organic Carbon
SCW	Supercritical Water
SCWG	Supercritical Water Gasification
SS316	Stainless steel 316
T	Thermocouple
TCD	Thermal Conductivity Detector
TOC	Total Organic Carbon (analytical method context)

LIST OF PUBLICATIONS

(1) Samanmulya, T.; Matsumura, Y., Effect of Activated Carbon Catalytic on Supercritical Water Gasification of Glycine as a Model Compound of Protein. *J. Jpn. Inst. Energy* **2013***, 92*, 894-899.

(2) Samanmulya, T.; Kanna, M.; Matsumura, Y., Activated carbon catalytic supercritical water gasification of glycine. *Proc. 21st European Biomass Conference and Exhibition,* **2013**.

(3) Samanmulya, T.; Inoue, S.; Inoue, T.; Kawai, Y.; Kubota, H.; Munetsuna, H.; Noguchi, T.; Matsumura, Y., Gasification characteristics of alanine in supercritical water. *J. Jpn. Petrol. Inst.* **2014**, accepted. (In press)

(4) Samanmulya, T.; Inoue, S.; Inoue, T.; Kawai, Y.; Kubota, H.; Munetsuna, H.; Noguchi, T.; Matsumura, Y., Comparison of glycine and alanine gasification in supercritical water conditions. *Proc. 22nd European Biomass Conference and Exhibition,* **2014**.

(5) Samanmulya, T.; Inoue, S.; Inoue, T.; Kawai, Y.; Kubota, H.; Munetsuna, H.; Noguchi, T.; Matsumura, Y., Gasification characteristics of amino acids in supercritical water. *J. Jpn. Inst. Energy* **2014**, accepted.

CHAPTER 1

Introduction

1.1 Introduction

Nowadays, the rising worldwide consumption of crude oil fuels has not only led to a major shortage of energy resources but also accelerated global warming. One approach to reducing the use of crude oil fuels is the utilization of biomass energy, which is a renewable and carbon neutral energy resource. This chapter will introduce

about biomass (section 1.2). Among the various technologies, fuel gas production from biomass is extremely attractive from the viewpoint of the efficiency associated with use of the product gas. Biomass gasification by thermochemical conversion is a cost-effective process for fuel gas production. This chapter therefore explains the fundamental of the supercritical water gasification (section 1.3). This chapter also informs the advantage of reaction in supercritical water gasification process of biomass conversion (section 1.4).

1.2 Biomass

What is biomass? Biomass is an organic substance, which can be considered as the natural source of energy. Biomass, which is a renewable energy source, refers to biological materials that could be used as fuel gas and energy production. It would be refer to plant materials, animal wastes, forestry, agricultural, and urban wastes. Examples of biomass resources are shown below:

- Corncobs
- Soy bean residue from extraction plants

- Straw and rice husk from field and rice mills
- Bagasse from sugar refineries factory
- Wood chips from forests and plantations or wood processing plants
- Residue from tapioca starch factories
- Empty bunches and/or coconut shell from coconut oil and/or milk plants
- Animals manure from livestock
- Sewage from production of food or agricultural factory or household
- Leftover food from household

Biomass stocks the materials that would be conversed to energy with the photosynthesis of plants which uses solar energy to convert CO_2 and H_2O into carbohydrates and keep them in various parts of the tree. In contrast to fossil fuels, biomass is energy source which is renewable as long as there is plant, water and sunlight. Biomass energy utilization would result in lower pollution and not gain Green House Effect gas due to the recycling process of CO_2 in plant rotation. Plantation as the sources of Biomass would absorb CO_2 as they grow. Even though

CO_2 is released during biomass conversion, it would be again utilized for the glowing process of the next plantation. As a result, there is no new CO_2 generates into the atmosphere as shown in Figure 1.1. The utilization of biomass energy would be called a renewable and carbon neutral energy resource.

Figure 1.1 CO_2 Recycling

Real biomass, it is not contained only lignocellulosic material but it also contains carbohydrate, fats, and protein. Proteins are biological molecules or macromolecules that consist of one or long chains of amino acids. The amino acids of protein are classified into 6 classes as shown in Table 1.1.

Table 1.1 Amino acids classification

Class	Amino acids
Aliphatic	Glycine, Alanine, Valine, Leucine, Isoleucine
Hydroxyl or Sulfer-containing	Serine, Cysteine, Threonine, Methionine
Cyclic	Proline
Aromatic	Phenylalanine, Tyrosine, Tryptophan
Basic	Histidine, Lysine, Arginine
Acidic and Amide	Aspartate, Glutamate, Asparagine, Glutamine

1.3 Supercritical water gasification (SCWG)

Supercritical water gasification (SCWG) is an innovation process for biomass conversion which uses advantage of the special properties of water at supercritical conditions. Supercritical water is stay above the critical point of temperature and pressure. Figure 1.2 indicates a critical point of water at 374 ^{o}C and 22.06 MPa. An increasing of temperature and pressure along the liquid-vapor saturation line, density of

liquid phase slightly decreases. Whereas, density of vapor phase slightly increases. The point that which is the density of those both phases are identical is defined to be the critical point. At this point and above area, the phase boundary between liquid and vapor disappears and the water becomes the one state fluid and it has gas-like and liquid-like properties.

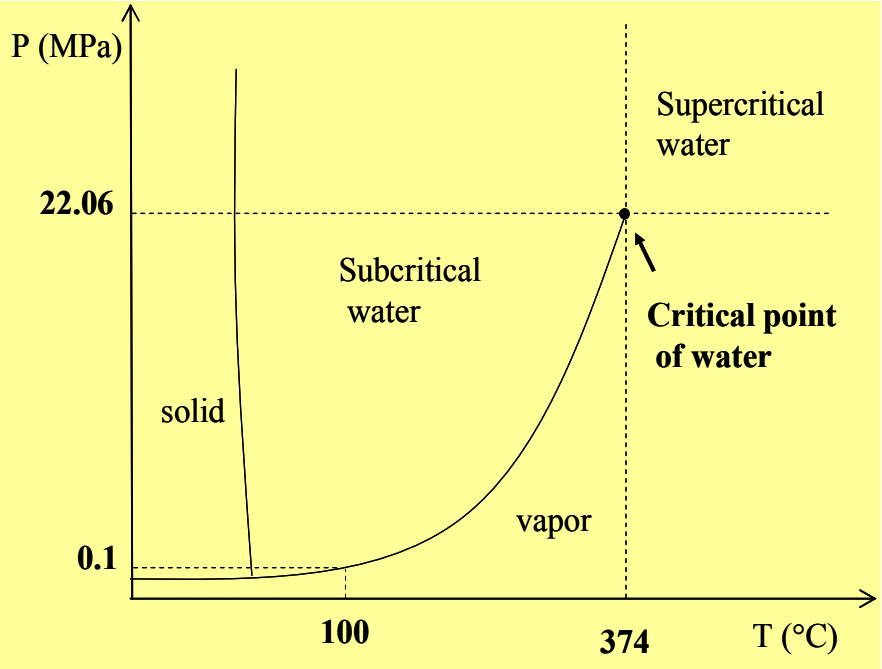

Figure 1.2 Phase diagram of water

The supercritical water has been applied for many thermo-chemical reactions and syntheses as the reaction medium, particularly for biomass utilization. This is due to an advantage of the specific properties of supercritical water, which are obtained by

changing temperature and pressure and it is different from those of gas or liquid. The dielectric constant (ε), water density (ρ) and ion product of water (K_w) as a function of temperature at a constant of pressure at 25 MPa are shown in Figure 1.3.

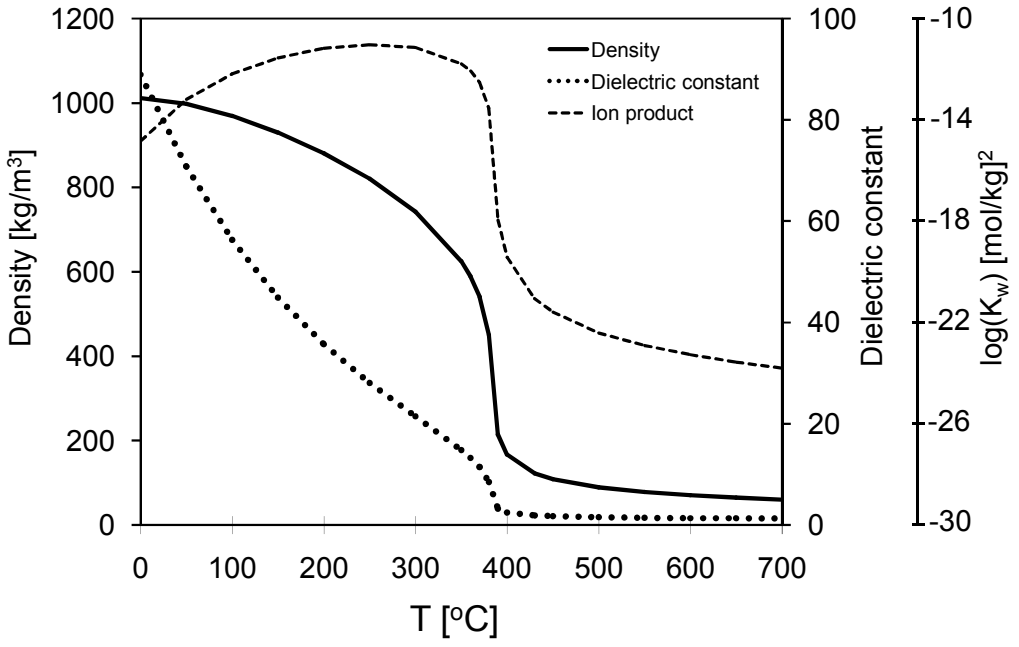

Figure 1.3 The changing if dielectric constant (ε), water density (ρ) and ion product of water (K_w) on temperature at 25 MPa (JSME steam tables, 1999).

Ion product refers to the constant of equilibrium for acid and base reaction of water, ($K_W = [H^+][OH^-]$). In subcritical region, the ion product increases to three order of magnitude higher than that in the ambient condition. The ionic-type reactions, therefore,

are being catalyzed by the H^+ and/or OH^- ions of the water isolation without any addition of acid/base catalysts. Many organic compounds cannot be dissolved in normal water. As approaching the critical point, the dielectric constant and ion product sharply decrease. The supercritical water behaves like an organic solvent. Under supercritical conditions, the amount of hydrogen bonds is much lower and their strength is much weaker while the temperature is increased (Mizan et al., 1996; Lu et al., 2006). The dielectric constant of supercritical water is much lower than when water stays in ambient conditions and increases the diffusivity under supercritical conditions (Shaw et al., 1991). With this change, the water turns into the nonpolar-like solvent with the high solubility of the organic compounds and gases. Supercritical water is a high reactive medium for hydrogen exchange, hydrolysis, hydration, and promote free radical reactions (Akiya and Savage, 2002). The ionic reaction, thus, is demoted and the radical reaction is enhanced instead, indicating that the reaction pathway can be controlled by manipulating the water conditions. In supercritical water conditions, cellulose, hemicellulose, polysaccharide, and protein are hydrolyzed to their monosaccharides and smaller compounds (e.g., glucose, xylose, amino acids, and organic acids) which are utilized further as the thermo-chemicals and bio-chemicals reactions. Additional, the reaction under sub- and supercritical water condition is the

environmental friendly system.

1.4 Supercritical water gasification (SCWG) of biomass – Introduction

Supercritical water gasification of wet biomass is a promising technology for producing combustible gas such as H_2 and CH_4 (Matsumura et al., 2005). Wet biomass contains much high water content which is the heat of vaporization of water exceeds the heat of combustion of the biomass, the drying process of gasification does not satisfied. Meanwhile, a lot of energy is consumed to evaporate water in biomass for biomass feedstock preparation more than the heating value of biomass utilization. Supercritical water gasification (SCWG) is another alternative which is taking the advantage of the high water content to use water as a reaction medium rather than being evaporated. Another good point of SCWG is a high solubility of organic compound of biomass in the supercritical water conditions. When temperature increases, the dielectric constant of water becomes lower, similar to that of organic compounds. As a result, homogeneous of the reaction is magnified, therefore speeding of the reaction rate and enhancing of the product yield. Moreover, a water-gas shift reaction has been highly promoted when the reaction temperature increases, CO converts to gaseous product

prosperous with H_2. CO yield is dramatically decreased while H_2 yield increases when then reaction temperature reaches the supercritical region (DiLeo et al., 2008). Water-gas shift reaction was also found to extent by high water density which was studied by Sato et al. (2004).

SCWG has been started at high temperature and high pressure, for example, the pilot scale of catalyst-suspended gasification of chicken manure was operated at 600 ^{o}C nad 25 MPa (Nakamura et al., 2008). At those conditions, it is such many challenges as reactor design, feedstock and/or catalyst homogenization, and a high stability of catalyst. For more details of SCWG improve and development is discussed in chapter 2.

The reaction in SCWG process of biomass are still much complex by the unique properties of hot-compressed water with different temperature and pressure, and biomass composition itself. The ionic reactions are promoted while the biomass feedstock heating up, starts in subcritical period. As a result, fast hydrolysis occurs, depolymerizing macro-molecular compounds (e.g., cellulose, hemicellulose, lignin, and protein) into smaller molecular compounds, oligomers, and monomers (e.g., glucose, xylose, phenols, and amino acids). As a basic compound of cellulose, many researchers use glucose to be a model compound of cellulose and its represents biomass

model compounds.

The decomposition mechanism had been investigated by using model compounds has shown some insight on biomass gasification behaviors. To understand SCWG process of biomass, the several reaction pathways of biomass model compounds are proposed. Sasaki et al. (1998) proposed the reaction pathway of cellulose, has shown in Figure 1.4, which is one of the main compounds in lignocellulosic biomass, in sub- and supercritical water. Hydrolysis of cellulose produces glucose and oligomer. Glucose isomerizes to fructose and decomposed to erythrose including glycolaldehyde or glyceraldehydes and dihydroxyacetone. Glyceraldehyde and dihydroxyacetone evaporated to pyruvaldehyde. Pyruvaldehyde, erythrose, and glycolaldehyde forward decompose to small compounds which are mostly acids, aldehydes and alcohols that are containing 1-3 carbons. 5-HMF (5-hydroxymethyl-2-furfural) is formed directly from glucose.

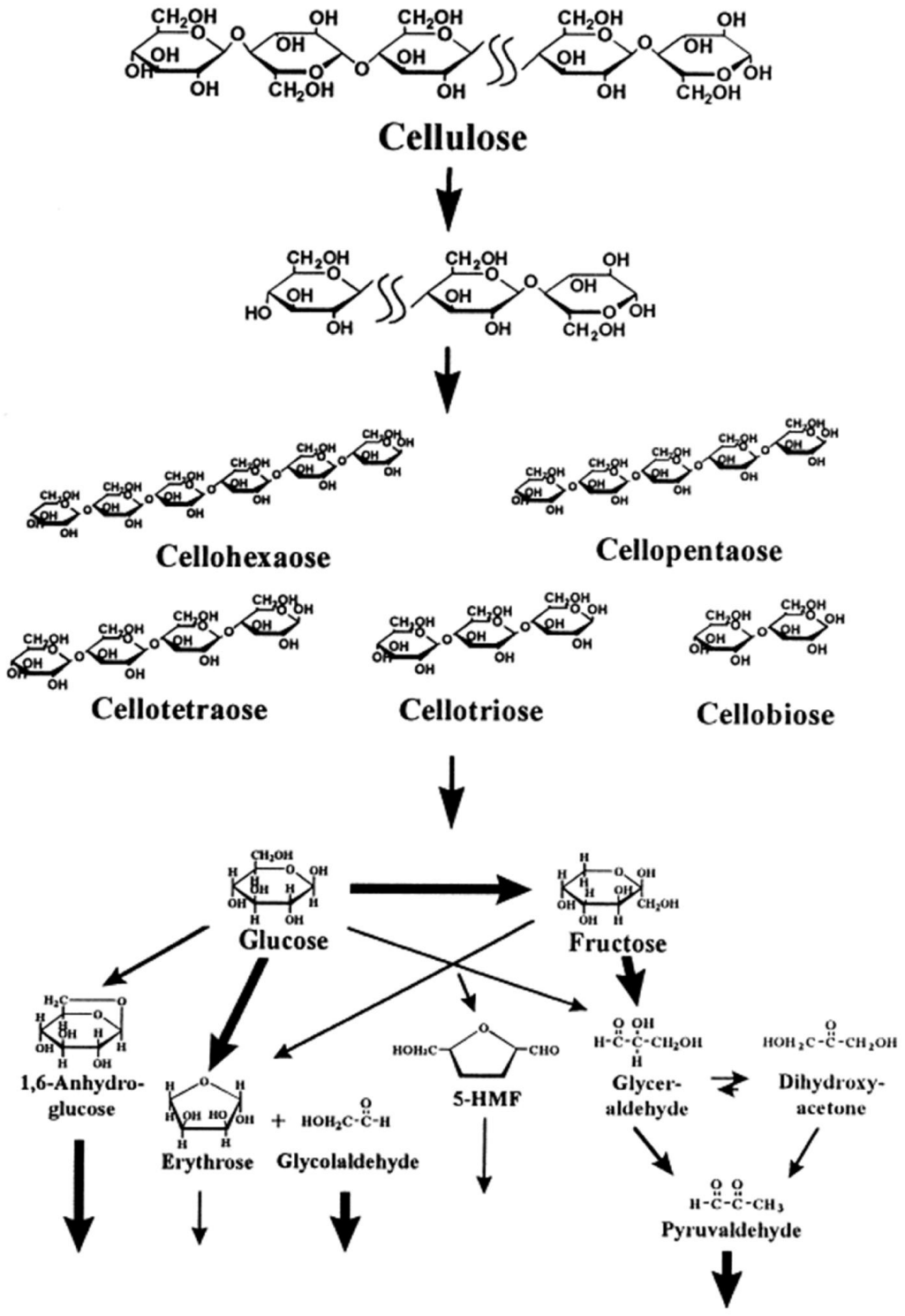

Figure 1.4 Proposed of cellulose hydrolysis reaction pathway in sub- and supercritical water (Sasaki et al., 1998).

After preheated, biomass is gasified in supercritical water conditions. Radical reactions necessary for gasification are promoted. The simplified reactions, as shown below, represents overall chemical conversion in SCWG process: (Antal et al., 2000)

Steam reformimg (glucose): $C_6H_{12}O_6 + 6H_2O \rightarrow 6CO_2 + 12H_2$ (1.1)

Water-gas shift reaction: $CO + H_2O \leftrightarrow CO_2 + H_2$ (1.2)

Methanation: $CO + 3H_2 \leftrightarrow CH_4 + H_2O$ (1.3)

In contrast, the products from hydrolysis and retro-aldol condensation, ring compounds would polymerize to form high-molecular-weight compounds as known as char and tarry material. Even though, SCWG shows a small amount of char and tarry material that those from drying process gasification by enhancing the higher solubility of organic compounds in supercritical water conditions. However, the high-molecular-weight compounds are difficultly gasified and reduced the carbon gasification of the process. The overview of reaction pathway of cellulose decomposed and gasified in SCWG process could be expressed as shown in Figure 1.5. (Kruse and Gawlik, 2003) To avoid the chat and tarry material formation, high reaction temperature, higher heating rate and catalyst would recommend (Sinag et al., 2004; Matsumura et al., 2006). Anyway, it means higher energy consumption is required.

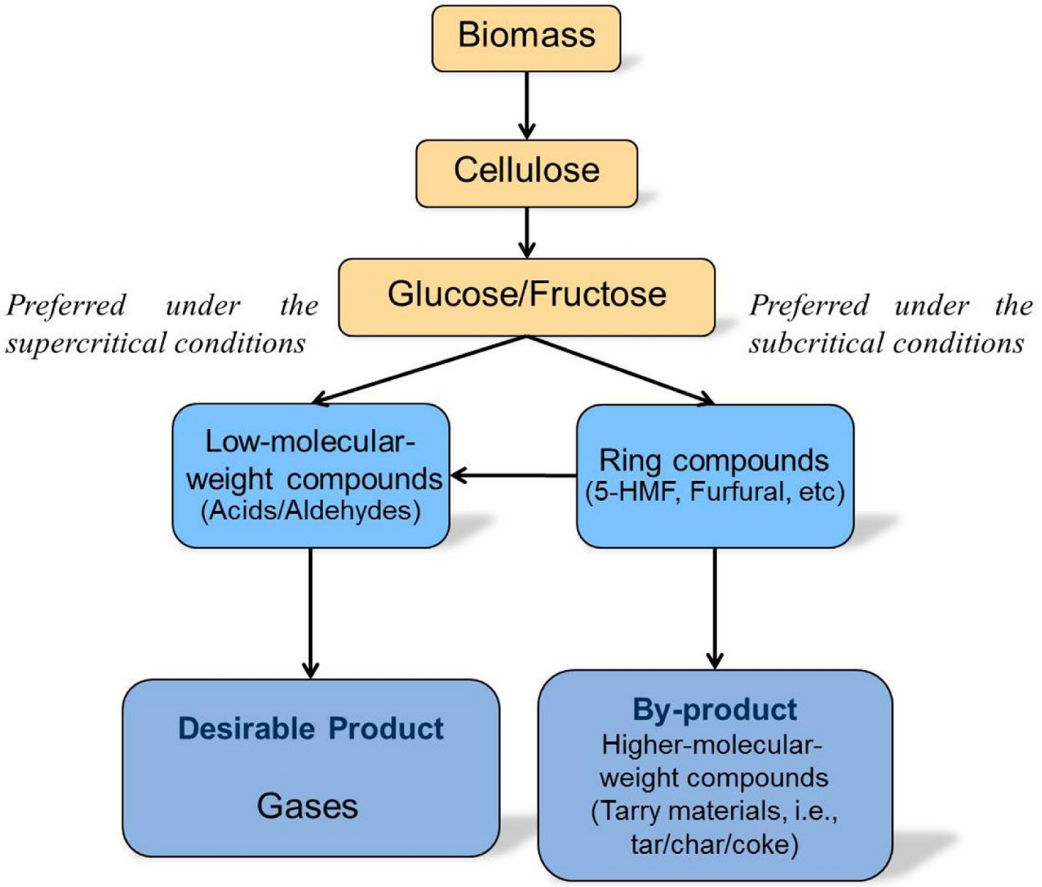

Figure 1.5 Biomass decomposition under sub- and supercritical conditions by simplified reaction pathway (Kruse and Gawlik, 2003).

Presently, there are three pilot plants of SCWG process of biomass, the VERENA plant in Karlsruhe with the operation of 2.4 t/d (Kruse, 2009), and one in the Chugoku Electric Power Company located in Higashi-Hiroshima which is operated in the Continuous Tests of SCWG Process with Shochu Residue of 1 t/d (Wada et al., 2013). Since SCWG is the chemical process, an in-depth understanding in undergoing

chemical reactions in the process is very important in the technology development and optimization. Lumped reaction mechanism is of interest in the field of biomass. This is due to the irregular composition of biomass, which makes it extremely difficult to track down all reactions of the biomass components. Our research groups in Thermal Engineering laboratory, Hiroshima University, studies reaction and formation mechanisms of gas and tarry materials in subcritical and super-critical water to make up the SCWG reaction mechanism based on main intermediate compounds. With our results obtained, the reaction kinetics was proposed by the reaction network model. The behavior of the reaction rates, however, has not been thoroughly elucidated yet. The present study therefore attempts to insight into the SCWG reaction mechanisms based on kinetics reaction, which is key for understanding the complex reaction behavior of biomass gasification and also further useful for developing biomass refinery process in the hot-compressed water and so on.

Additional, there has been on report on the systematic investigation on protein contained biomass. The behavior of the proteins is important, especially for food waste, sewage, and household waste, but has yet to be fully elucidated. By gasifying amino acids, model compounds of protein would show some insight significant on gasification characteristics in supercritical water.

CHAPTER 2

Literatures Review

2.1 Introduction

The 21st century and beyond, World-wide experts have agreed that propitiation of climate change is humanity's greatest threat and challenge. Fossil fuel is about 80% of the world energy consumption. Greenhouse gas emission and pollution progressive

particularly from power plants generators are identified as the global warming mainly effect. Renewable energy is interest and attractive with vast immediate of studies and researches established throughout the year. A world-wide energy crisis and enhancing environmental problems have been caused as long as the dependency on fossil fuels then the urgent need to find an alternative replaced method.

Biomass is an alternative which it can be converted into energy by many appropriate technologies. Sub- or/and Supercritical water gasification technology is a promising conversion technology for high water content biomass (wet biomass). Even though, there are several methods for conversion of waste biomass to energy, especially thermochemical conversion process such as pyrolysis, combustion, and liquefaction. Thermochemical conversion is the method which extremely uses high temperature to reform the chemicals of the organic compounds. The molecules have broken and formed intermediate molecules fructifying in gaseous compounds which content high fraction of fuel gas such as hydrogen and methane and also hydrocarbon liquid fuels (Cantrell et al., 2007). However, biomass waste that contains high water content requires a high drying process. Therefore, hydrothermal biomass conversion is a suitable technology for high water content when its reaction has been taken under water, then it is no need to dry the waste biomass before.

This literatures review provided a thorough analysis and background study on the plant biomass conversion in sub- and supercritical water with the aim of well understanding of the process especially the field of studies based on established research and their results obtained long ago. In this chapter, the reviews are divided into many sections. The preliminary are focused on sub- and supercritical water gasification of real plants biomass compounds. It could show the effect of water properties under sub- and supercritical water conditions that influenced the biomass decomposition. Next, the studies on model compounds are also interest and important part of this review. Because the complication of real biomass compounds, cellulose, hemicellulose, and lignin biopolymer, the studying of biomass model compounds is a necessary first step to determine the primary reaction mechanism of its decomposition and gasification under sub- and supercritical water conditions. Additional, it is also important to find out the reaction mechanism and pathways towards the formation of desirable products (gaseous and liquid compounds) and unexpected product formation, char formation, which is inhibited the conversion process. The effects of the vital operating parameters such as reaction temperature, pressure, residence time, biomass concentration, and additional of catalyst are also reviewed for better understanding.

2.2 Supercritical water gasification of real biomass

Review on the comprehensive study of SCWG for various kinds of feedstocks to predicate and optimize operating conditions. The feedstocks are ranging from biomass, such as agricultural and industrial wastes, livestock manure and algae.

Many works have proved that it is hardly converse biomass at atmospheric pressure, including the study of Herguido et al. (1992). They studied lignocellulosic residues, pine wood chips, pine sawdust, thistles, and cereal straw, gasified with steam at normal pressure. Their results obtained only tar, char, and gaseous product with hydrocarbons contents. The formation of these unexpected by products inhibits hydrogen production.

Since the discovery of the principle of supercritical water gasification by Modell (1985), many researchers have pointed out that biomass gasification in supercritical water is a promising technology for the production of fuel gases, such as hydrogen and methane (Xu et al., 1996; Yoshida et al., 2004; Matsumura et al., 2005; Peterson et al., 2008; Matsumura et al., 2013).

Hawaii Natural Energy Institute (HNEI) accomplished an extensive investigation of the gasification of sawdust and sewage sludge at 600^{o}C and 34.5 MPa.

Antal et al. (2000) found 100% gasification efficiency was achieved under supercritical water conditions. Antal et al. (2000) investigated the gasification of corn, potato and wood sawdust in supercritical water gasification using tubular reactor and found the gas yield more than 2 L/g with hydrogen content of 57 mol%. D'Jesus and co-workers (2005 and 2006) determined the feedstock preparation, corn silage, and reaction conditions effect on the gasification efficiency. The gasification was found to be strongly dependent on the temperature than on the pressure. Yanik et al. (2007) studied the gasification of various kinds of agricultural and leather wastes and compared gaseous and liquid products which are obtained from. They found that the obtained products were different however with biomasses those have similar components. Cheng et al. (2009) explored the study of rapid conversion in subcritical water of switch grass. Kruse's research group focused on the hydrothermal gasification of biomass in various types; for example, artichoke stalk, pine cone, and stalk. High reaction rate in SCWG, the gaseous product can be obtained with high feedstock concentrations. However, the side reaction of the hydrothermal biomass gasification such char and coke formation as unwanted are also revealed.

There are also many researches using SCWG method for gasifying the waste from industry and livestock manure; such as black liquor from the paper factory (Cao et

al., 2011 and Sricharoenchaikul, 2009), empty palm fruit bunch (Akhtar et al., 2010), food wastes (Okajima et al., 2007), municipal solid waste (Onwudili and Williams, 2007), poultry manure (Yanagida et al., 2007; Nakamura et al., 2008) and olive mill wastewater (Erkonak et al., 2008). However, the results were not so impressive since the reaction was not complete and so far from equilibrium state of its ideal, due to the tar and char formation.

Algae gasification has drawn attention to gasification with supercritical water recently. It is due to the fact that algae are versatile biological factories and have high photosynthetic efficiency (Stucki et al., 2009; Brown et al., 2010; Ross et al., 2010; Biller and Ross, 2011; Guan et al., 2012)

As all above mentioned, it can be clearly noted that, the challenges in working on real biomass is special roles and irregular properties of the compositions of biomass clearly posture. The strategy used to overcome this problem is to use the biomass model compounds in order to reduce the reaction complexity. The main reaction mechanism, therefore, could be revealed, which is useful for the process development and optimization.

2.3 Supercritical water gasification of model biomass

Due to the reaction mechanism of biomass in SCWG is complexity mechanism, biomass model compounds have drawn attention to elucidate the reaction mechanism. Table 2.1 exhibits the real biomass in SCWG and their model compounds.

Table 2.1 Real biomass and its model compounds

Real biomass	***Model biomass***	
Lignocellulosic biomass	***Group I.***	***Group II.***
	Cellulose	Glucose
	Hemicellulose	Xylose
	Lignin	Catechol and Guaiacol
Protein	Amino acid, Glycine and Alanine etc.	
Algae	Glycerol	

Lignocellulosic biomass, consists of cellulose, hemicelluloses and lignin, is one of the well-known model. Cellulose, hemicelluloses and lignin (Group I.) also can hydrolyze to glucose, xylose, catechol and guaiacol respectively as their model biomass at hydrothermal condition. Antal et al. (1990 and 1991) elucidated the mechanism of ring compound formation from D-xylose, D-fructose and sucrose. Yu et al. (1993) successfully studied the gasification of glucose in supercritical water and its carbon

gasification efficiency was over 85%. Minowa's group (1999) elucidated the hot compressed water hydrogen production from cellulose. Yoshida et al. (2001 and 2004) studied cellulose, hemi-celluloses and lignin mixtures gasification at 350 ^{o}C and 25 MPa. Kruse et al. (2000) gasified pyrocatechol, as model compound of lignin. Schmieder et al. (2000) efficiently gasified biomass model compounds, glucose for cellulose, catechol and vanillin for lignin, glycine for proteins.

These model compounds have been proposed the reaction mechanism in SCWG process. (Goodwin and Rorrer, 2010; Aida et al., 2010; Qi and Xiuyang, 2007 and Resende, F. et al., 2007 and 2008). Figures 2.1-2.3 illustrate the reaction pathway of model biomass; glucose, xylose and guaiacol which are model compounds of cellulose, hemicelluloses and lignin, respectively.

Many fundamentals underlying the biomass gasification characteristics were discovered by the experiments of the model compounds. This is due to the simplified reaction parameters that make the identification of the reaction pathways possible.

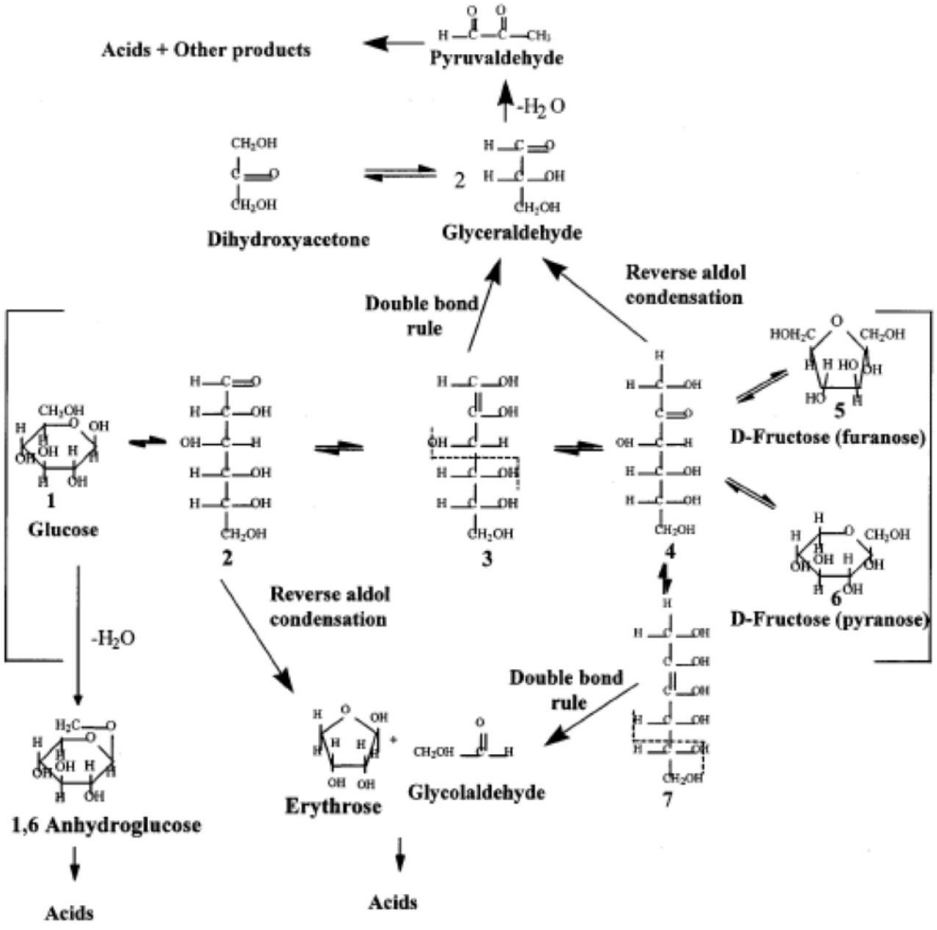

Figure 2.1. Propose pathway of glucose in SCWG. (Kabyemela et al, 1999).

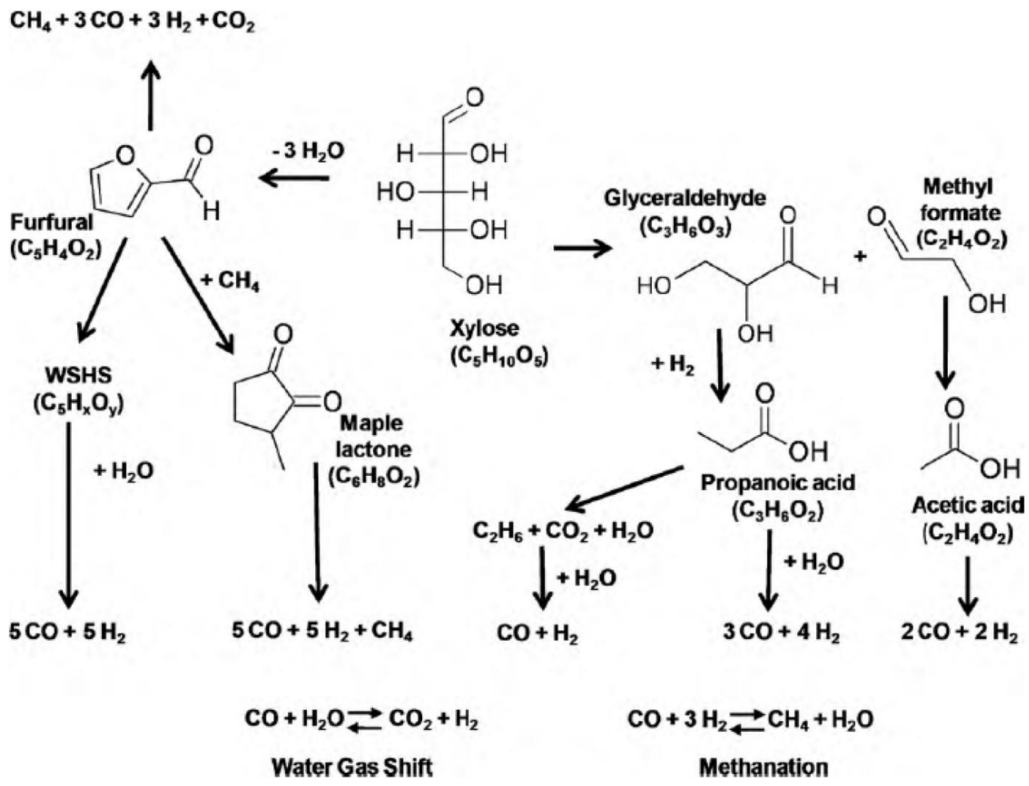

Figure 2.2. Proposed reaction mechanism model of xylose decomposition and gasification (Goodwin and Rorrer, 2010).

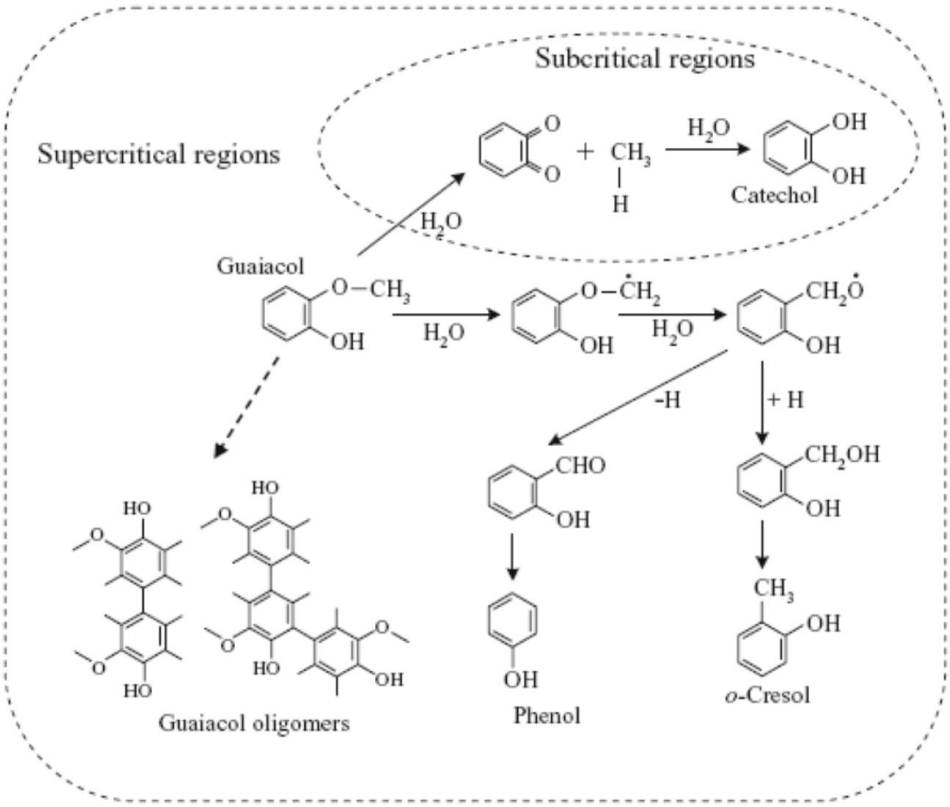

Figure 2.3. Proposed reaction pathways for guaiacol decomposition. (Wahyudiono et al., 2011).

Glucose, a biomass model obtained from cellulose hydrolysis, is effectively to be used for the SCWG reaction characteristics. Many research works employed glucose as a biomass model compound, and showed its behavior in hot compressed water which is advertent decomposition (Fang et al., 2008; Kabyemela et al., 1997; Luijkx et al., 1993; Matsumura et al., 2006, Yoshida et al, 2007; Knežević, et al, 2009). Some recent studies (Sinağ et al, 2004; Fang et al, 2008) show a hydrogen production of glucose by catalytic hydrothermal gasification, supercritical water gasification of glucose with thermodynamic analysis, (Letellier et al., 2010; Voll et al., 2010) and production of valuable intermediate; 5-HMF and furfural for fine chemicals, pharmaceuticals and polymers (Girisuta et al., 2006; Qi et al, 2008; Blasi et al, 2010).

Many by-products have been found during the hydrothermal gasification. Decomposition of glucose is not a typical pyrolysis to produce product gases. Many linear (as glyceraldehyde, dihydroxyactonce, pyruvaldehyde and levulinic acid) and ring compounds (as 5-HMF, furfural and 1,2,4-benzenetriol) were produced. Kabyemela et al.(1997 and 1999) elucidated the decomposition of glucose in hydrothermal process and explained the existence of dehydration, retro-aldol, hydration and isomerization reactions. Dehydration reaction to 5-HMF and furfural occur in decomposition of glucose by C-O bond breaking. Retro-adol reaction also takes place in this

decomposition by C-C bond breaking to form glyceraldehyde, dihydroxyacetone which further dehydrate to pyruvaldehyde. Both of reactions come together about the critical point of water. Aldehyde compounds are intermediates to produce the desirable gaseous products. On the other hand, aromatic compounds reduce the carbon gasification efficiency of the SCWG process by the formation of tar material via the polymerization reaction. Aida et al.(2007) reported the increasing pressure in a range of 40 MPa to 80 MPa and temperature in a range of 350 to 400 ^{o}C provide 5-HMF production by enhanced dehydration reactions, but enhanced hydrolysis of 5-HMF leads to the 1,2,4-benzenetriol production. At 623 K, 80 MPa and 1.6 s residence time, the maximum yield, 8%, of 5-HMF was obtained.

Chuntanapum and Matsumura (2010) pointed out the mechanism of char formation by 5-HMF and glucose in SCWG process. They also proposed the formation of char, from 5- HMF and glucose, reaction pathway in SCWG (Figs. 2.4-2.5). The concentration of 5-HMF has no effect on the gasification pathway, but the increasing concentration of 5-HMF securely promotes the polymerization pathway. In the glucose experiment, the rate of char formation was higher than that for the 5-HMF experiment and found to be 2 orders of magnitude.

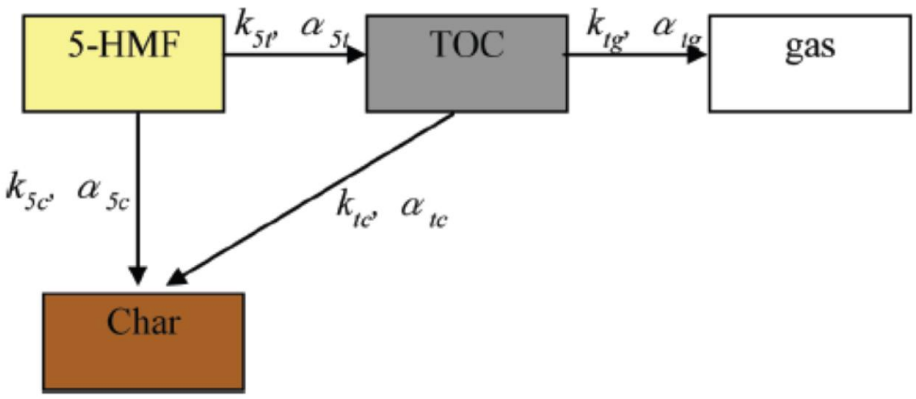

Figure 2.4. Reaction pathway of char formation from 5-HMF(Chuntanapum and Matsumura, 2010)

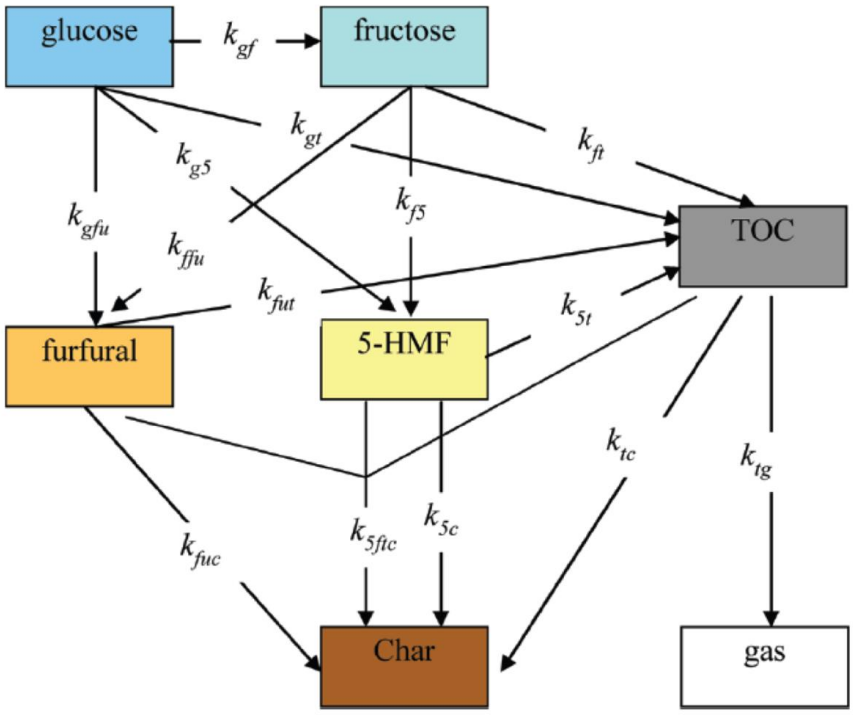

Figure 2.5. Reaction pathway of char formation from glucose (Chuntanapum and Matsumura, 2010).

Biomass, protein content, is a new interesting task. The behavior of the proteins is important, especially for food waste and house-hold waste, including sewage. Minowa et al., 2003 studied hydrothermal reaction of biomass model compounds, the mixture of glucose and glycine, in hot compressed water between 150 to 350^{o}C. At 200 ^{o}C, char was observed and gas product contained almost of carbon dioxide. Maillard reaction, a reaction between amino acids and condensing sugars, was clarified. The Mailard product, melanoidin, was decomposed over 200^{o}C to produce the char, gas, ammonia, and decomposed products in aqueous solution product. Kruse et al., 2005 and 2007 studied a protein presence of real and model compounds biomass effect on hydrothermal gasification. They reported that nitrogen atom of amino acid is a key point which mailard reaction produced mailard products that is N-containing ring compounds. These N-containing ring compounds may form coke at lower temperature operation.

2.4 Effect of variable process parameters on SCWG

2.4.1 Reaction Temperature

Temperature plays a vital role on the reaction due to the changing properties of water with temperature, which can significantly influence the consequence. This effect on the reaction has been determined by several research works. Xu et al., 1996 demonstrated that glucose concentration of 1.0 mol/dm^3 was completely gasified at 600 ^{o}C. When the temperature was under 580 ^{o}C, liquid effluent is yellowish and by-product like tar was observed. Kaybyemela et al.(1997) studied decomposition of

glucose at 300-400^{o}C and pressure of 25-40 MP with a short residence time. In the view point of reaction mechanism, Sasaki et al. (2002) reported the dehydration was dominant at lower temperatures (350 ^{o}C), whereas the retro-aldol reaction mainly occurred at higher temperatures (400 to 450 ^{o}C). Kruse and Gawik (2003) reported that the subcritical temperature favored the furfural formation due to the high ion product of water, meanwhile the supercritical temperature favored the gasification due to the free radical reaction dominantly. Qian et al. (2005) liquefied woody biomass in supercritical water at 280-420 ^{o}C and found that reaction temperature is a key of liquefaction. Higher temperature provided an increasing of heavy oil yield but the highest temperature results in a low yield due to the decomposition of heavy oil formed some small amounts compounds.

2.4.2 Reaction Pressure

From the literatures done, in SCWG process, it was established that the pressure effect did not influence both gasification and carbon gasification efficiency (Hao et al., 2003; Lu et al, 2006 and Guo et al., 2007). The effect of pressure does not influence on biomass gasification too much. Gas product yield of each pressure values does not increase much from 17 to 30 MPa. Especially, Carbon gasification efficiency dose not improve when increasing pressure. The parameters, as carbon gasification efficiency and

gasification efficiency, are not monotonic function of pressure (Lu et al., 2006). Demirbas (2004) also demonstrated hydrogen yield increased as pressure increased from 23 to 48 MPa with fruit shell gasification in SCW. It is due to the fact that high pressure favors water-gas shift reaction. D'Jesus et al., 2005 gasified corn silage in supercritical water and found that gasification yield was not changed by pressure.

In the point of reaction behavior, the change of pressure leads to the value of physical properties of water, such as dielectric constant, ion product, and water density. An increasing pressure, free-radical reaction is restrained and the ion reaction rate increases. Therefore, the hydrolysis rate also increases when with the increasing pressure. Aida et al.(2007) reported that dehydration reactions were enhanced and 5-HMF was provided by the increased pressure from 40 MPa to 70 and 80 MPa with the temperature range of 350 to 400 ^{o}C and its lead 1,2,4-benzenetriol production.

2.4.3 Residence time

SCWG process can complete fully gasification efficiency since short residence time the reason could be the special property of water at this conditions. Schmieder et al., 2000 found that short residence time of 30 s the gasification efficiency was dropped and methane yield decreased. At higher concentration and short residence time provided the formation of tar and char. Lee et al. (2002) examined the effect of

residence time on the gasification of glucose and observed that total yield of all gas was not affected by the residence time but the only shortest residence time of 10.4s affected. To insight the reaction kinetics, the effect of residence time influenced with the product yield such as glucose and fructose decomposition in SCWG. (Kabyemela et al., 1999). Longer residence time, yield of gasification was increased until a maximum was reached (D'Jesus et al., 2005).

2.4.4 Feedstock Concentration

Hao et al., 2003 studied glucose gasification under 923 K and 25 MPa. As glucose concentration increased from 0.1M to 0.8M, the hydrogen fraction in product gas mixture and gasification efficiency was found to reduce. When the glucose concentration was 0.8M the product liquid was very thick, and not analyzed by the total organic analyzer. Franco et al., 2003 gasify real waste biomass, pine, eucalyptus, and holm-oak, and found that at higher steam/biomass ratio (w/w), hydrogen and hydrocarbons production were reduced but tars was produced. At low temperature and high concentration of biomass feedstock, there was plugging occur. Only increasing concentration of biomass feedstock does not improve the gas product yield (Lu et al., 2006).

2.4.5 Catalysts

From the literatures done, in SCWG process, it was established that the presence of catalyst significantly reduced the tar content of the product gas and conversion to

hydrogen and methane. Ni, Ru and activated carbon, Heterogeneous catalyst, are known that can promote the water–gas shift reaction, the methanation, and the hydrogenation reaction. With metal catalysts, the complete gasification could be achieved at the lower reaction temperature (Matsumura et al., 1997; Yoshida et al., 2004; Byrd et al., 2007; Furusawa et al., 2007; Lee and Ihm, 2009; Azadia et al., 2008). Matsumura et al. (2003) gasified cellulose, lignin, and their mixture in supercritical water condition of 673 K and 25 MPa with nickel as a catalyst. Efficiency of gasification is low when lignin is containing in the feedstock but it increases with the amount of the catalyst. The tarry product from reaction between cellulose and lignin deactivated the nickel catalyst. Appropriate amount of catalyst gives high gasification efficiency when cellulose and lignin were mixed for the feedstock. They used sawdust and rice straw for the real biomass feedstock. These real biomass were gasified in the same condition.

Homogenous catalyst such alkali salts was early reported by Sinag et al. (2003) and Kruse and Faquir (2007) as they found that the gasification results of the real biomass were in the same trend as that of the mixture of glucose and K_2CO_3. The hydrogen yield is dramatically increased with the alkali salts addition, as the water-gas shift reaction is promoted by a result of the catalysis via the formation of the formate salt (e.g., HCOOK). Hao et al. (2003) found alkali addition can reduce the CO fraction

in the gas product of glucose gasification. Glucose are readily dehydrated with the absence of alkali additives to form furfural and 5-HMF, the expected precursor to tar and char formation. The additional of alkali, furfural and 5-HMF are not formed, and rather glucose is broken down into derivatives which are ketones, aldehydes, carboxylic acids and their alkylated and hydroxylated derivatives (Onwudili and Williams, 2009). The tar and char formation, therefore, dramatically reduces. An addition of alkali and alkali salts was tested in the gasification of brominated fire-retardant plastics (Onwudili and Williams, 2008), pyrocathechol (Kruse et al., 2000), Municipal Solid Waste or MSW (Onwudili and Williams, 2007) and food wastes (Okajima et al., 2007).

To study the catalyst effect in SCWG, the dissociation constant of H^+ and OH^- was elucidated by Ho et al. (2000 and 2001). Asghari et al. (2006) studied the effect of acid catalyst on 5-HMF reaction and found that at very low pH, 5-HMF further hydration to levulinic and formic acids and also further polymerization at high pH, as they tried to produce 5-HMF from fructose under subcritical condition. Chuntanapum et al. (2011) methodically determined the kinetics of char formation from 5-HMF and glucose, the biomass model compounds. For the glucose, the rate of char formation was higher than that for the 5-HMF and found to be 2 orders of magnitude.

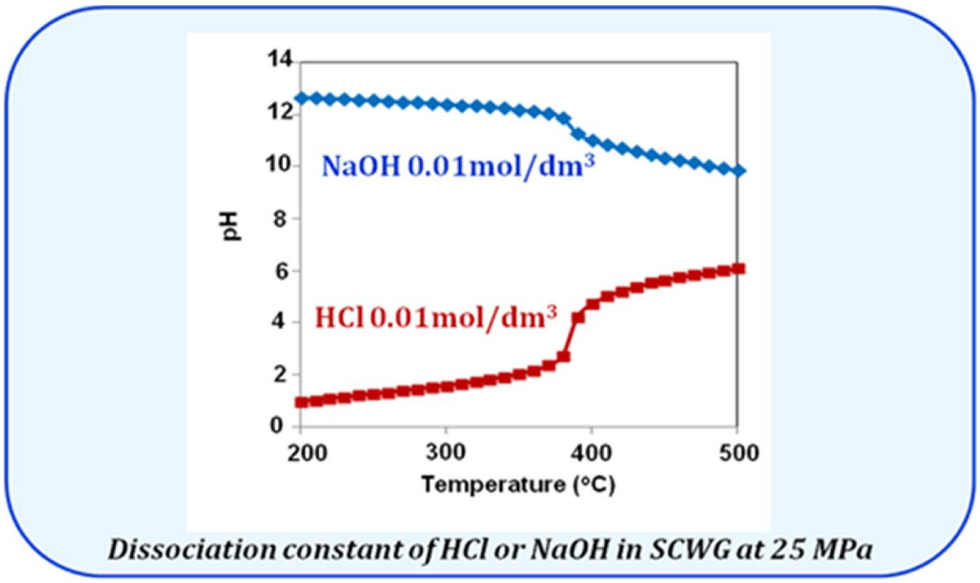

Figure 2.6. Dissociation constants of HCl and NaOH in SCWG at 25 MPa (Ho et al., 2000 and 2001).

Activated carbon catalyst is of interest because it is cheap, recoverable, and also made from abundant agricultural waste. An activated carbon catalyst is effective to achieve high gasification efficiency (Xu et al., 1996). The activated carbon catalyst, it has been found to be effective for glucose- and cellulose-containing feedstock (Matsumura et al., 2013).

2.4.6 Heating rate

Signag et al (2004) explain the effect of heating rate on the hydropyrolysis of glucose in SCWG. The result showed the fast heating up enhanced the gasification of

biomass. They also found out the fast heating up also increases the decarboxylation and the formation of acetic acid.

2.5 Reaction mechanism and kinetics in SCWG

2.5.1 Reaction mechanism

Watanabe et al. (2004) demonstrated the main reaction pathways in SCW are identified to be an ionic or radical character. In liquid water, high pressure of SCW, and the intense gas phase, the reaction seen to proceed via pathways of ionic reaction. In contrast, the steam and less intense SCW promote radical reactions and seem to be the main reaction pathways in these phases. Ionic and radical reactions are competitively conducted around the critical point of water.

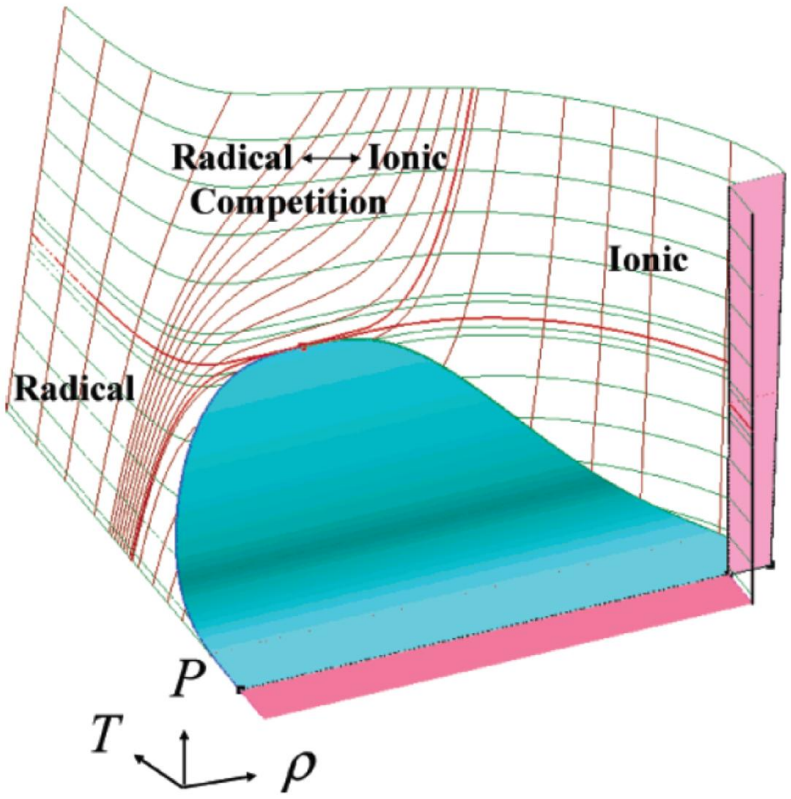

Figure 2.7. The main reaction regimes of P-ρ-T surface of water. (Watanabe et al., 2004)

Katritzky et al. (2001) suggested many reactions progress in SCW via radical or ionic reactions and the competition between radical and ionic reaction pathways depends on the conditions and both compounds. Akiya and Savage (2002) concluded that water can be a catalyst, proton donator or hydration agent for organic reactions.

Few researchers proposed the reaction pathway of model biomass in SCWG which is ionic and radical reactions. Kruse and Edenjus (2007) demonstrated the reaction pathway of glycerol in ionic and radical pathways. On the ionic mechanism

(350 ^{o}C), the protonation of glycerol is the most important step. This means the self-dissociation of water (Fig. 2.8). On the free radical pathway (470 ^{o}C), the abstraction of an OH group from glycerol is the first step. Then, methanol and gases are formed (Fig. 2.9).

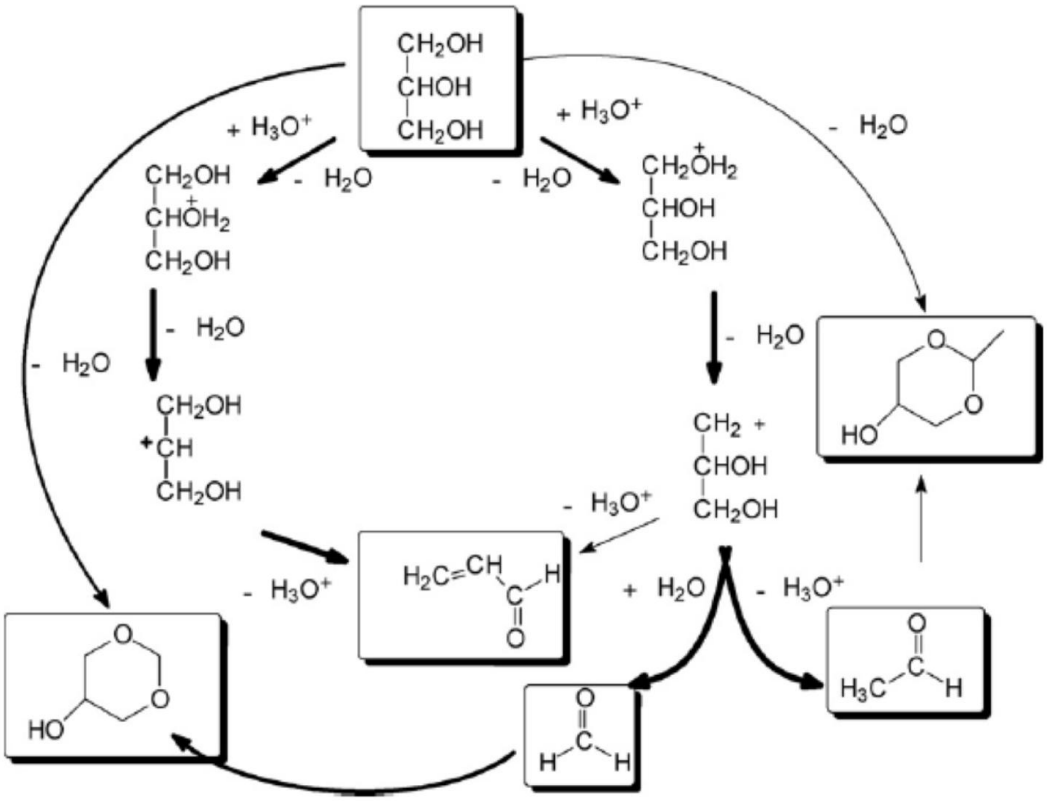

Figure 2.8 The main ionic reaction pathways of 45 MPa, 350^{o}C (Kruse and Edenjus, 2007).

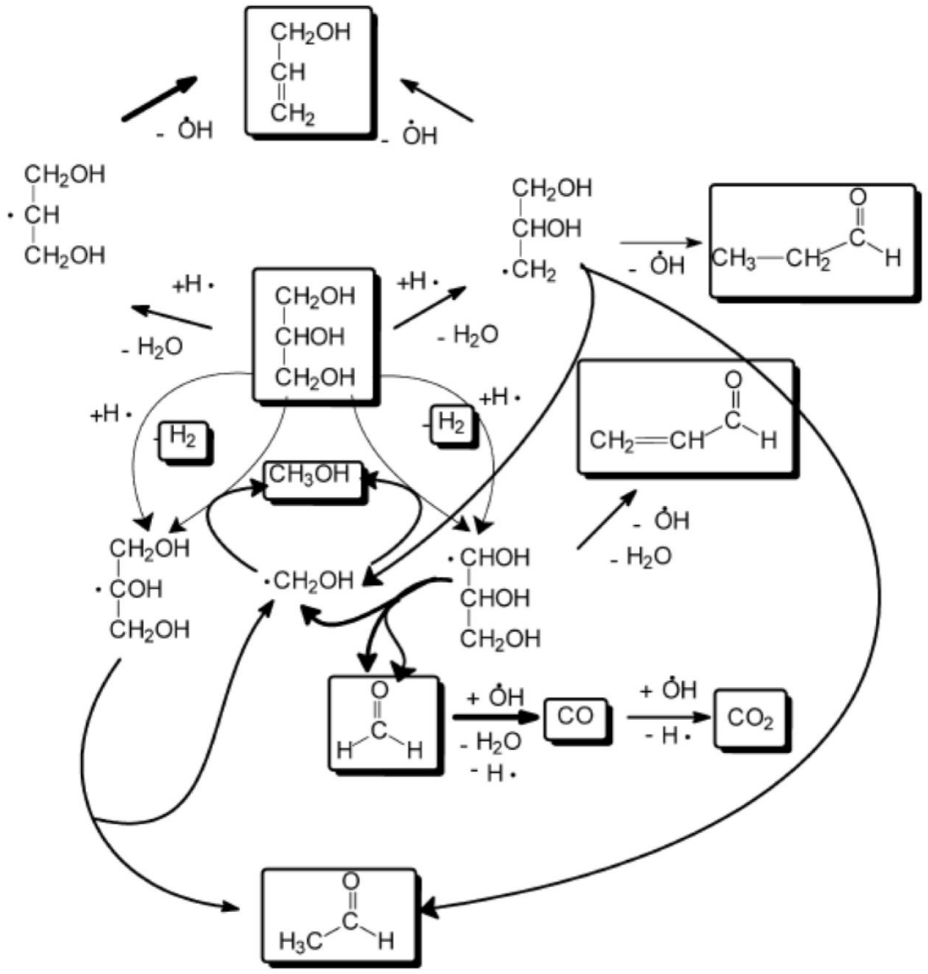

Figure 2.9 The main free radical reaction pathways of 45 MPa, 470^{o}C (Kruse and Edenjus, 2007).

2.5.2. Development of reaction kinetic in supercritical region

Here, there are two method correlated with the reaction rate in SCW. First, Kirkwood relation is the correlation between the rate of chemical reaction and the

polarity of the solvent. Second, transition theory is the relation between the reaction rate and tj activation volume.

Subramanlam and McHugh (1986) reviewed the reactions in supercritical fluid (SCF). The rate enhancement at high pressure can be explained by Transition-state analysis (Laidler, 1965; Ehrlich, 1971; and Eckert, 1972). Eckert (1972) stated that a chemical equilibrium is assumed between the reactants "A" and "B" and the transition state "M" for a bimolecular reaction.

$$A + B \leftrightarrow M^{\pm} \rightarrow products \tag{2.1}$$

The reaction rate constant k variation with pressure is given by

$$\frac{\partial \ln k}{\partial p} = -\Delta V^{\pm} / RT \tag{2.2}$$

where $\Delta V^{\pm}$ = the activation volume, which is the difference between the activated complex volume of partial molar and the reactants and it is given by

$$\Delta V^{\pm} = \overline{V}_M - \overline{V}_A - \overline{V}_B \tag{2.3}$$

If the activation volume is positive, then the pressure will prevent the reaction. However, if $\Delta V^{\pm}$ is a negative quantity, then the pressure will accumulate the reaction rate.

In addition, Subramanlam and McHugh (1986) also mentioned supercritical fluid has unusual physical properties. These properties may have an effect on reaction behavior in critical region. At moderate to high pressures, the diffusivity of supercritical fluid is more gas-like than liquid-like. Also in the critical region, the viscosity of supercritical fluid is more gas-like. These properties should be enhancing the mass-transfer characteristics of supercritical fluid reaction separation process.

In the supercritical fluid phase, the increased reaction rates were reviewed by Subramanlam and McHugh (1986). The reaction rates are enhanced in supercritical fluid by the associated with free-radical pairs efficient production. The free radicals formation is explained in the below reaction when a geminate radical pair $(A \bullet B\bullet)$ is formed by the molecule AB dislocates which may further diffuse apart to form a free radical pair or remerge before it can diffuse apart. It can be called "cage-effect".

$$AB \leftrightarrow (A \bullet B\bullet) \rightarrow A \bullet + B \bullet \qquad (2.4)$$

The resistance diffusion in the mixture critical region will be lower than that in the liquid phase, therefore in the critical region, it would be expected that the $(A \bullet B\bullet)$ radical pair should more readily diffuse. Even though the remerging of $(A \bullet B\bullet)$ to form AB favors in the increased pressure, it can be assumed that the rate of diffusion dominates the pressure effect with reasonable on condition that below 1000 atm of system pressure. Accordingly, the free radicals formation should be encouraged in the supercritical fluid phase.

Above mentions are examples for Development of reaction kinetic. Our laboratory research team, Yong and Matsumura, 2012 and 2013, had also developed and used the kinetics analysis for lignin and guaiacol conversion which obtained agreement results. The present work hence attempted to fill this gap in the research field of SCWG by elucidating the kinetic reaction in SCWG process of glucose. To elucidate the reactions during the heating up period of the supercritical water gasification, and for designing an effective reactor, above and previous mention knowledge will be useful for these purposes.

CHAPTER 3

Aim and Objectives

3.1 Research motivation

The increasing worldwide consumption of fossil fuels has not only led to a major shortage of energy resources but also accelerated pollution and global warming (United States DOE Report, 2004). To reducing the use of fossil fuels, renewable and sustainable energy sources, as sunlight, wind, and biomass would be useful. The

utilization of biomass energy, which is a renewable and carbon neutral energy resource, released carbon dioxide during biomass conversion. But it would be again utilized for the glowing process of the next biomass material plantation. As a result, there is no new carbon dioxide generates into the atmosphere. Biomass, which is an abundant resource that has the potential to produce high heating value fuel: either liquid or gaseous. Among the various technologies, fuel gas production from biomass is extremely attractive from the viewpoint of the efficiency associated with use of the product gas. A variety of biomass resources can be used to provide energy, including conversion to hydrogen and methane.

Nowadays, there is significant global interest in the biomass utilization as an energy resource in order to reduce the use of fossil fuels because biomass is renewable and carbon neutral. Wet biomass, which includes food waste, is one of the most interesting types of biomass because it comprises half of the biomass resources available in Japan. Wet biomasses are abundantly available and the amount of biomass used in Japan has increased significantly (Ministry of Agriculture, Forestry and Fisheries of Japan, 2009). Direct combustion is the preferred method for utilizing biomass due to its simplicity and inexpensive equipment. High content of water in biomass, i.e., moisture content > 70 – 80 wt% (Nakamura, 2008; van Rossum et al.,

2009; Kruse, 2009), its high moisture content impedes the combustion of wet biomass. As an alternative to combustion, supercritical water gasification is expected to be a better technology for the utilization of wet biomass as a source of renewable energy.

Supercritical water gasification (SCWG) is a promising process for gasifying the wet biomass or organic waste into pleasurable products such as hydrogen and methane. Supercritical water gasification takes the advantage of high water content in wet biomasses. The water acts as a reaction medium, eradicating the feedstock evaporation step and cost. Supercritical water gasification is also environmental friendly, which uses only water, and the potential of controlling chemical reactions. At supercritical conditions, water is an excellent gases and organic solvent, and also acts to be an acid/base catalyst. Moreover, supercritical water gasification presents a fewer amounts of tarry materials formation than that of the dry gasification due to the enhanced organic solubility in supercritical water conditions. The tarry materials, char and tar, are extremely hard to gasify and they are inhibitor for the complete gasification.

A wide variety of real biomass and also model compounds have been gasified in supercritical water. Glucose, the most famous biomass model compound, and 5-hydroxymethylfurfural (5-HMF), the well-known dehydrated product of glucose which is expected to be a key compound in the char formation mechanism, have been

previously studied by our research team (Chuntanapum and Matsumura, 2011, and Promdej and Matsumura, 2011). In case of real biomass, softwood lignin and guaiacol, a model compound of lignin, have been also studied by our research team, Yong and Matsumura, 2013.

To understand the reaction mechanism of real biomass or model compounds gasification in supercritical water, the correlation of kinetic rate and temperature has been found to be useful. For the reactions between intermediates, radical and ionic reactions were distinguished by their conformity to Arrhenius behavior (Promdej et al., 2010; Promdej and Matsumura, 2011; Yong and Matsumura, 2013). As the gasification and decomposition of glucose, the decomposition product of cellulose which is the main element of agricultural biomass, has been clarified by many previous work. But a predicting the gasification rate of a specific feedstock remains difficult. There are another abundant biomass resource which is not a kind of agricultural waste such as food waste and sewage from household that is mainly contain proteins. The behavior of the proteins is important, especially for food waste, but has yet to be fully elucidated.

Anyway, an activated carbon catalyst is known to be effective to achieve high gasification efficiency. But it was recently reported that the effectiveness of this

catalyst differs by the kind of feedstocks. Glucose- and cellulose-containing feedstocks has been found to be effective for activated carbon catalyst, but quite limited for fermentation residue (Matsumura et al., 2013). Thus, it is extremely important to find out for which biomass materials the activated carbon catalyst is effective. However, there has been no report on a systematic investigation to achieve this. Especially, its effectiveness for the gasification of compounds with heteroatoms, such as proteins, is of interest.

Inspired by all the considerations above, the study of reaction kinetics of amino acids, a model compound of protein, gasification in supercritical water is methodologically investigated in the present work by changing the process variable parameters (feedstock concentration, residence time, temperature, and catalyst). The different structure of each amino acid would give some insight effect on gasification rate and it would be clarified. Then, the reaction rate kinetics of amino acids in this study could be useful to predict and specify the reaction type of biomass protein-content in supercritical water gasification. To elucidate the reactions network of amino acid decomposition and gasification during the heating up period of the supercritical water gasification, and for designing an effective reactor, above information will be useful for these purposes.

3.2 Aim and objectives

The aim of this work is to carry out detailed studies on the amino acids gasification in supercritical water conditions to determine the detailed reaction network , mechanism and subsequently to elucidate its reaction rate and effect of gasification parameters. The measurable objectives of this study are followings:

1. To determine effect of gasification parameters of amino acid in supercritical water conditions which are feedstock concentration, residence time, reaction temperature and catalyst additional.
2. To evaluate the various reaction products obtained (gas, liquid and solid fractions) are evaluated based on qualitative and quantitative manner.
3. To determine the effect of different functional group and structure of amino acids in supercritical water gasification.
4. To elucidate the kinetics parameters for the reaction rate of amino acids gasification.
5. To propose the reaction network of amino acids decomposition and gasification in supercritical water conditions.

CHAPTER 4

Experimental Method

4.1 Introduction

Experimental methods for all the experiments conducted in the present work are explained in this chapter. Experimental procedures of continuous flow reactor, product analyses (including those for gas, liquid and solid, if it has), experimental conditions and materials are also described.

4.2 Experimental procedures

All gasification runs were performed using the tubular flow reactor schematically illustrated in Figure 4.1. The reactor was made of SS316 steel tubing (i.d., 2.17 mm; o.d., 3.18 mm) with a length of 12 m. The desired temperature was reached by only feeding deionized water before the addition of the feedstock and he reactor pressure was maintained at 25 MPa. The residence time was changed in the range of 63 to 188 s by adjusting the feedstock flow rate. The reactor effluent was cooled down by the cooler before the remaining solid was separated from suspension by a solid−liquid separator and filter. At the back-pressure regulator, the effluent was depressurized to atmospheric pressure and then sampled. The feedstock used in this study was a mixture of commercialized amino acids and deionized water.

In case of catalyst additional, activated carbon from coconut shell (PDX-1, Kuraray Co., Ltd.) with median particle size of 29 μm was used in this work and its concentration was fixed at 0.5 wt%. Feedstock containing the activated carbon catalyst was fed into the reactor by a piston pump (Toyo Koatsu Co.).

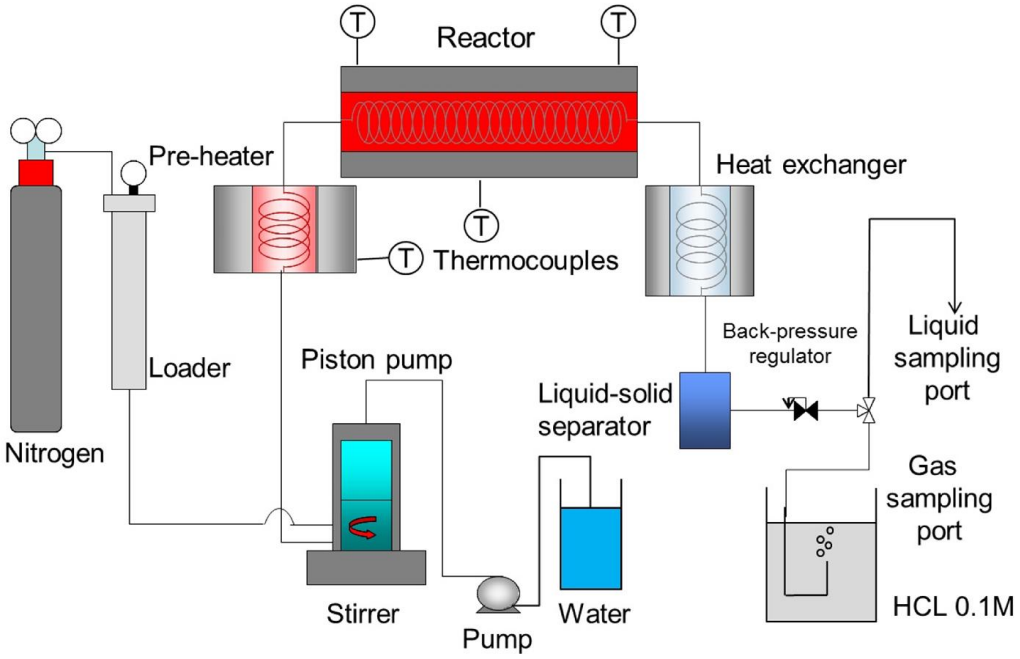

Figure 4.1 Experimental apparatus

4.3 Products Analytical

The reaction effluent products are separated into gas and liquid as follows. The product analyses overview that used in this study is illustrated in Figure 4.2.

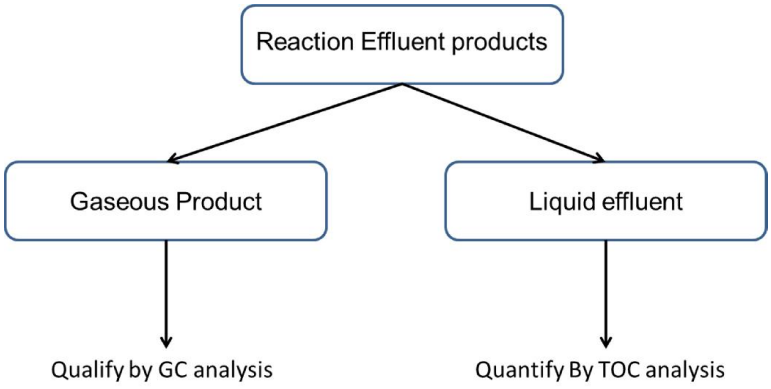

Figure 4.2. Product analyses.

The gas generation rate was determined by measuring the time for effluent gas to fill a vial of known volume under 0.1M of HCl solution.

4.3.1 Gas product

A gas chromatography (GC) is an analysis accessory for separating chemicals in a complex gas sample. A gas chromatography conducts with a flow of gas samples through a small tube, as known as the column, where the different chemical composition of a sample pass in a gas stream, carrier gas or mobile phase, which has different rates. The rates depend on their various properties of chemical and physical and also their interaction with a specific column filling which is called the stationary phase. The chemicals gases are electronically detected and identified at the exit of the end of the column. In the column, the stationary phase work as a separator of each different component, begetting each identified components exit the column with a different time which is called retention time. The flow rate of carrier gas, temperature and the length of column are the parameters that can affect the order of separation or retention time.

In this work, gas chromatography (GC), Shimadzu GC-14B, Japan, is used for product gases analysis. GC-TCD, a thermal conductivity detector GC, will detect CO_2 and CO with He as the carrier gas. GC-FID, a flame ionization detector GC will detect

CH_4, C_2H_4, and C_2H_6 with He as the carrier gas. GC-TCD with N_2 as the carrier gas will detect H_2.

4.3.1.1 Gas Chromatography Procedures

1) Open the carrier gas (nitrogen or helium depend on what components we want to measure) N2 for hydrogen, He for carbon gas
2) Open hydrogen gas stopcock and turn on the air compressor (only for measuring carbon components)
3) Check the pressure gauge, set the following pressure PRIMARY CARRIER (P): 500kPa AIR: 50kPa HYDROGEN: 50kPa
4) Turn on the GC
5) Press [FILE] – [0] – [ENT] for measuring carbon components Press [FILE] – [1] – [ENT] for measuring hydrogen
6) Press start
7) Wait around 2 hours 30minutes to 3 hours for the instrument to setup and heat up To check the temperature, press [MONIT] – [COL], [INJ] or [DET-T]
8) After the wait, press {IGNITE} and ignite the FID detector 1 (on the left hand side). To check whether the detector is ignited or not, hold a gas sample bottle over the detector and check if there is a water vapor forming at the bottom of

bottle

9) Turn on the printer; check the voltage by pressing (COMMAND) – (M) – (1) or (2) – (ENTER)

10) Conduct slope test to check the instrument stability Press (COMMAND) – (,) – (1) – (ENTER) and (COMMAND) – (,) – (2) – (ENTER) Press (MONIT) to see whether the voltage still changing or not, if not then the stabilization is completed.

11) Set the value to 0 by pressing (COMMAND) – (N) – (1) or (2) – (ENTER)

12) To analyze the gas sample

1. Check whether the READY light on the GC is on or not, if not wait for it

2. Use the syringe, take 0.3 ml of sample (less or more would be fine, but remember the used volume for calculation)

3. Inject a sample into the inlet (left), use the other hand to press [START] on the GC and slowly pull the syringe out

4. The analysis would take about 30 minutes for one sample injection as shown in the sample GC chart of Figure 4.10.

In case of measuring hydrogen, one can press [STOP] after 5 minutes since the peak that we are interested in, come out at around 1.7 – 3.0 minutes

13) To end the analysis, press [FILE] – [9] – [ENTER] and wait around 30 minutes to let the temperature drop.

14) After 30 minutes, if the temperature drops below 100°C, turn off the printer and GC

15) Turn off the gas stopcock and air compressor. Let the air inside the compressor out.

Remarks : [ ] represent button on GC control panel

( ) represent button on the printer

*The printer will start printing automatically after pressing [START] on the GC, but there is an exception when we press [STOP] and (STOP1) before the GC finish its cycle during hydrogen measurement. We have to press (START) manually after pressing [START] on the GC.

For clearly understanding, GC parts have been shown in following figures, Figure 4.3, 4.4, 4.5, and 4.6. Subsequently, the example GC chart and including peaks explanation is shown in Figure 4.7.

Figure 4.3 GC Control panel

Figure 4.4 GC Printer

Figure 4.5 Gas pressure gauge

Figure 4.6 Igniters and Injectors

The detectors, almost commonly used, are the FID (flame ionization detector) and the TCD (thermal conductivity detector). They are a wide range of components sensitivity, and they work over a wide concentrations range. Although, TCD is used to

detect any universal component essentially and other than the carrier gas on condition that their thermal conductivities are different from that of the carrier gas. Hydrocarbons are primarily sensitive detected at FIDs more than TCD. However, water cannot be detected by FID. TCD, a non-destructive, can be operated in-series before FID, a destructive. So, it provides the same analyses of complementary detection with impregnable.

Meanwhile, TCD can show all peak of gases that contain in gas sample which is injected to GC. But FID could show only the peak of hydrocarbon gases. An example GC graph is shown in Figure 4.7 with remarks of gas products of each retention times.

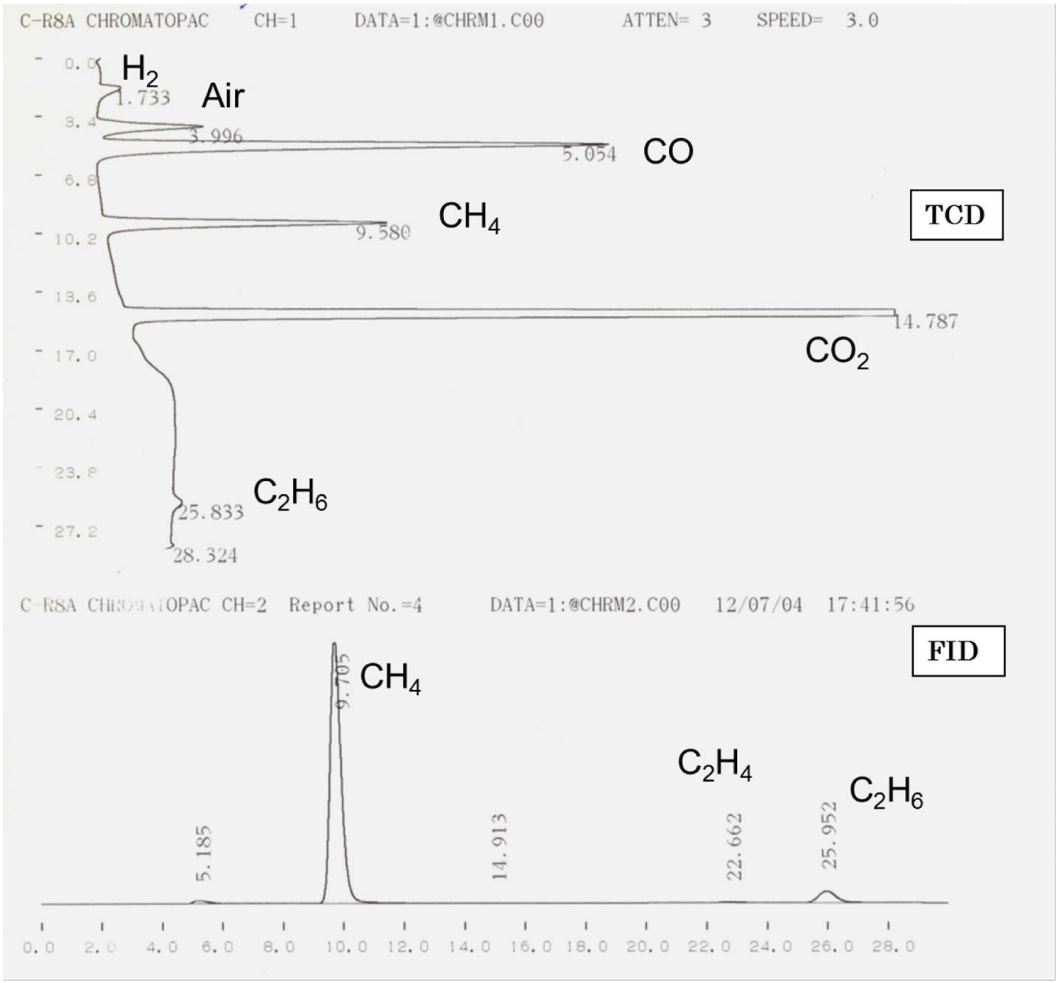

Figure 4.7 The example GC chart, including specified gas product at retention time peaks

4.3.2 Liquid product

Total organic carbon (TOC) analysis is the analysis used to measure the amount of carbon bound in an organic compound. IC, inorganic carbon, is a typical analysis of TOC measurements, aka the amount of carbon gases dissolved in the liquid sample such as carbon dioxide and carbonic acid salts. IC portion was involved

removing first for TOC analysis and then it was measured the carbon which leftover. After that an acidified sample was involved purging with carbon-zero air or nitrogen gas before measurement. It is called non-purgeable organic carbon (NPOC). NPOC gives the amount of carbon dissolved in liquid form. The result of TOC analysis shows up as mg/l of carbon in the sample.

In this work, the liquid effluent was also analyzed by a total organic carbon (TOC) analyzer (Shimadzu TOC-V CHP, Japan) to measure the NPOC or non-purgeable organic carbon which is the amounts of carbon in the liquid product and the IC or inorganic carbon which is the dissolved gas product using compressed air as the carrier gas.

4.3.2.1 Total Organic Carbon Analyzer (TOC) procedures

1) Open the TOC and check the water level inside

2) Open the stopcock of the air cylinder and set the pressure to 0.3MPa

3) Turn on the TOC analyzer

4) Run the program TOC-Control V

5) Open the sample data (left) then click [OK] (right)

6) Click ‘new’ and choose ‘sample measurement’ (left) then click [OK] (right)

7) On the menu bar, click the lightning symbol ‘Connect the machine’ to connect

the computer with the analyzer

A window will pop up (left), click (P) and another window will appear (right). Wait until it says 100% and 'now Initializing' then close the window

8) Check that water flow rate and pressure is 150 ml/min and 200 kPa respectively

9) Click on 'monitor' and the status window will appear

Wait at least 1 hour 30 minutes or until all red '!' turn into green 'check mark' and the graph below is stabilized

10) After stabilization is completed, select measurement method, (I) —>(M)

11) A new window will appear (left). To insert method, click browse […], a set of method will appear (right), then select the method to use and click open (O)

12) Click next (N) (left) and set the number of measuring sample (right)

13) Click next (N) and finish until a new window appear (upper). Insert the sample number corresponding to the location of sample on a tray (lower). Then click [OK]

14) The method we enter will appear on the table. Repeat step 11 to 13 if we want to use more than one method to measure the sample. To start analyze the sample, click on the green light symbol

15) A window will appear and ask to save the file, click (S)

Originally the file name is TOC_year_month_date_hour_minute_second_0.t32, the program automatically set the name to the current time, however this can be change to anything you want

16) After click save, the program will ask what to do after it finish analyzing the sample. Mark (K) to let it stand by for other to use Mark (S) to let the program shutdown by itself and disconnect the computer from the analyzer After that, click the bottom left button to continue

17) The program will confirm the analysis method again; check the method and the sample number. After that, click [OK] and another window will pop up, click the left button to start analyze

The process will take around 20minutes per sample per method and cannot be paused

18) When the instrument finish analyze, the results will show as the following image.

19) The results are the average of all analysis of all samples and cannot be used. To get the result for each sample, we have to print the results.

Remarks: To print the result, click file (F) -> print (P)

Choose (T) to print the same table as shown on the program

Choose (S) to print the results for each sample

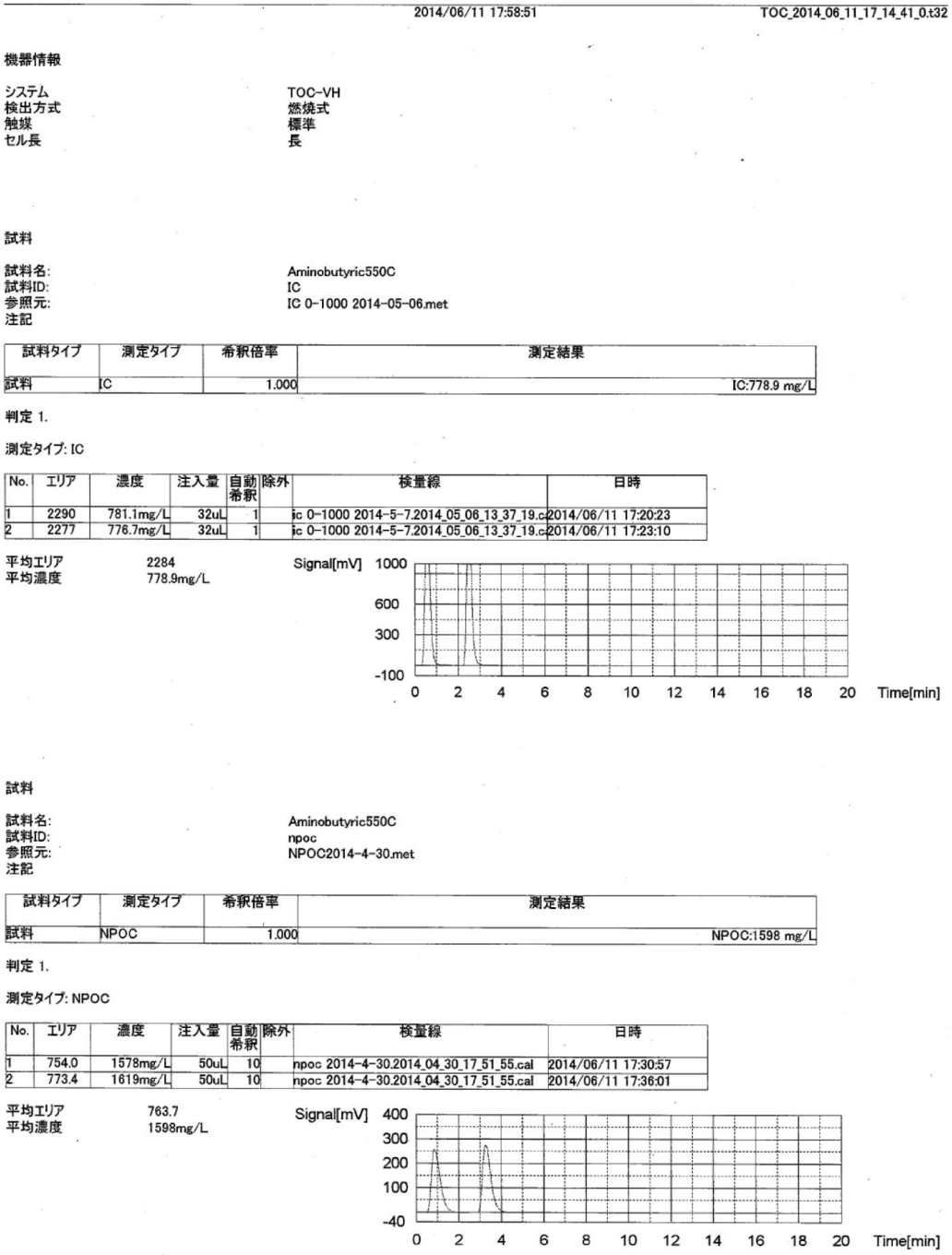

2014/06/11 17:58:51 TOC_2014_06_11_17_14_41_0.t32

機器情報

システム	TOC-VH
検出方式	燃焼式
触媒	標準
セル長	長

試料

試料名:	Aminobutyric550C
試料ID:	IC
参照元:	IC 0-1000 2014-05-06.met
注記	

試料タイプ	測定タイプ	希釈倍率	測定結果
試料	IC	1.000	IC:778.9 mg/L

判定 1.

測定タイプ: IC

No.	エリア	濃度	注入量	自動希釈	除外	検量線	日時
1	2290	781.1mg/L	32uL	1		ic 0-1000 2014-5-7.2014_05_06_13_37_19.c	2014/06/11 17:20:23
2	2277	776.7mg/L	32uL	1		ic 0-1000 2014-5-7.2014_05_06_13_37_19.c	2014/06/11 17:23:10

平均エリア 2284
平均濃度 778.9mg/L

試料

試料名:	Aminobutyric550C
試料ID:	npoc
参照元:	NPOC2014-4-30.met
注記	

試料タイプ	測定タイプ	希釈倍率	測定結果
試料	NPOC	1.000	NPOC:1598 mg/L

判定 1.

測定タイプ: NPOC

No.	エリア	濃度	注入量	自動希釈	除外	検量線	日時
1	754.0	1578mg/L	50uL	10		npoc 2014-4-30.2014_04_30_17_51_55.cal	2014/06/11 17:30:57
2	773.4	1619mg/L	50uL	10		npoc 2014-4-30.2014_04_30_17_51_55.cal	2014/06/11 17:36:01

平均エリア 763.7
平均濃度 1598mg/L

Figure 4.8 TOC example results chart

4.4 Data Analysis

4.4.1 Carbon Gasification Efficiency (CGE)

Carbon gasification efficiency represent by the fraction of carbon in feedstock which gasified into other product. The results are obtained from IC and GC as defined.

$$\text{CGE} = \frac{\text{rate of carbon gasified [mol/min]}}{\text{flow rate of carbon in feedstock [mol/min]}} + \frac{\text{carbon in IC [mgC/L]}}{\text{carbon in feedstock [mgC/L]}} \qquad (4.1)$$

When, the flow rate of carbon in feedstock are defined as follow

$$\textbf{carbon in feed flow rate } [\frac{\text{mol}}{\text{min}}]$$

$$= \frac{\text{flow rate } \left[\frac{\text{g}}{\text{min}}\right] \times \text{feed concentration } \left[\frac{\text{g}}{\text{L}}\right] \times \text{carbon percentage in feedstock}}{12\ [\frac{\text{gC}}{\text{mol}}]} \qquad (4.2)$$

Example

1.0 wt% of alanine = 10 g of alanine/L

Flow rate: 2 g/min = 2mL/min = 0.002 L/min

Carbon percentage in alanine = $\frac{36}{89.09}$ = 0.4041

$$\frac{\left(0.002\frac{\text{L}}{\text{min}}\right) \times \left(10\frac{\text{g}}{\text{L}}\right) \times (0.4041)}{2\ \frac{\text{gC}}{\text{mol}}} = 6.735 \times 10^{-4}\ \frac{\text{mol of carbon}}{\text{min}}$$

Rate of carbon gasified

$$= \sum_{k=0}^{n} (carbon\ component\ of\ gas\ \times gas\ generation\ rate)$$

Leads to

$$= \frac{[CO+CO_2+CH_4+2(C_2H_4)+2(C_2H_6)]\times \text{gas generation rate}[\text{ mL/min}]}{\text{volume of 1 mol of gas during the day of experiment } [\frac{\text{mL}}{\text{mol}}]} \quad (4.3)$$

Volume of 1 mol of gas during the day of experiment ($V_{1 \text{ mol of product gas}}$) is fined as follows

$$\mathbf{V_{1 \text{ mol of product gas}}} = (1 \text{ mol})\times(0.08206 \text{ L} \cdot \text{atm/mol} \cdot \text{K})\times(T+273.15)\times(\frac{1013.25 \text{ hPa}}{P}) \quad (4.4)$$

Where T = the room temperature on the day of experiment [^{o}C]

P = the room pressure on the day of experiment [hPa]

Carbon component of gas product can be found as defined equations below

$V_{product\ gas} = V_{total} - V_{air}$

V_{total} = volume of injected gas

V_{air} = volume of air

V_{CO} = volume of carbon monoxide

V_{CO2} = volume of carbon dioxide

$V_{methane}$ = volume of methane

$V_{ethylene}$ = volume of ethylene

V_{ethane} = volume of ethane

$$\textbf{Carbon component of gas} = \{V_{CO}+V_{CO2}+V_{methane}+(2\times V_{ethylene})+(2\times V_{ethane})\}/V_{product\ gas} \quad (4.5)$$

4.4.2 Reaction Rate Equation

The reaction rate equation is derived from the carbon gasification efficiency. From the equation, when determining the optimum conditions, the carbon gasification efficiency can be predicted using the reaction temperature or residence time of effluent in reactor. We assumed that the gasification reaction rate is first-order with respect to the amount of carbon in feedstock. Using the Arrhenius rate law for the reaction rate constant, the following equation can be obtained.

$$\text{Rate} = \frac{dC}{dt} = -kC \tag{4.6}$$

$$\text{When } \mathrm{k} = k_0 \exp\left(\frac{E_a}{RT}\right) \tag{4.7}$$

$$\text{Leads to } \frac{dC}{dt} = -k_0 \exp\left(\frac{-E_a}{RT}\right)C \tag{4.8}$$

But C in Eq. (4.8) can be defined to carbon gasification efficiency that means amounts of carbon in feedstock has been changed by time. However, the carbon gasification efficiency can be determined by below equation.

$$CGE = \frac{n_{Cg}}{n_{C0}} \tag{4.9}$$

Then, Eq. (4.8) is modified to be

$$\frac{dn_{Cg}}{dt} = -k_0 \exp\left(\frac{-E_a}{RT}\right)\left(n_{C0} - n_{Cg}\right) \tag{4.10}$$

which leads to

$$n_{C0} - n_{Cg} = n_{C0} \exp\left[-k_0 \exp\left(\frac{-E_a}{RT} \right) t \right] \tag{4.11}$$

$$\frac{n_{Cg}}{n_{C0}} = 1 - \exp\left[-k_0 \exp\left(\frac{-E_a}{RT} \right) t \right] \tag{4.12}$$

where n_{C0} = initial amount of carbon [mol],

n_{Cg} = amount of gasified carbon [mol],

k_0 = pre-exponential factor [s^{-1}],

E_a = activation energy [J mol^{-1}],

R = gas constant [J mol^{-1} K^{-1}],

T = Temperature [K],

t = time [s]

and CGE = carbon gasification efficiency [-].

4.5 Experimental Conditions

The experiments were carried out under the supercritical water conditions (reaction temperature above 400^{o}C), and the reaction pressure 25 MPa in order to systematically study the gasification characteristics parameters which are reaction temperature, feedstock concentration, residence time (the time of effluent stays in reactor), and catalyst additional. The feedstock used in this study is commercialized

amino acids that it was varied the concentration in a range of 1.0 to 5.0 wt%. The experimental reaction temperature was used in a range of 500 to 650 ^{o}C. The changing of residence time had been adjusted by feedstock flow rate which are 1.0, 2.0, and 3.0 g/min. and it made the residence time were in a range of 63 to 188 s. In case of catalyst additional, activated carbon from coconut shell with median particle size of 29 μm from PDX-1, Kuraray Co., Ltd. was used in this work and its concentration was fixed at 0.5 wt%. This mixture is thoroughly stirred in piston pump (Toyokoatsu Co., designed for our use) while it is fed. Hydrochloric acid (HCl) with a concentration of 0.1 M was used for product gas sampling method as an ideal of product gas cannot dissolve into acid solution. The experimental conditions will be explained with more details again in Chapters 5-7.

CHAPTER 5

Supercritical Water Gasification of Amino acid: A parametric study

5.1 Introduction

The use of model compound is effective to determine the gasification rate kinetic parameter and also elucidate the reaction mechanism of biomass in SCWG process.

Amino acids have been chosen to be a model compound of protein. Because the behavior of the proteins is important, especially for food waste and sewage from household, but have not yet to be clearly determined. Glycine is the simplest amino acid, which can be a good model compound of protein.

There are many parametric that effect on gasification characteristics, such as reaction temperature, reaction pressure, residence time, types of reactor, reactor geometrical shape, the properties of reactor wall, heating rate, types of biomass, particle size of biomass, catalysts and/or types of catalyst and feedstock concentration.

Y. J. Lu et al. (2005) studied the parameters effect on gasification of hydrogen production from biomass model compounds and real biomass in supercritical water.

The effect of pressure does not influence on biomass gasification too much. Gas product yield of each pressure values does not increase much from 17 to 30 MPa. Especially, Carbon gasification efficiency does not improve when increasing pressure. It can be seen that the carbon gasification efficiency and gasification efficiency, are not a function of pressure.

The effect of temperature has significant influence on biomass gasification. Gas product yield was improved when temperature was increased. The reason might be the

free–radical reactions have been promoted at high temperature region which are needful for gas formations.

The effect of residence time has influence on biomass gasification. With increasing residence time, the carbon gasification efficiency increase and also leaded the amount of carbon in liquid product decreases. This information showed that longer residence time is needed to reach the highest gasification efficiency.

Higher reaction temperature or high heating rate and catalyst addition are required for a higher concentration of biomass feedstock. At low temperature and high concentration of biomass feedstock, there was plugging occur. Only increasing concentration of biomass feedstock does not improve the gas product yield.

To achieve high gasification efficiency, activated carbon catalyst is known to be effective (Xu X. et al., 1996). However, recently it was reported that the effectiveness of activated catalyst differs from feedstock to feedstock. It is effective for glucose and cellulose containing feedstock, but it quite limited for fermentation residue. Then, it is important to find out for which biomass the activated carbon catalyst is effective. However, there has been on report on the systematic investigation on the effectiveness of

activated carbon catalyst for various feedstock. Especially, its effectiveness on gasification of compound with hetero atoms is of interest.

Then, in this chapter shows investigation of feedstock concentration effect, residence time effect, activated carbon catalyst effect, and reaction temperature effect. Furthermore, reaction temperature effect on the glycine gasification under supercritical water conditions is considered by measuring the changes in the carbon gasification efficiency and product gas at different reaction temperatures. Then, based on the experimental results, we go on to determine the reaction parameters by assuming the first-order reaction for glycine. However, evaluation of the various reaction products obtained (gas and liquid fractions) are evaluated based on qualitative and quantitative manner. Glycine gasification reaction rate constant was also determined by the Arrhenius equation.

5.2 Experimental procedures

Details on the experimental procedures used in this study have been described in Chapter 4. Briefly, a desired concentration of glycine solution was prepared by mixing glycine with deionized water. The reactor pressure was maintained at 25 MPa by feeding only water and the desired temperature was reached before the addition of the feedstock. The SS316 steel tubular with inner diameters of 2.17 mm and outer

diameters of 3.18 mm, and the length of 12 m was used as the reactor. An aqueous solution of glycine was delivered to the reactor by a high-pressure pump at a desired feedstock flow rate. In case of activated carbon catalyst, glycine solution was mixed with activated carbon before it was fed by piston pump (Toyo Koatsu Co.). Activated carbon made from coconut shell with median particle size of 29 μm from PDX-1, Kuraray Co., Ltd. was used in this work and its concentration was fixed at 0.5 wt%. The mixture of feedstock solution and activated carbon is thoroughly stirred in piston pump while it is fed. By adjusting the feedstock flow rate, the residence time was changed. After feedstock passed through the reactor, the effluent product was cooled by a heat exchanger. The remaining solid was separated from suspension by a solid−liquid separator and filter. The effluent was depressurized by a back pressure regulator, and then sampled.

At sampling port, gas samples were measured their gas generation rate by the time for effluent gas to fill a vial of known volume by water replacement. The gaseous product was qualified and quantified by a gas chromatography (GC) installed with TCD and FID. GC-TCD, a thermal conductivity detector GC, will detect CO_2 and CO with He as the carrier gas. GC-FID, a flame ionization detector GC will detect CH_4, C_2H_4, and C_2H_6 with He as the carrier gas. GC-TCD with N_2 as the carrier gas will detect H_2.

Liquid product was also collected at the sampling port. The liquid product was analyzed by a TOC analyzer (total organic carbon analyzer) to quantify the carbon content in the liquid product (NPOC) and the dissolved carbon gas product (IC).

Carbon balance was calculated based on the carbon content in glycine concentration and the carbon content in products and its was defined by following equation.

$$\text{Carbon Balnce} = \frac{C \text{ in gas product } (GC) + C \text{ in liquid product } (IC \text{ and } NPOC)}{C \text{ in feedstock}} \quad (5.1)$$

Noted, the carbon balance between the products (gaseous carbon, IC, and NPOC) and feedstock carbon was closed within the range from 0.96 to 1.1.

5.3 Experimental conditions

Glycine gasification experimental runs were performed using the experimental conditions which are shown in Table 5.1

Table 5.1. Experimental conditions for the glycine gasification

Feedstock	glycine
Feedstock concentration	1.0-5.0 wt%
Reaction temperature	500 - 650 ^{o}C
Reaction pressure	25 MPa
Feedstock flow rate	1.0, 2.0 and 3.0 g/min
Residence time	188, 94 and 63 s
Catalyst	Activated carbon (0.5 wt%)
Reactor type	Flow reactor
Reactor length	12 m

5.4 Results and discussion

To clearly explain the concentration effect, residence time effect, and temperature effect on the characteristics of glycine gasification and kinetic rates of glycine gasification under supercritical water conditions, results of 5-HMF in

Supercritical Water Gasification of Glucose (Chunatapump's thesis, 2010, and Chuntanapum and Matsumura, 2011) are beneficially discussed in this chapter.

5.4.1 Effect of glycine concentration

The experiment was conducted for glycine concentrations of 1.0, 3.0, and 5.0 wt% at 600 ^{o}C and 25 MPa with a residence time of 94 s. The carbon gasification efficiency (CGE) of all experiments are calculated based on of the carbon content in glycine solution feedstock as it has defined in below equation:

$$CGE \equiv \frac{n_{Cg}}{n_{C0}} = \frac{n_{Cgas} + n_{IC}}{n_{C0}} \tag{5.2}$$

where n_{C0} = initial amount of carbon [mol],

n_{Cg} = amount of gasified carbon [mol],

n_{Cgas} = total amount of carbon in gas products obtained after subtracting the effect of activated carbon gasification [mol],

n_{IC} = total amount of organic carbon in the liquid products [mol],

CGE = carbon gasification efficiency [-].

The effect of glycine concentration on the carbon gasification efficiency (CGE) is shown in Figure. 5.1. The effect of activated carbon is also shown in the same figure.

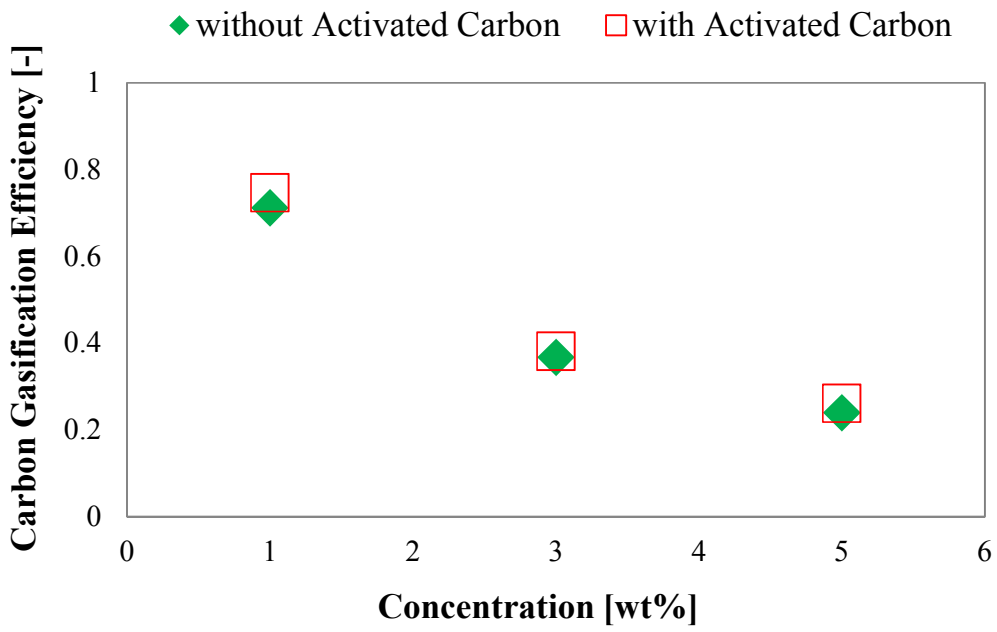

Figure 5.1 Effect of glycine concentration on carbon gasification efficiency, reaction temperature of 600 ^{o}C, reaction pressure of 25 MPa., and feedstock flow rate of 2 g/min

It can be seen that a high feedstock concentration resulted in lower carbon gasification efficiency, which is likely due to the production of tarry material. In a previous report on glucose gasification, the order of the reaction of tarry material

production was found to be higher than unity, with high concentration resulting in a preference for tarry material production over gasification (Chuntanapum and Matsumura, 2011). The same trend was therefore expected here. Thus, at higher concentration, the effect of tarry material production cannot be neglected. As the intention of this study was to assess the gasification characteristics, the effect of tarry material production needed to be omitted so that the gasification rate was first order. For this reason, we employed the low feedstock concentration of 1 wt% in the subsequent experimental runs.

5.4.1.1 Gas Product

The effect of feedstock concentration on gas composition is shown in Figure 5.2. The effect of activated carbon on product gas composition is also shown in the Figure 5.2.

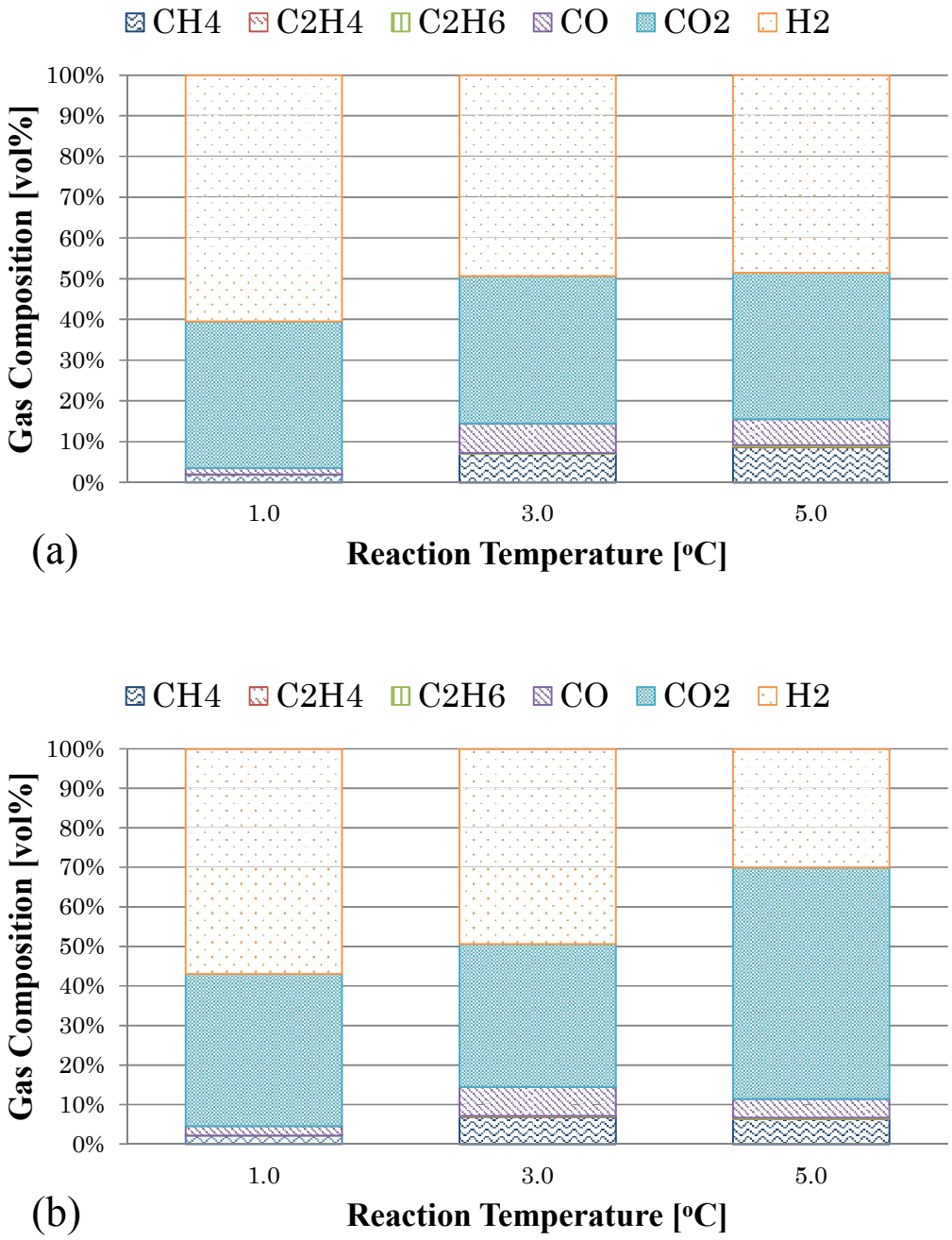

Figure 5.2 Effect of glycine concentration on product gas composition, reaction temperature of 600 °C, reaction pressure of 25 MPa., and feedstock flow rate of 2 g/min. (a) without Activated carbon (b) with Activated carbon

A low feedstock concentration gave a higher hydrogen content, while a higher feedstock concentration provided a higher methane content. Thermodynamics has been found to be effective to predict the gas composition, where gas composition to minimize Gibbs free energy is calculated (Xu et al., 1996). Thermodynamics for supercritical water gasification predicts that higher feedstock concentration favors methane production. Thus, the experimental result agrees with thermodynamic prediction. Thermodynamics also predicts that little carbon monoxide is to be found due to the water-gas shift reaction with being of large amount of water, but carbon monoxide is observed because the water-gas shift reaction is slow, and has not reached the equilibrium. The amount of carbon dioxide was found to increase when activated carbon was applied to high feedstock concentration, possibly due to its effect as catalyst for water gas shift reaction.

5.4.1.2 Liquid Product

Liquid product was quantified the amount of carbon which is containing in liquid product by a total organic carbon analyzer (TOC). TOC measures amount of carbon in liquid sample and reports into 2 type of values which are IC (inorganic carbon) and NPOC (non-purgeable organic carbon). IC refers to inorganic carbon that dissolved into liquid phase temporarily such as carbon dioxide. NPOC refers to

organic carbon that is in liquid phase and could not be purged. The IC value would be treated together with the product gas. Figure 5.3 shows liquid products from the study of the effect of glycine concentration. All samples are clear and colorless. As analyzed by TOC, higher concentration of glycine results higher carbon content in liquid product. It may refer to carbon amounts in feedstock does not change to carbon amounts in gas product.

(a)

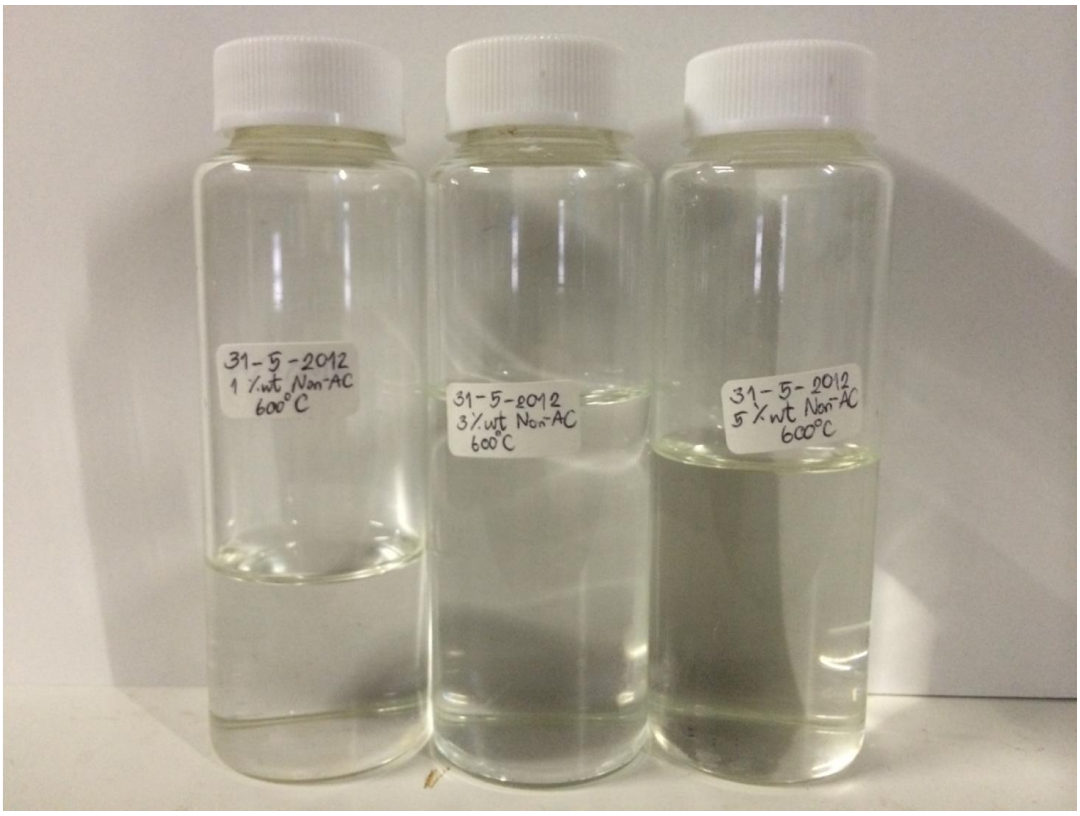

(Left) 1.0wt%, (Middle) 2.0wt%, (Right) 3.0wt%

(b)

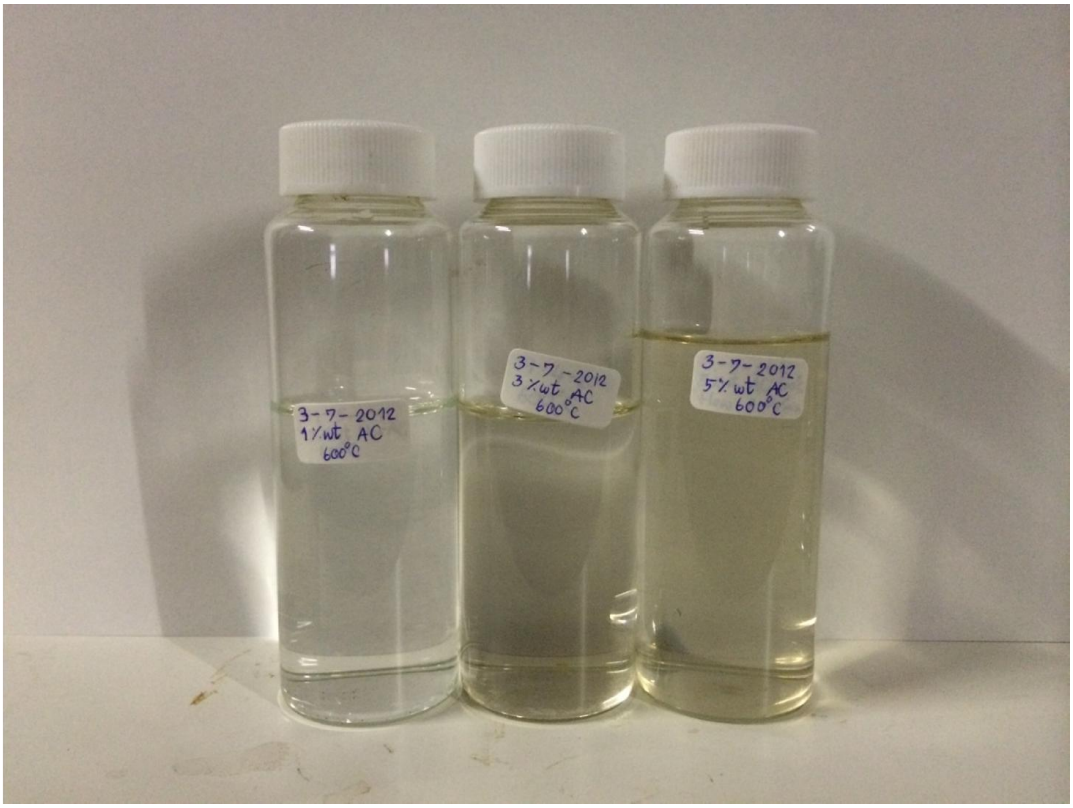

Figure 5.3 Liquid samples of experimental on effect of glycine concentration, reaction temperature of 600 ^{o}C, reaction pressure of 25 MPa., and feedstock flow rate of 2 g/min. (a) without Activated carbon (b) with Activated carbon

Noted, we did not attempt to identify or quantify individual compounds remaining in the liquid phase. There is no particle observed and remained in filter and liquid-solid separator.

5.4.2 Effect of residence time

Glycine solution of 1.0 wt% was gasified at 600 °C and 25 MPa, for different residence times with and without the catalyst. The employed residence times were 188, 94, and 63 s, had been set by adjusting the feedstock flow rate. The carbon gasification efficiency is increased by increasing of residence time as it is shown in Figure 5.4.

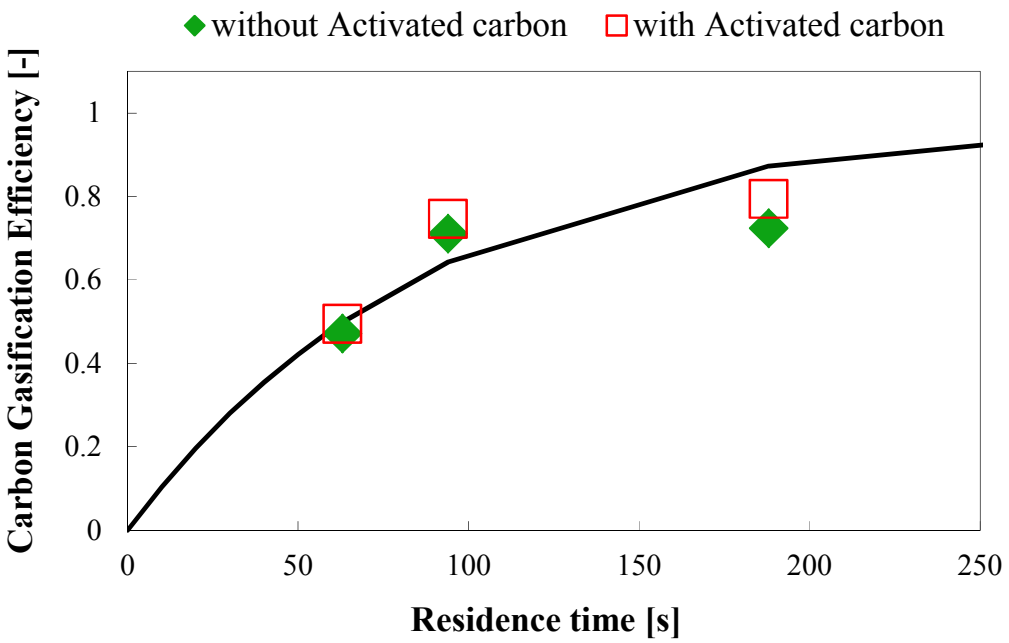

Figure 5.4 Effect of residence time on carbon gasification efficiency, reaction temperature of 600 °C, reaction pressure of 25 MPa, and feedstock concentration of 1.0wt%.

Assuming that the gasification reaction rate is first order in terms of the ungasified carbon, the following equation is obtained

$$\frac{dn_{Cg}}{dt} = -k_0 \exp\left(\frac{-E_a}{RT}\right)\left(n_{C0} - n_{Cg}\right) \tag{5.3}$$

which leads to

$$n_{C0} - n_{Cg} = n_{C0} \exp\left[-k_0 \exp\left(\frac{-E_a}{RT}\right)t\right] \tag{5.4}$$

$$CGE \equiv \frac{n_{Cg}}{n_{C0}} = 1 - \exp\left[-k_0 \exp\left(\frac{-E_a}{RT}\right)t\right] \tag{5.5}$$

where n_{C0} = initial amount of carbon [mol],

n_{Cg} = amount of gasified carbon [mol],

k_0 = pre-exponential factor [s^{-1}],

E_a = activation energy [J mol^{-1}],

R = gas cons tant [J mol^{-1} K^{-1}],

T = Temperature [K],

t = time [s]

and CGE = carbon gasification efficiency [-].

Fitting with this first-order-reaction rate equation is also shown in Fig. 4, and is in good agreement with the experimental data, indicating that 1.0 wt% is sufficiently dilute for the gasification characteristics to be expressed as a first order reaction with little error. This is also in agreement with many other reports on the effect of residence time on biomass gasification, where the gasification efficiency approached unity with time in an exponential manner (Lee et al., 2002 and Hao et al., 2003).

5.4.2.1 Gas product

The effect of glycine concentration on gas composition is shown in Figure 5.5. The effect of activated carbon on product gas composition is also shown in the Figure 5.5.

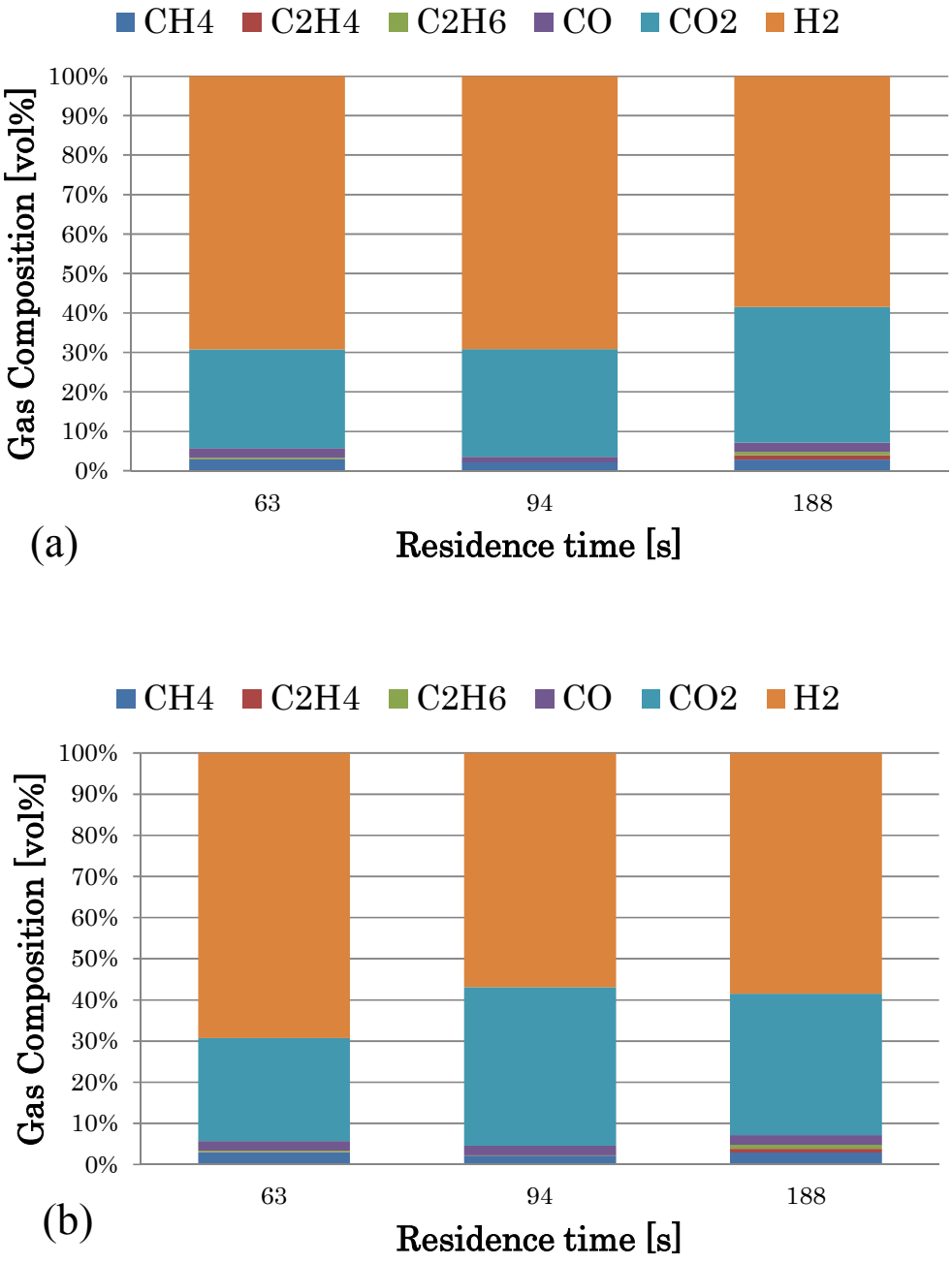

Figure 5.5 Effect of residence time on product gas composition, reaction temperature of 600 ^{o}C, reaction pressure of 25 MPa., and feedstock flow rate of 2 g/min. (a) without Activated carbon (b) with Activated carbon

Carbon dioxide was increased with increasing residence time. Same expectation as previous, it may cause water-gas shift reaction is slow, and has not reached the equilibrium. Thermodynamics predicts that little carbon monoxide is to be found due to the water-gas shift reaction with being of large amount of water, but carbon monoxide has been observed in this effect study. Gas composition has not much changed which compares to the additional of activated carbon.

5.4.2.2 Liquid product

Liquid product was quantified the amount of carbon which is containing in liquid product by a total organic carbon analyzer (TOC). Again, we did not attempt to identify or quantify individual compounds remaining in the liquid phase. Figure 5.6 shows liquid product of the effect of residence time. It can be seen that all liquid product is clear and colorless. No particle suspense in liquid product.

Here again, we had check the solid particle that may remain in filter and liquid-solid separator. But there is no particle observed and remained in filter and liquid-solid separator.

(a)

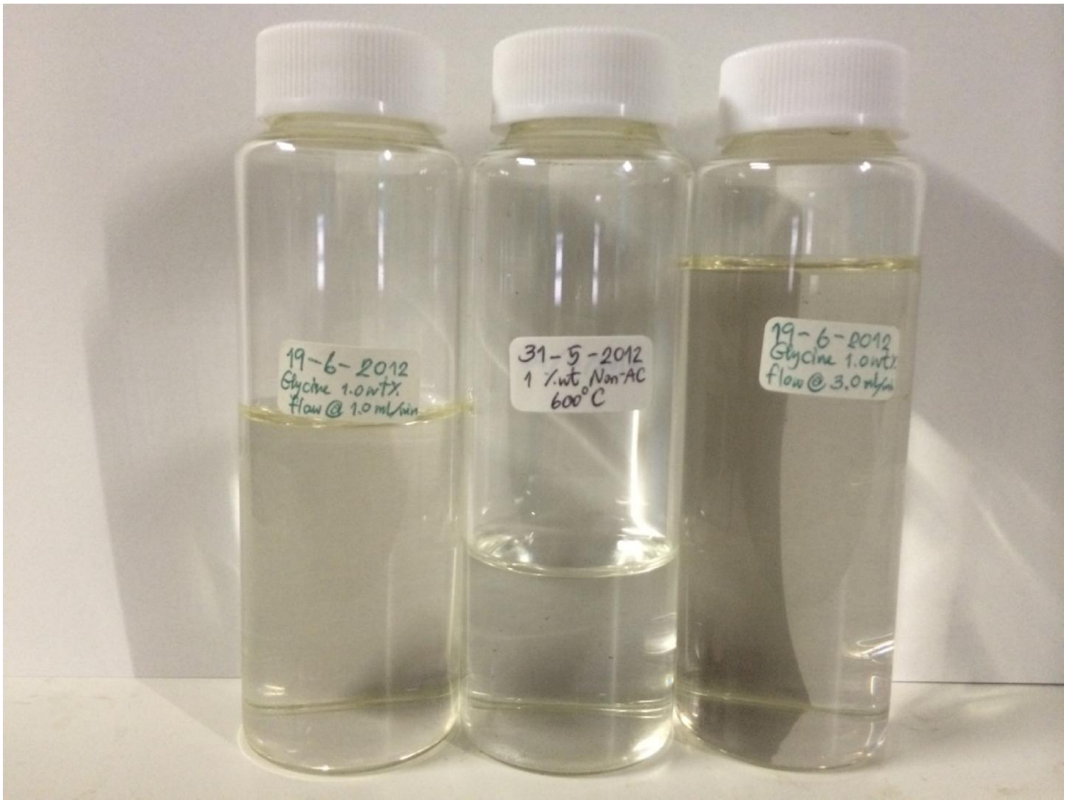

(Left) 1.0 g/min., (Middle) 2.0 g/min., (Right) 3.0 g/min.

(b)

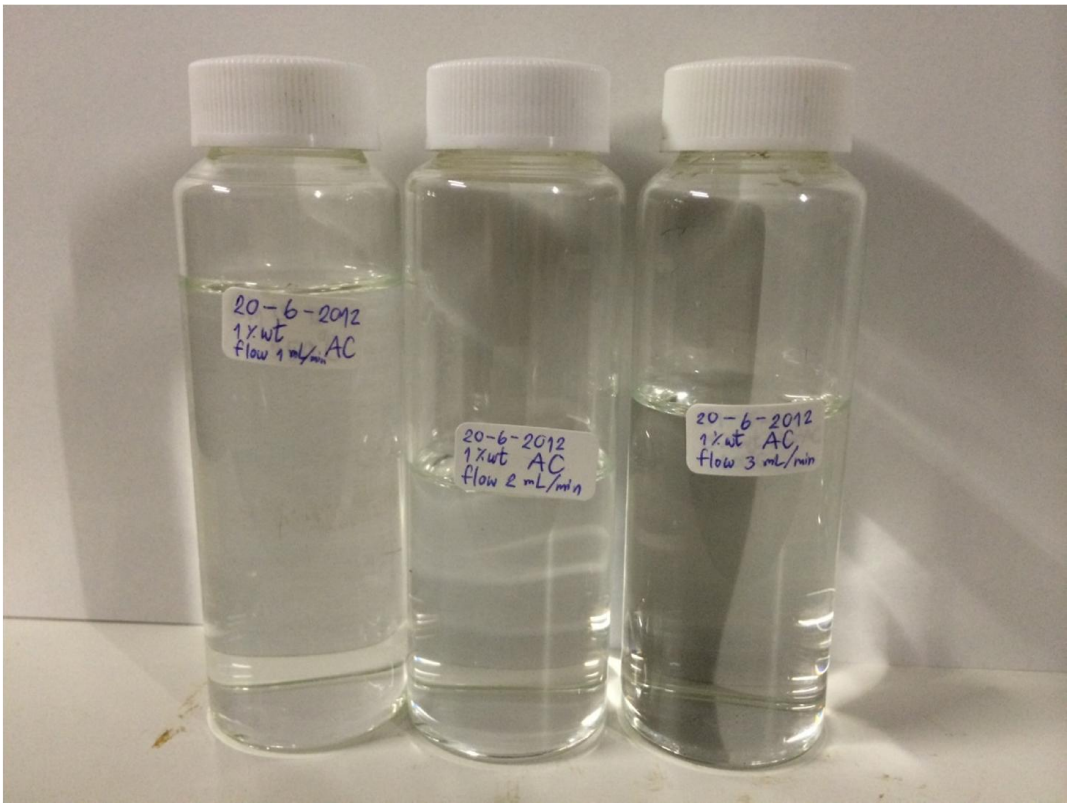

(Left) 1.0 g/min., (Middle) 2.0 g/min., (Right) 3.0 g/min.

Figure 5.6 Liquid samples of experimental on effect of residence time, reaction temperature of 600 ^{o}C, reaction pressure of 25 MPa., and feedstock concentration of 1.0wt%. (a) without Activated carbon (b) with Activated carbon

5.4.3 Effect of reaction temperature

Effect of reaction temperature was studied by changing operated temperature from 500 to 650 ^{o}C and controlled reaction pressure at 25 MPa with fixed glycine concentration of 1.0 wt%. The reaction temperature effect on the carbon gasification efficiency is shown in Figure 5.7. As is characteristic for supercritical water gasification, an increasing temperature leads the efficiency increased significantly. By changing reaction temperature, the residence time had been changed a little in a range of 86 to 119 s. Higher reaction temperature provides a shorter residence time. But the reaction temperature has significant on supercritical water gasification as many works have been done. As previously found, the carbon gasification efficiency of the effect of residence time follows the first order reaction with the sufficient glycine concentration of 1.0 wt%. The same expectation is assumed to the effect study. Assuming the Arrhenius rate law, a pre-exponential factor of 2.73×10^{4} s^{-1} and an activation energy of 106.9 kJ mol^{-1} were obtained from the experimental results without activated carbon.

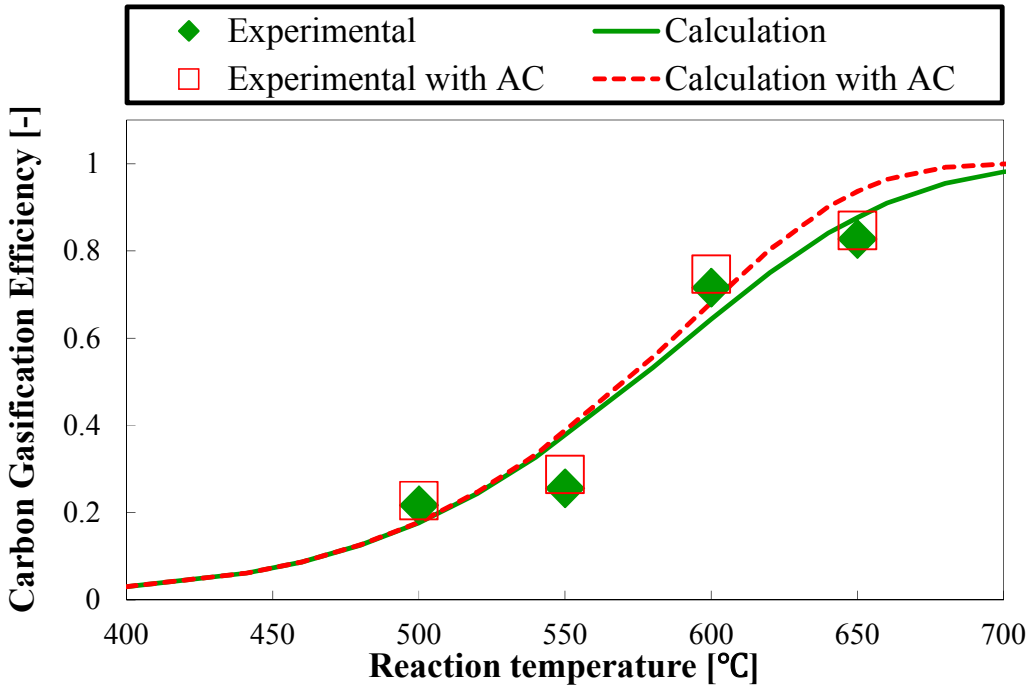

Figure 5.7 Effect of reaction temperature on carbon gasification efficiency, glycine concentration of 1.0 wt%, reaction pressure of 25 MPa, and feedstock flow rate of 2 g/min.

Figure 5.8 shows the Arrhenius plot to show the validity of this assumption. Good agreement between experimental and theoretical results using the Arrhenius parameters was obtained, as shown in Figure 5.7.

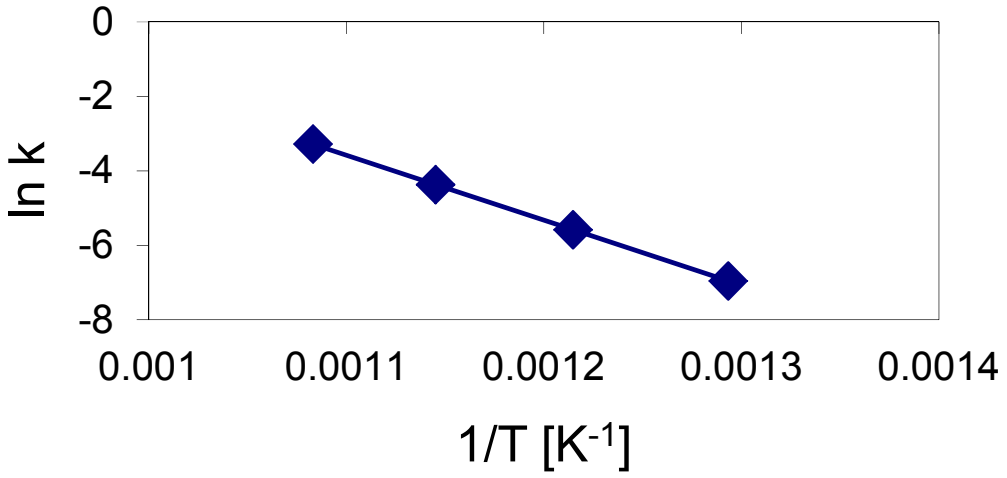

Figure 5.8 Arrhenius plot of the reaction rate constant for glycine gasification without activated carbon

5.4.3.1 Gas Product

The effect of reaction temperature on the gas composition is shown in Figure 5.9. Hydrogen content is not affected by the reaction temperature so much. This may be characteristic to the decomposition of glycine. Thermodynamics predicts higher Hydrogen content for higher temperature. However, to achieve this equilibrium, methane generation has to proceed. Glycine, which is a small molecule with no methyl group, may not easily produce methane. This is just speculation, and further study is wanted.

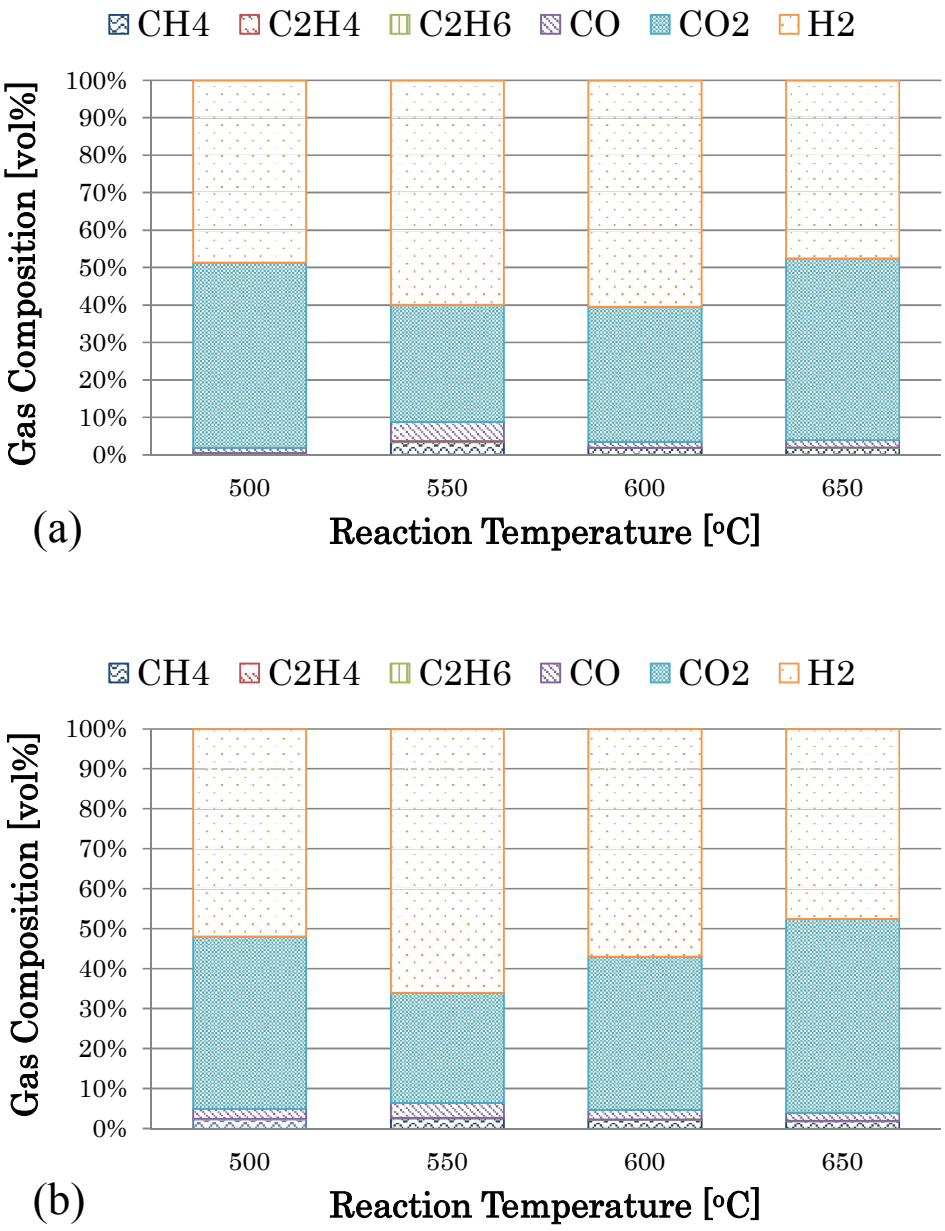

Figure 5.9 Effect of reaction temperature on gas product composition, glycine concentration of 1.0 wt%, reaction pressure of 25 MPa., and feedstock flow rate of 2 g/min. (a) without Activated carbon (b) with Activated carbon

5.4.3.2 Liquid product

All liquid products of the effect of reaction temperature experimental were also quantified the amounts of carbon which is containing in liquid product by a total organic carbon analyzer (TOC). Here again, we did not attempt to identify or quantify individual compounds remaining in the liquid phase. It can be seen that all liquid product is clear, colorless and there is no particle suspense in liquid product as shown in Figure 5.9.

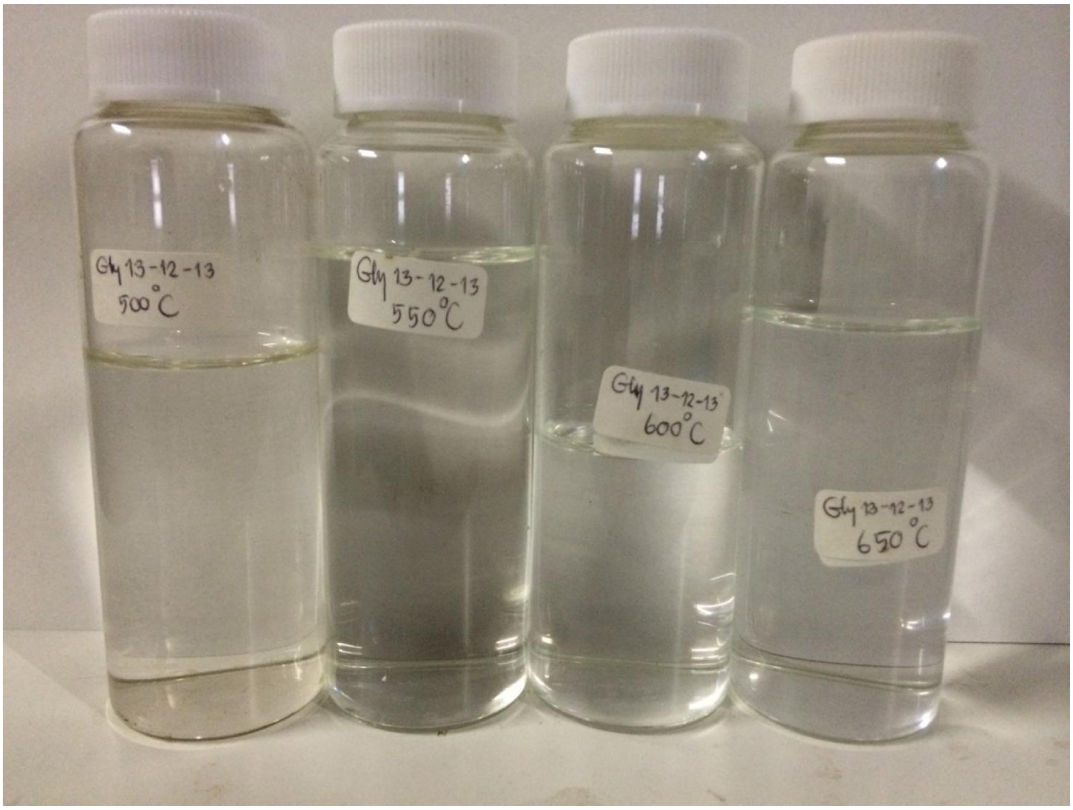

(a) Left : 500°C, Center-left : 550 °C, Center-right : 600 °C, Right : 650 °C

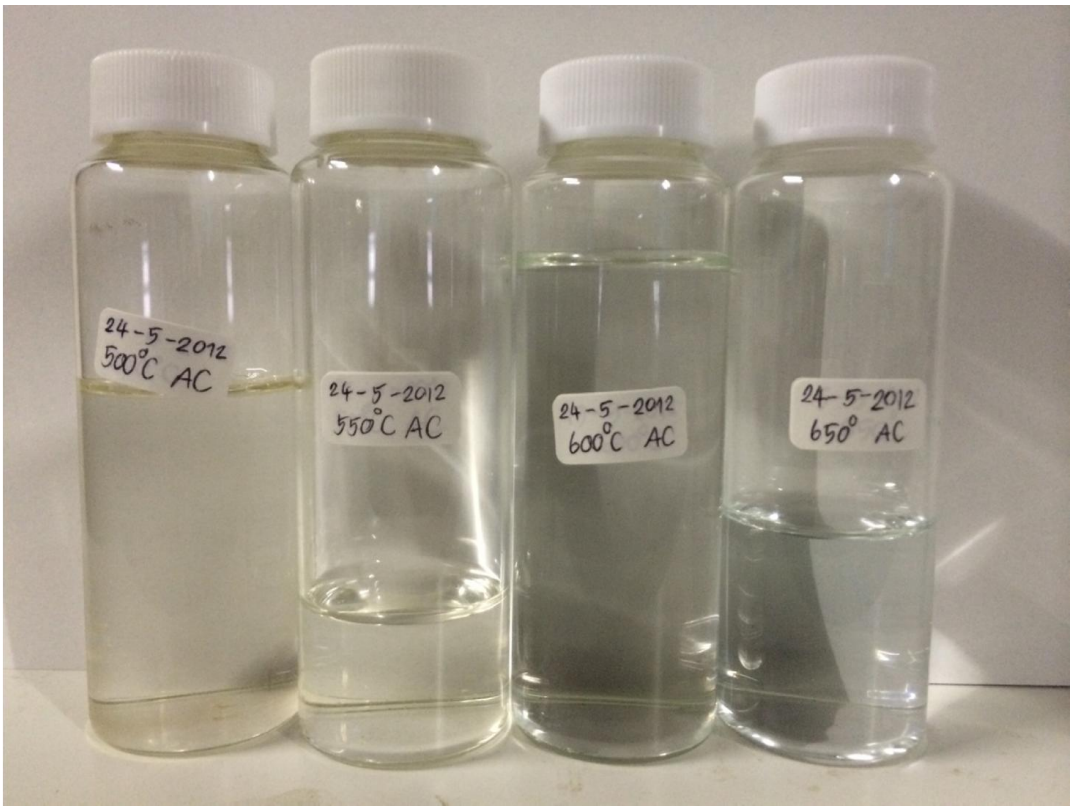

(b) Left : 500°C, Center-left : 550 °C, Center-right : 600 °C, Right : 650 °C

Figure 5.10 Liquid samples of experimental on effect of reaction temperature, reaction pressure of 25 MPa., feedstock concentration of 1.0wt%, feedstock flow rate of 2g/min..

(a) without Activated carbon (b) with Activated carbon

5.4.4 Effect of activated carbon catalyst

To achieve high gasification efficiency, it is known that catalyst is effective. Many works have proved by using various types of catalyst. Activated carbon is one of catalyst kinds that it can be regenerated and environmental friendly. Xu et al., 1996 had shown that glucose gasification in supercritical water conditions was effected by activated carbon catalyst. However, there was recently reported that the effectiveness of this catalyst differs from feedstock to feedstock. Matsumura et al., 2013 reported that it quite limited for fermentation residue feedstock but has been found to be effective for glucose- and cellulose-containing feedstocks. Then, in this work is interest to find out for which biomass materials the activated carbon catalyst is effective. Anyway, there has so far been no report on a systematic investigation to achieve this. Especially, the effect of activated carbon catalyst for the gasification of compounds with heteroatoms, such as proteins, is of interest. Activated carbon powder, used in this work, is shown Figure 5.10. Activated carbon, was used in this work, is made from coconut shell with median particle size of 29 μm, supplied from PDX-1, Kuraray Co., Ltd. and its concentration was fixed at 0.5 wt%.

Figure 5.11 Activated carbon powder made from coconut shell with median particle size of 29 μm supplied from PDX-1, Kuraray Co., Ltd..

As it can be seen in Figure 5.1, Figure 5.4, and Figure 5.6, The effect of activated carbon was found to be negligible, indicating that this particular catalyst is not

effective for enhancing the supercritical water gasification of glycine. Matsumura et al., 2013 classified biomass feedstock into three groups in terms of the effect of activated carbon: high cellulose content, low cellulose content, and lignin-containing, among which the low cellulose content group was not affected by the activated carbon catalyst. Glycine does not include cellulose or lignin, and so is most suited to the low (or no) cellulose content group. The lack of an effect by the carbon catalyst on the glycine feedstock therefore is in agreement with these previous results.

Anyway, the amount of carbon dioxide was found to increase when activated carbon was applied to high feedstock concentration and longer residence time as they are shown in Figure 5.2 and Figure 5.5, respectively. It is possibly due to its effect as catalyst for water gas shift reaction.

The authors did not recover activated carbon from the reactor effluent. Activated carbon can be gasified in supercritical water to produce H_2 and CO_2 as elucidated by Matsumura et al., 1997. Then, the yield of carbon gaseous compounds which is produced from the activated carbon gasification in the reaction was subtracted from the product gas when calculating the carbon gasification efficiency. The

gasification rate of activated carbon catalyst needed for this purpose was determined only sending activated carbon to the reactor.

Remark: In this study, behavior of nitrogen was not followed, because it was beyond the scope of this study that effect of activated carbon is to be verified for glycine gasification, and because hetero atom behavior is difficult to trace by the small scale reactors as was employed in this study.

5.5 Conclusion

The investigation of glycine (representative of amino acid) gasification under supercritical water conditions by using a tubular flow reactor with the variation of parameters supports the following conclusion:

1) When the feedstock concentration was high, carbon gasification efficiency became lower. At a sufficiently low concentration of 1 wt%, the carbon gasification reaction followed the first order reaction rate as it was observed on the effect of residence time.

2) Its reaction rate constant was expressed by the Arrhenius equation well with a pre-exponential factor of 2.73×10^4 s^{-1} and an activation energy of 106.9 kJ mol^{-1}.

The gaseous product was constituted of Hydrogen, Methane, Carbon dioxide, Carbon monoxide, and a small amount of Ethene and Ethane. The effect of operation parameters on its composition agreed with the thermodynamic predictions.

3) The activated carbon catalyst was found to be ineffective for glycine.

Note that there is no particle observed and remained in filter and liquid-solid separator for all experimental runs of each effect study.

CHAPTER 6

Effect of methyl functional group on supercritical water gasification of amino acid

6.1 Introduction

Previously, Promdej et al., 2010 has found the reaction mechanism of biomass gasification in supercritical water by using the relation between kinetic rate and

temperature. For the reactions between intermediates, radical and ionic reactions were distinguished by their conformity to Arrhenius behavior (Promdej et al., 2010, Promdej and Matsumura, 2011 and Yong and Matsumura, 2013). Anyway, the prediction of gasification rate in supercritical water is still difficult, and it is a major problem in reactor design. It is expected that the molecular structure should have some effect on the reaction rate, since it surely affects the first decomposition of the molecule. Since we have already measured the gasification rate of glycine, a model protein compound, in supercritical water conditions with the variation of parameters as already described in Chapter 5. The determination of gasification of other amino acids and comparison of their gasification rates would be interesting. In particular, if we can compare the two similar compounds that differ by only one functional group, it might give some insight into the effect of the functional group on decomposition rate in supercritical water. Thus, the purpose of this study is to compare the gasification rate of glycine and alanine. By gasifying alanine, which is different from glycine by one methyl group, the effect of the methyl group would be clarified. Figure 6.1 shows molecules structure of glycine and alanine.

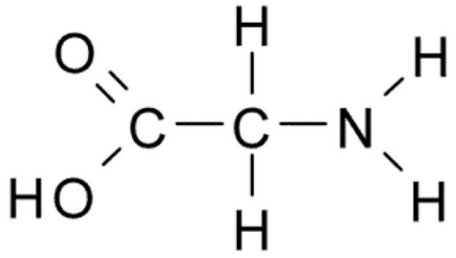

Glycine

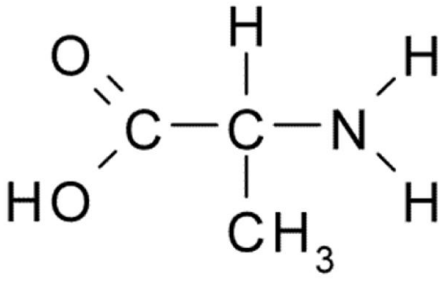

Alanine

Figure 6.1 Molecules structure of glycine and alanine, different by one methyl group

6.2 Experimental procedures

The details of the procedures and the continuous flow reactor used this this study have been describe in Chapter 4. Briefly, deionized water was only fed into the equipment by high pressure pump in order to make the system pressure up to 25 MPa. The tubular reactor was heated and reached to the desired temperature before the feedstock was fed. Alanine was mixed with deionized water to the desired concentration. The reactor, which is used in this study, is the same as previous study in Chapter 5. But it is no activated carbon catalyst added into the alanine solution. The loader and the piston pump had been cut. Then, the experimental apparatus has been revised as shown in Figure 6.2.

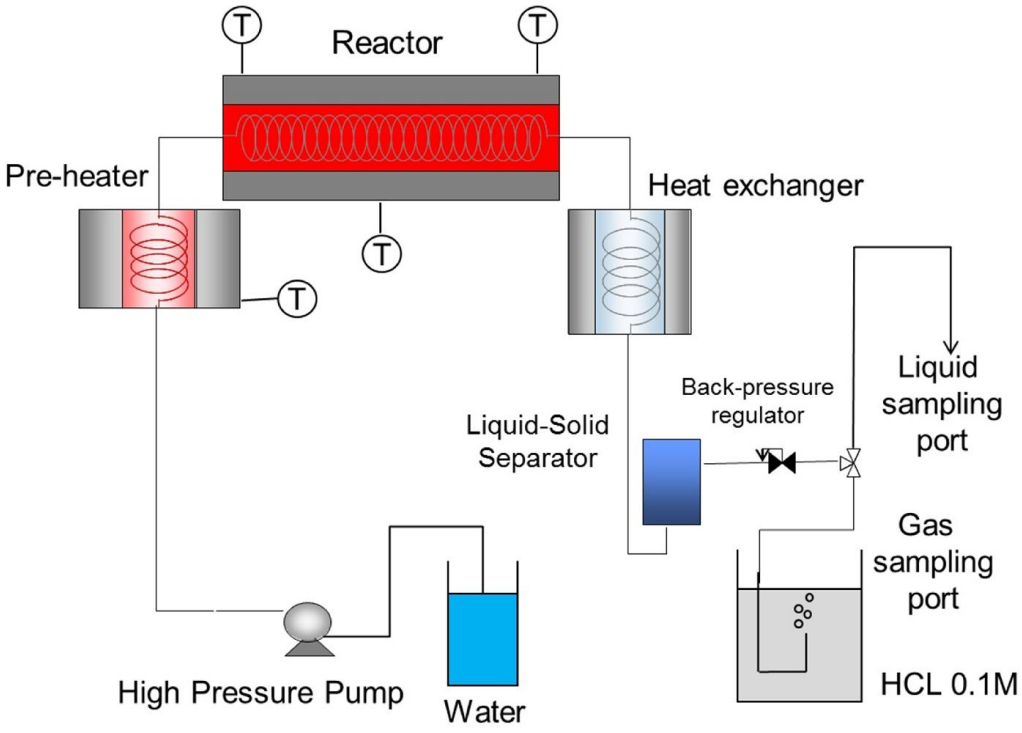

Figure 6.2 Experimental apparatus (cut off loader and piston pump, directly feed to the system)

The alanine aqueous solution was directly fed into the system by a high-pressure pump at a feedstock flow rate of 2 g/min. The reaction temperature was varied from 500 to 650 ^{o}C (residence times in a range of 86–119 s) and reaction pressure was controlled at 25 MPa. After feedstock passed through the reactor, the effluent product was cooled by a heat exchanger. Solid product, if it has, was separated by sedimentation at liquid-solid separator then filtrated by filter. After that, the effluent

was depressurized by a back pressure regulator, and then sampled. At the liquid sampling port, the liquid effluent with dispersed solid particle was collected. The gas product was collected under 0.1 M of HCl. The rate of gas production was measured by the time for effluent gas to fill a vial of known volume by water replacement. The gas product was also sampled and further qualified the composition.

Gas chromatography (GC), Shimadzu GC-14B, Japan, is used for product gases analysis. GC-TCD, a thermal conductivity detector GC, will detect CO_2 and CO with He as the carrier gas. GC-FID, a flame ionization detector GC will detect CH_4, C_2H_4, and C_2H_6 with He as the carrier gas. GC-TCD with N_2 as the carrier gas will detect H_2.

Liquid product was quantified the amount of carbon which is containing in liquid product (NPOC) and in the dissolved gas product (IC) by a total organic carbon analyzer (TOC). Dissolved gas product, IC value, that was detected by TOC refers to CO_2 which can be dissolved into liquid phase for a while. Then this IC value could be included with gas product which is measured by GC to calculate the carbon gasification efficiency.

6.3 Experimental conditions

Alanine gasification experimental runs were performed using the experimental conditions which are shown in Table 6.1

Table 6.1. Experimental conditions for the alanine gasification

Feedstock	Alanine
Feedstock concentration	1.0, 2.0, and 3.0 wt%
Reaction temperature	500 - 650 ^{o}C
Reaction pressure	25 MPa
Feedstock flow rate	2.0 g/min
Residence time	119, 108, 94, and 86 s
Catalyst	No catalyst
Reactor type	Tubing flow reactor
Reactor length	12 m

6.4 Results and discussion

To elucidate the effect of methyl group on supercritical water gasification of alanine, the results of glycine gasification has been also shown in this study. The appearance of methyl group in supercritical water gasification would be clarified. The effect of methyl group in alanine can be shown by gasifying alanine with the study of alanine concentration (1.0, 2.0, and 3.0 wt%) and reaction temperature (500 – 650^{o}C) and compare with those results of glycine. Noted, the alanine experimental was repeated at least three times.

The carbon gasification efficiency (CGE) of all experiments are calculated based on of the carbon content in glycine solution feedstock as it has defined in below equation:

$$CGE = \frac{n_{Cg}}{n_{C0}} = \frac{n_{Cgas} + n_{IC}}{n_{C0}} \tag{6.1}$$

where n_{C0} = initial amount of carbon [mol],

n_{Cg} = total amount of gasified carbon [mol],

n_{Cgas} = amount of carbon in gaseous products [mol],

n_{IC} = amount of inorganic carbon in the liquid products [mol].

6.4.1 Effect of alanine concentration

The experiment was conducted for alanine concentrations of 1.0, 2.0, and 3.0 wt% under 25 MPa, 600 ^{o}C and feedstock flow rate was controlled at 2 g/min. that provides a residence time of 94 s. The effect of alanine concentration on carbon gasification efficiency is shown in Figure 6.3. Figure 6.3 has also shown the results of glycine for comparison.

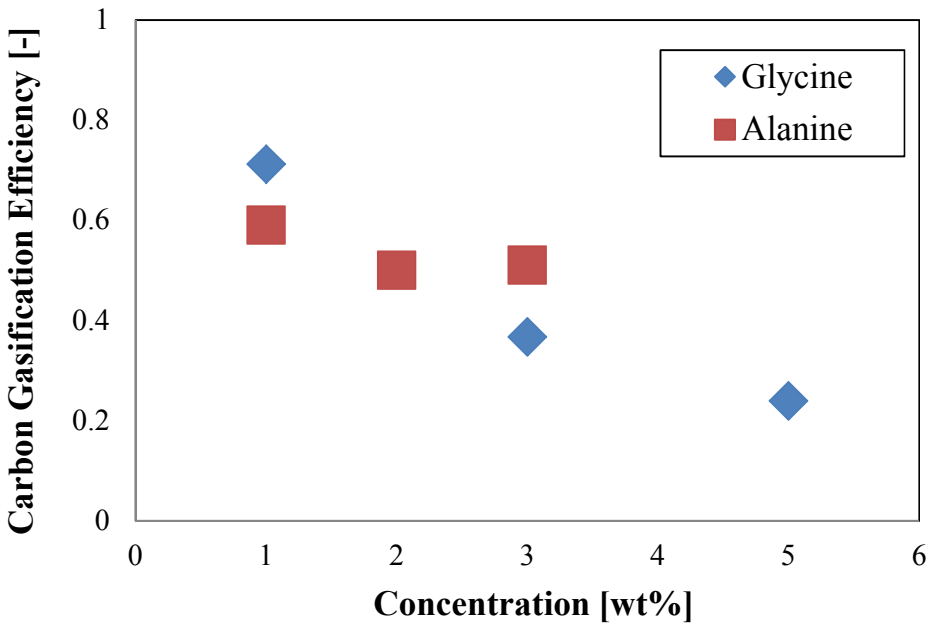

Figure 6.3 Effect of alanine concentration on carbon gasification efficiency compares with glycine's, reaction temperature of 600 ^{o}C, reaction pressure of 25 MPa., and feedstock flow rate of 2 g/min.

The carbon gasification efficiency of alanine is not affected by the increasing alanine concentration employed here, which corresponds to first order behavior. For the case of glycine, the carbon gasification efficiency decreased with concentration. This is expected to be due to tarry material production at high concentrations. It is known that the order of the reaction for tarry material production is higher than unity for the case of glucose (Chuntanapum and Matsumura, 2011). The same can be expected for amino

acids. To determine the gasification characteristics, the effect of tarry material production should be omitted. It is not possible to completely get rid of it, but judging from the effect of residence time, 1.0 wt% was found to be sufficiently dilute so that the gasification characteristics is expressed as a first order reaction with a small error as it has already described and shown in Chapter 5. For the case of alanine, the effect of tarry material production is negligible, and we can safely assume first order kinetics. Maybe the methyl group has the ability to suppress tarry material production.

6.4.1.1 Gas Product

The effect of alanine concentration on gas composition is shown in Figure 6.4. No activated carbon catalyst has been used in this study.

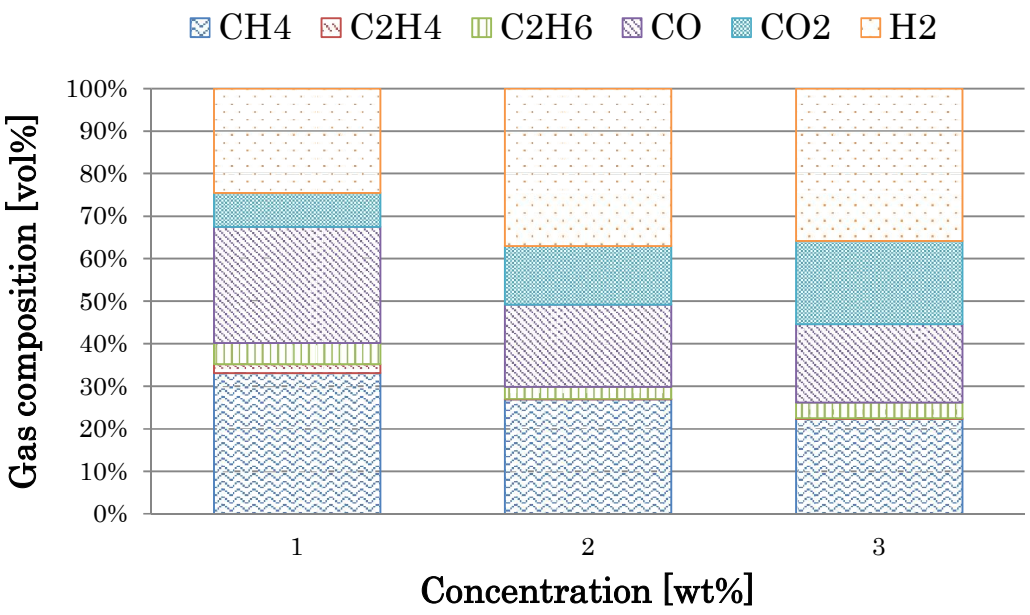

Figure 6.4 Effect of alanine concentration on product gas composition, reaction temperature of 600 ^{o}C, reaction pressure of 25 MPa., and feedstock flow rate of 2 g/min.

Thermodynamics predicts that little carbon monoxide is to be found due to the water-gas shift reaction with the existence of large amounts of water, but carbon monoxide is observed because the water gas shift reaction is slow, and has not reached equilibrium. Increase in feedstock concentration results in increased hydrogen and carbon dioxide yields. Remembering that increase in feedstock concentration did not affect the carbon gasification efficiency, increase in hydrogen and carbon dioxide yields implies the proceeding of the water-gas shift reaction. A corresponding reduction in

carbon monoxide yield supports this idea. Considering that amino groups can produce ammonia or amine molecules, what we observed ammonium ion in our liquid samples, the alkalinity of the liquid should also increase with feedstock concentration. This alkali might have functioned as the catalyst for the water gas shift reaction. Alkali stabilizes the carbon dioxide, and enhanced water gas shift reaction is expected.

6.4.1.2 Liquid product

Liquid products of all experimental were only quantified the amount of carbon which is containing in liquid product (NPOC) and in the dissolved gas product (IC) by a total organic carbon analyzer (TOC). Figure 6.5 shows the liquid product of alanine gasification on the effect of alanine concentration. Note that there is no particle observed and remained in filter and liquid-solid separator for all experimental runs of each effect study. At concentration of 3.0wt% of alanine, liquid product is yellowish but is still clear, no solid particle suspense. The yellowish in higher concentration may cause char formation from Mailard products (Minowa et al., 2004; Kruse et al., 2005 and 2007).

Figure 6.5 Liquid samples of experimental on effect of alanine concentration, reaction temperature of 600 oC, reaction pressure of 25 MPa., feedstock flow rate of 2g/min.

6.4.2 Effect of reaction temperature

Alanine concentration was used at 1.0 wt%. The reaction temperature was changed from 500 to 650 ^{o}C and controlled reaction pressure at 25 MPa to determine the effect of reaction temperature. The feedstock flow rate had been fixed at 2 g/min. By changing reaction temperature and fixed the flow rate, the residence time had been changed a little in a range of 86 to 119 s. Figure 6.6 shows the reaction temperature effect on the carbon gasification efficiency. The carbon gasification efficiency results

of 1.0 wt% glycine have also shown in Figure 6.6 in order to compare with those of alanine. Glycine gasification was conducted four times, and alanine gasification was conducted three times to obtain sufficient reproducibility.

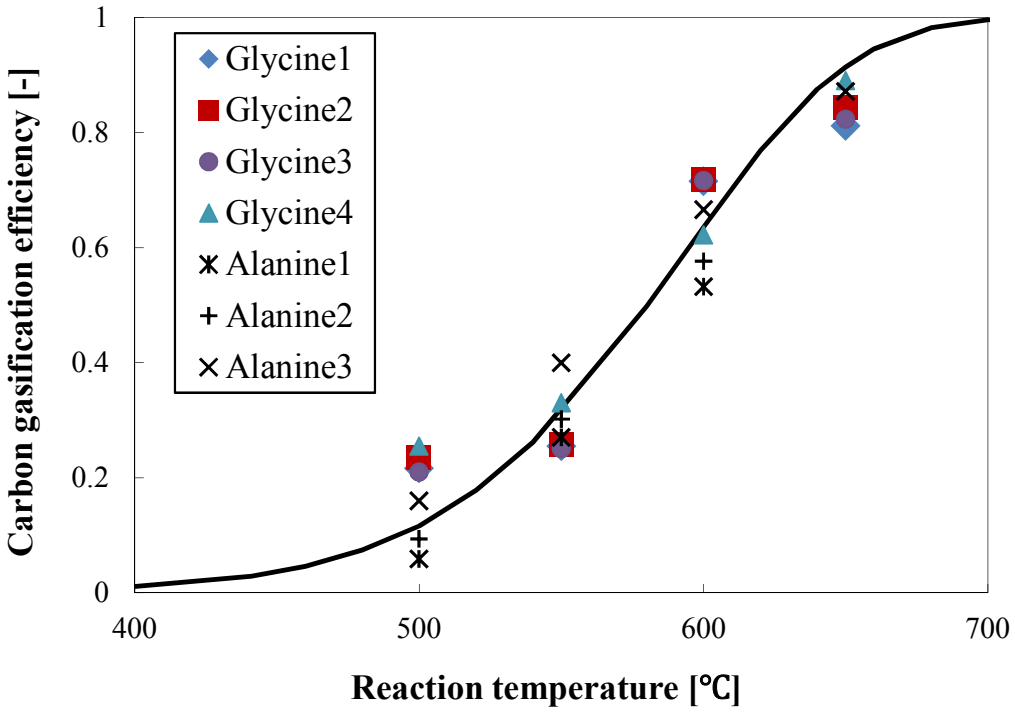

Figure 6.6 Effect of reaction temperature on carbon gasification efficiency, glycine and alanine

The carbon gasification efficiency increases with reaction temperature. As is characteristic for supercritical water gasification, the efficiency increases significantly

with increasing temperature, as was observed for glucose by Xu et al., 1996, and Xu and Antal, 1997.

Considering the experimental error of the carbon gasification efficiency, the gasification rates of glycine and alanine are identical. This fact implies that the methyl group in alanine does not have a significant effect on carbon gasification efficiency. One of the possibilities is that the carboxyl group, which is common to both glycine and alanine, is reacting first. Since the carbon atom is not strongly electrophilic or nucleophilic, the methyl group will not affect the reactivity of the carboxyl group. This mechanism can explain why the methyl group does not affect the carbon gasification rate.

Assuming that the gasification reaction rate is first order in terms of the feedstock carbon amount, and assuming the Arrhenius rate law, the following equation is obtained.

$$\frac{dn_{Cg}}{dt} = k_0 \left\{ \exp\left(\frac{-E_a}{RT} \right) \right\} \left(n_{C0} - n_{Cg} \right) \tag{6.2}$$

which leads to

$$n_{C0} - n_{Cg} = n_{C0} \exp\left[-k_0 \left\{ \exp\left(\frac{-E_a}{RT} \right) \right\} t \right] \tag{6.3}$$

$$CGE = \frac{n_{Cg}}{n_{C0}} = 1 - \exp\left[-k_0 \left\{ \exp\left(\frac{-E_a}{RT} \right) \right\} t \right] \tag{6.4}$$

where n_{C0} = initial amount of carbon [mol],

n_{Cg} = amount of gasified carbon [mol],

k_0 = pre-exponential factor [s^{-1}],

E_a = activation energy [J mol^{-1}],

R = gas constant [J mol^{-1} K^{-1}],

T = Temperature [K],

t = time [s]

and CGE = carbon gasification efficiency [-].

The parameters in Eq. (6.4) were determined by fitting to the experimental data. Assuming the same reaction rate, the pre-exponential factor and the activation energy of glycine and alanine were determined to be 7.37×10^5 s^{-1} and 131 kJ/mol, respectively. The fitting result using these parameters is also shown in Figure 6.6. Good agreement between experimental and calculation results are obtained.

6.4.2.1 Gas Product

Gas composition of alanine gasification as a function of reaction temperature is shown in Figure 6.7. The product gas composition for glycine is also shown for comparison purposes. It is clear that in comparison to glycine, alanine results in a higher yield of methane. This methane would have been produced from the methyl group. Another clear difference between glycine and alanine is that water gas shift reaction proceeds to a greater extent for glycine. Since both amino acid solutions were created at 1 wt%, and considering that molecular weight is smaller for glycine, the number of nitrogen atoms is higher for the case of glycine; thus, a stronger alkali effect is expected. Again, the alkali can stabilize carbon dioxide, resulting in a greater progress of the water gas shift reaction.

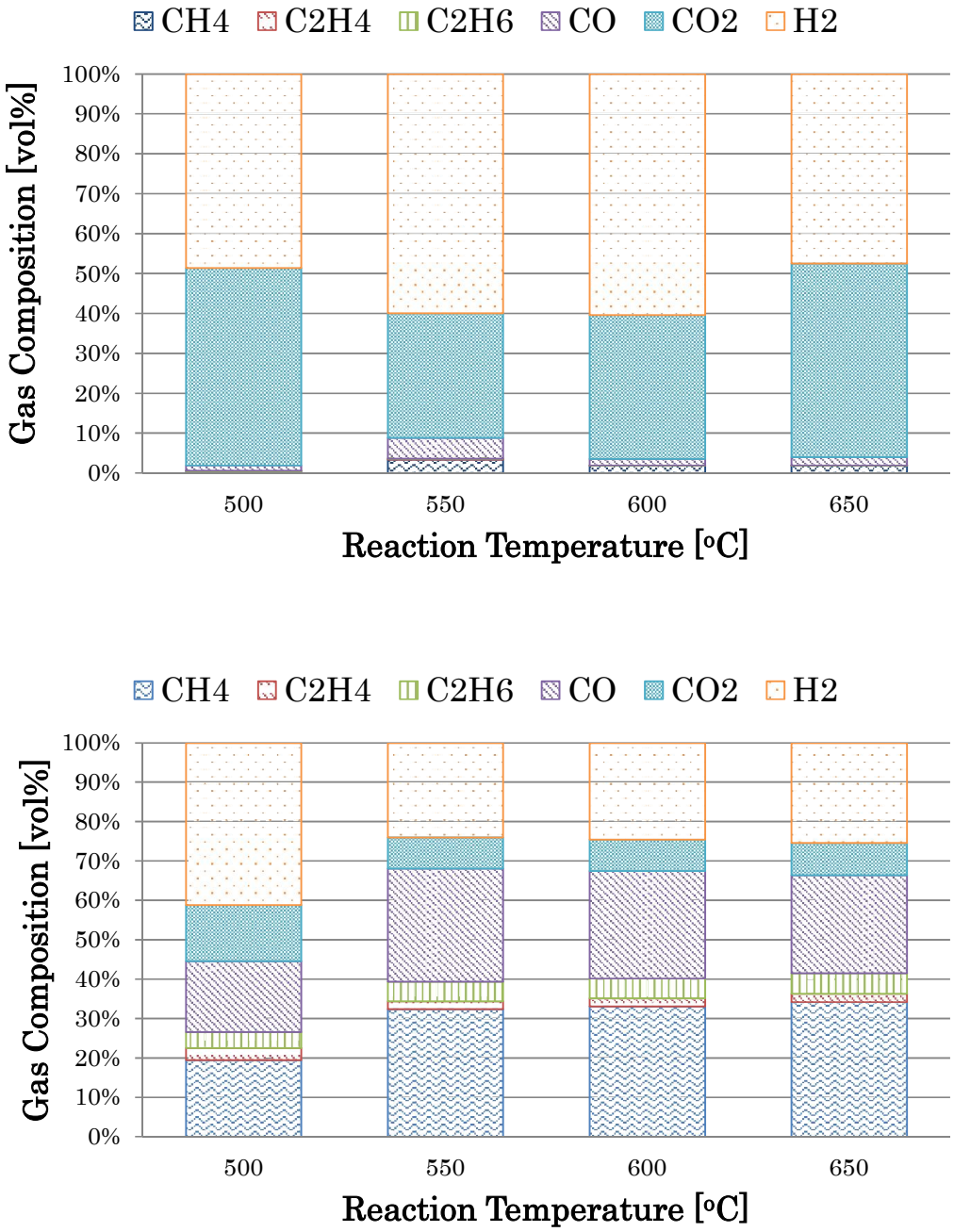

Figure 6.7 Effect of reaction temperature on product gas composition of glycine and alanine gasification at 1 wt% of concentration, 25 MPa and 2 g/min of flow rate.

In this respect, the effect of the methyl group in alanine should be two-fold: 1. it is converted into methane, and 2. it dilutes nitrogen so that the alkaline effect is suppressed. The former explains the higher methane yield, whereas the latter results in the high carbon monoxide yield.

6.4.2.2 Liquid Product

Liquid products of the effect of reaction temperature experimental were also quantified the amount of carbon which is containing in liquid product (NPOC) and in the dissolved gas product (IC) by a total organic carbon analyzer (TOC). At lower reaction temperature, it can be seen that liquid product is yellowish but it is going to be lighter and colorless when was treated at higher reaction temperature as it is shown in Figure 6.8. The yellow color of liquid product at lower reaction temperature may cause from char. Here again, we did not attempt to identify or quantify individual compounds remaining in the liquid phase.

Note that there is no particle observed and remained in filter and liquid-solid separator for all experimental runs of each effect study.

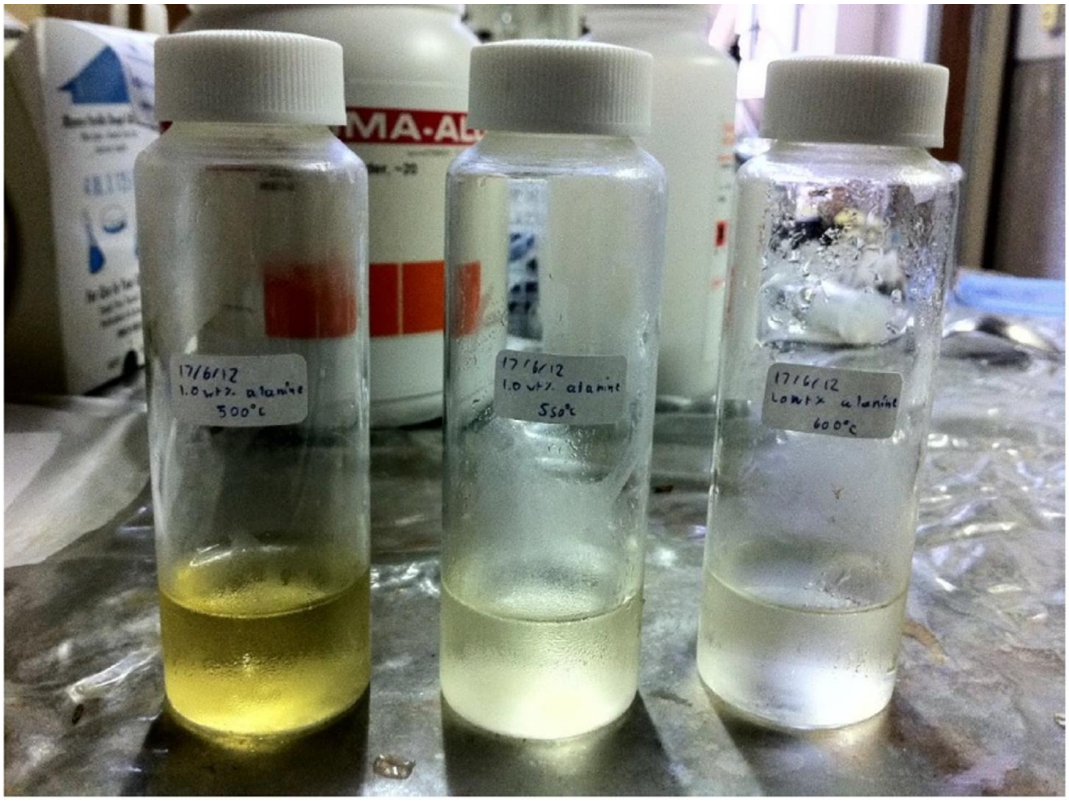

Figure 6.8 Liquid samples of experimental on effect of reaction temperature, reaction pressure of 25 MPa., feedstock concentration of 1.0wt%, feedstock flow rate of 2g/min.

6.4.3 Effect of methyl functional group

As it has already determined the effect of alanine concentration and the effect of reaction temperature on alanine gasification compared with those of glycine. It is clear that the methyl group in alanine does not have a significant effect on carbon gasification efficiency. It might due to the carboxyl group, which is common to both

glycine and alanine, is reacting first. And the carbon atom is not strongly electrophilic or nucleophilic, the methyl group will not affect the reactivity of the carboxyl group. This mechanism can explain why the methyl group does not affect the carbon gasification rate. Then, the gasification rate of glycine and alanine are determined to be identical.

The effect of methyl group on product gas composition, as it has shown in Figure 6.7 that alanine results in a higher yield of methane. This methane have been produced from the methyl group. Water gas shift reaction proceeds to a greater extent for glycine which is another clear difference between glycine and alanine. As both amino acid solutions, glycine and alanine, were prepared at 1 wt% concentration, and considering that molecular weight of glycine is smaller, the number of nitrogen atoms is higher for the case of glycine; thus, a stronger alkali effect is expected. Again, the alkali can stabilize carbon dioxide, resulting in a greater progress of the water-gas shift reaction.

Considering, the effect of the methyl group in alanine should be provides into 2 steps. First, it is converted into methane, and second, it dilutes nitrogen. Thus, the alkaline effect is suppressed. The former explains the higher methane yield, whereas the latter results in the high carbon monoxide yield.

6.5 Conclusion

Gasification of alanine was conducted using a tubular flow reactor. When the feedstock concentration was high, the carbon gasification efficiency does not much change, but 1.0 wt% of glycine is sufficiently dilute for gasification. The carbon gasification reaction of alanine followed first order kinetics. Gasification rate is identical for both glycine and alanine, and the reaction rate parameters were determined. Its reaction rate constant was expressed by the Arrhenius equation well by a pre-exponential factor of 7.37×10^{5} s^{-1} and an activation energy of 131 kJ mol^{-1}. The gaseous product was constituted of Hydrogen, Methane, Carbon dioxide, Carbon monoxide, and a small amount of Ethene and Ethane. The effect of the methyl group in alanine is the production of methane, and the dilution of nitrogen so that the alkaline effect is suppressed. The former explains the higher methane yield, whereas the latter results in the high carbon monoxide yield.

Note that there is no particle observed and remained in filter and liquid-solid separator for all experimental runs of each effect study.

CHAPTER 7

Gasification characteristics of aliphatic amino acids in supercritical water conditions

7.1 Introduction

As we have already described the effect of methyl group in Chapter 6 and it shows that methyl group in alanine molecule has no effect. The gasification efficiency

of glycine and alanine has been showed to be practically the same. There are more three amino acids that are in the same aliphatic class as glycine and alanine which are valine, leucine, and iso-leucine. Amino acids in aliphatic class differ by functional groups that are hydrogen for glycine, methyl for alanine, propyl for valine, and butyl for leucine. Figure 7.1 shows molecule structure of valine and leucine.

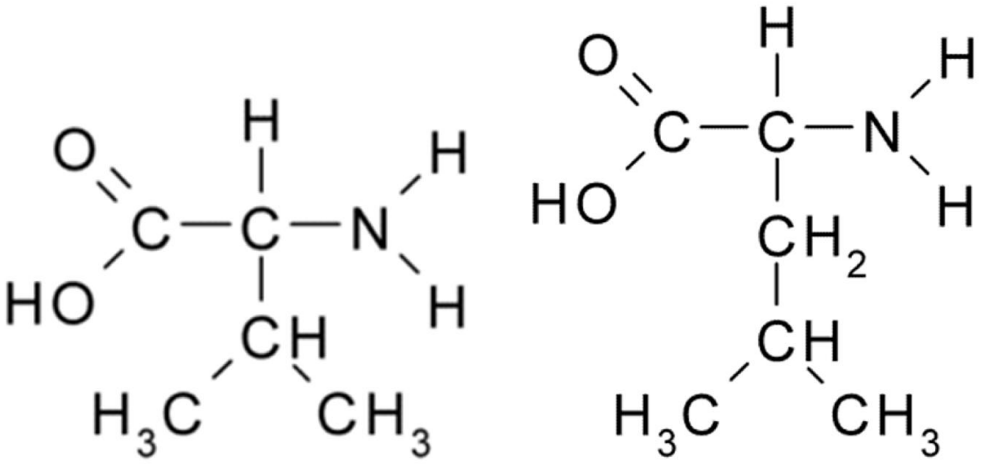

Valine Leucine

Figure 7.1 Molecules structure of valine and leucine, different by one functional group and classified into aliphatic group

If other amino acids also incur gasification at the same rate, it could be able to apply this gasification rate to other amino acids safely and likely proteins as well. Thus,

valine and leucine have been chosen to determine their gasification characteristics in supercritical water conditions and also compared to those of glycine and alanine.

7.2 Experimental procedures

As it has been described the continuous flow reactor and procedures in previous, Chapter 4, this effect study used practically the same experimental apparatus and procedures. Briefly, the valine and leucine feedstock solution were prepared to desirable concentration by dissolving commercially obtained amino acids in deionized water. The experiments involved delivery of an aqueous solution of the both amino acids into a tubular SS316 steel reactor (inner diameter: 2.17 mm, length: 12 m) at a controlled feedstock flow rate of 2 g/min using a high-pressure pump, feeding directly the same as it is shown and described in Chapter 6. After decomposition of the amino acids at reaction temperature in a range of 500–650 °C and 25 MPa in the reactor, the effluent was cooled down by a heat exchanger, depressurized using a back-pressure regulator, and then sampled. The residence time in the reactor ranged from 86 to 119 s depending on the reaction temperature. The gas-generation rate was determined using the time required for the effluent gas to fill a vial of known volume by water replacement under 0.1M of HCl solution.

The gaseous product was qualified and quantified by a gas chromatography (GC) installed with TCD and FID. GC-TCD, a thermal conductivity detector GC, will detect CO_2 and CO with He as the carrier gas. GC-FID, a flame ionization detector GC will detect CH_4, C_2H_4, and C_2H_6 with He as the carrier gas. GC-TCD with N_2 as the carrier gas will detect H_2. Liquid product was quantified the amount of carbon which is containing in liquid product. Note that the IC value from TOC refers to CO_2 which can be dissolved into liquid phase for a while. Then this IC value could be included with gas product which is measured by GC to calculate the carbon gasification efficiency.

Note that there is no particle observed and remained in filter and liquid-solid separator for all experimental runs in this study.

Carbon gasification efficiency is defined as the ratio of the molar amount of carbon in the gas product to that carbon content in the feedstock solution as it has been described in Chapter 6, equation (6.1).

7.3 Experimental conditions

Valine and leucine gasification experimental runs were performed using the experimental conditions which are shown in Table 7.1.

Table 7.1. Experimental conditions for the valine and leucine gasification

Feedstock	Valine and Leucine
Feedstock concentration	1.0 wt%
Reaction temperature	500 - 650 ^{o}C
Reaction pressure	25 MPa
Feedstock flow rate	2.0 g/min
Residence time	119, 108, 94, and 86 s
Catalyst	No catalyst
Reactor type	Tubing flow reactor
Reactor length	12 m

7.4 Results and discussion

To determine the gasification characteristics of valine and leucine in supercritical water condition, the effect of reaction temperature has been used to

clarified by varying in a range of 500 – 650 ^{o}C as same as our previous study. The results of glycine and alanine gasification have also shown in this Chapter for comparison purpose.

As we have found decomposition of glycine and alanine in this reaction temperature region followed the first order reaction rate (Samanmulya and Matsumura, 2013 and Samanmulya et al., 2014), we assumed that the gasification reaction rate is first-order with respect to the amount of carbon feedstock here too. Using the Arrhenius rate law for the reaction rate constant, the following equation can be obtained:

$$\frac{dn_{Cg}}{dt} = k_0 \left\{ \exp\left(\frac{-E_a}{RT} \right) \right\} \left(n_{C0} - n_{Cg} \right). \tag{7.1}$$

This equation leads to

$$n_{C0} - n_{Cg} = n_{C0} \exp\left[-k_0 \left\{ \exp\left(\frac{-E_a}{RT} \right) \right\} t \right] \tag{7.2}$$

And $$CGE = \frac{n_{Cg}}{n_{C0}} = 1 - \exp\left[-k_0 \left\{ \exp\left(\frac{-E_a}{RT} \right) \right\} t \right], \tag{7.3}$$

where n_{C0} is the initial amount of carbon [mol],

n_{Cg} is the amount of gasified carbon [mol],

k_0 is the pre-exponential factor [s^{-1}],

E_a is the activation energy [J mol^{-1}],

R is the gas constant [J mol^{-1} K^{-1}],

T is the temperature [K],

t is the time [s],

and CGE is the carbon gasification efficiency [-].

7.4.1 Gasification characteristics of valine

Figure 7.2 shows the carbon gasification rate of valine relative to the previous reported results for glycine and alanine. The results are shown as the carbon gasification efficiency at each temperature. Considering, the gasification rates of glycine and alanine are practically identical (Samanmulya et al., 2014). Unexpectedly, and to our disappointment, the gasification rate of valine is much lower than that of glycine and alanine. This is attributed to the effect of the isopropyl functional group. Glycine, alanine, and valine vary only in the functional group that is attached to the alpha carbon, i.e., hydrogen, methyl, and isopropyl, respectively. Previous study showed that radical reaction is favored under the reaction conditions employed in this study (Promdej and

Matsumura, 2011). The parameters in Eq. (7.3) were determined by fitting the resulting carbon gasification efficiencies to the experimental data and also shown in Figure 7.2. The resulting pre-exponential factors and activation energies of the valine are 6.97×10^{1} s^{-1} and 70 kJ/mol, respectively.

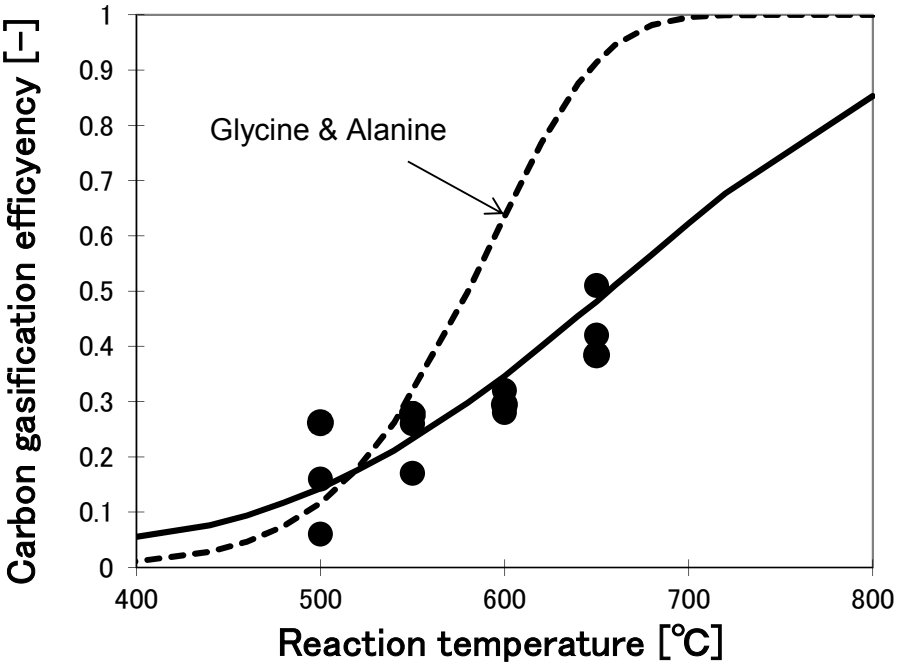

Figure 7.2 Gasification characteristics of valine compares with that of glycine and alanine

Decomposition of the amino acid most likely leads to the production of hydrogen, methyl, and isopropyl radicals from the corresponding amino acids, as shown in Figure 7.3.

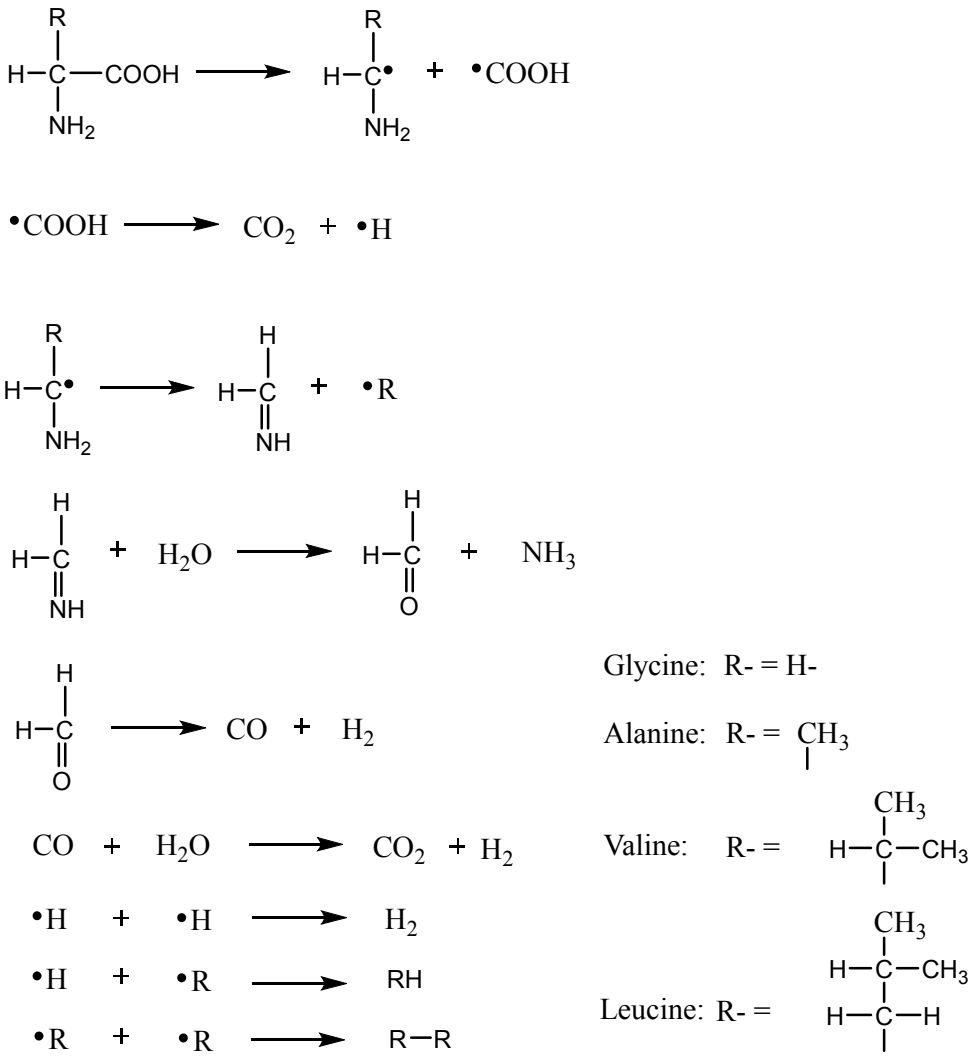

Figure 7.3 Reaction scheme of amino acids decomposition, glycine, alanine, valine, and leucine

These radicals have quite different reactivities: Hydrogen and methyl radicals are much more reactive than isopropyl radicals and rapidly react with other radicals or molecules. Since hydrogen and methyl radicals are small and the product of the radical

reaction can be gaseous, e.g., hydrogen, methane, and ethane, their reactivity leads to a high carbon-gasification efficiency. In contrast, isopropyl radicals are secondary radicals, which are relatively stable; therefore, they can exist longer than hydrogen or methyl radicals allowing them to interact with other heavy radicals to produce tarry material. In addition, the reaction of isopropyl radicals with each other generates 2,3-dimethylbutane, which is a liquid-phase product. The formation of this bulky molecule could lead to the production of polymers, as shown in Figure 7. 4, because radicals of higher carbon numbers are more stable than smaller radicals and are relatively easily produced.

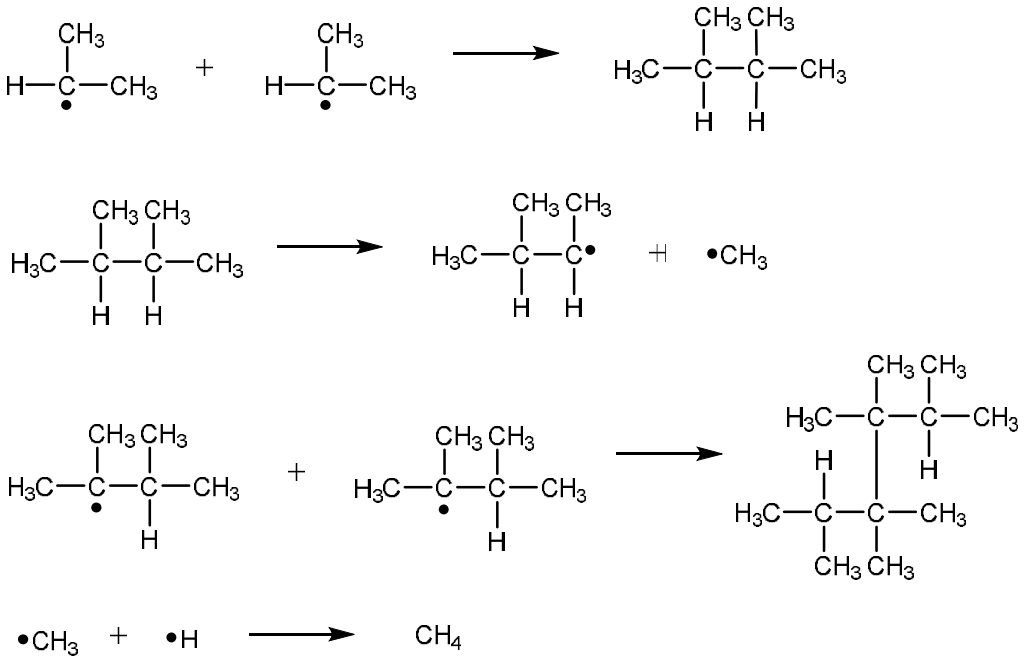

Figure 7.4 Reaction of isopropyl radical of valine

7.4.1.1 Gas product

The composition of the effluent gas also supports this hypothesis. Figure 7.5 shows the composition of the gases generated from glycine, alanine, and valine. Gasification of glycine should generate carbon dioxide and hydrogen, as shown in Figure 7. 3 (R = H), at a ratio of 3 to 2, as observed in Figure 7.5, leaving ammonia in the water phase. Accordingly, gasification of alanine should generate methane and ethane in addition to hydrogen and carbon dioxide, as demonstrated in Figure 7.3 (R = CH_3). These gases were experimentally observed. Gasification of valine results in a significant amount of methane in the product gas, which indicates that the methyl radical production shown in Figure 7.4 does occur.

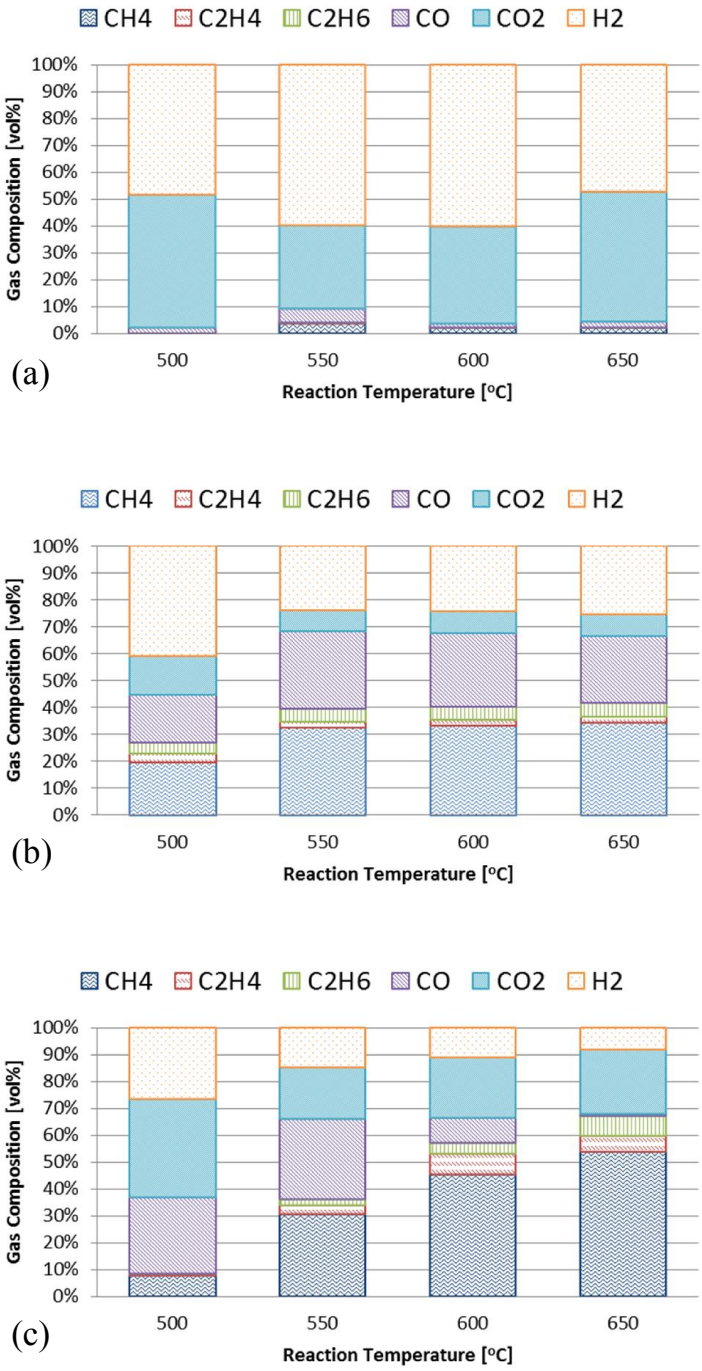

Figure 7.5 Effect of reaction temperature on product gas composition, (a) Glycine (b) Alanine (c) Valine, concentration of 1.0 wt%, 25 MPa, and flow rate of 2 g/min.

7.4.2 Gasification characteristics of leucine

Figure 7.6 shows the gasification characteristics of leucine in supercritical water. Noticeably, the gasification rate of leucine is much faster than that of valine and similar to those of glycine and alanine. Thus, an increase in the carbon number on the functional group from three in valine to four in leucine results in a faster gasification rate. This is attributed to the effect of the isobutyl functional group: The isobutyl group of leucine will produce an isobutyl radical, as shown in Figure 7.3, which is a primary radical and less stable than a secondary radical. The parameters in Eq. (7.3) were determined by fitting the resulting carbon gasification efficiencies to the experimental data and also shown in Figure 7.6. The resulting pre-exponential factors and activation energies of the leucine are 7.37×10^{1} s^{-1} and 135 kJ/mol, respectively.

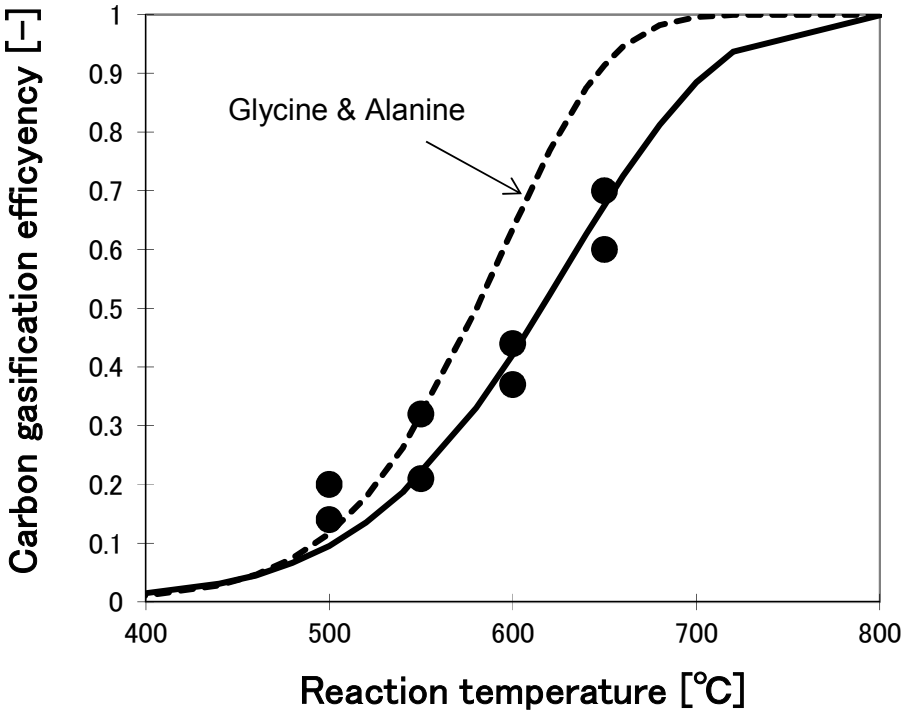

Figure 7.6 Gasification characteristics of leucine compares with that of glycine and alanine

Accordingly, it can react with water to produce isopropyl alcohol, as shown in Figure 7.7. The methyl radical can be removed, which generates methane.

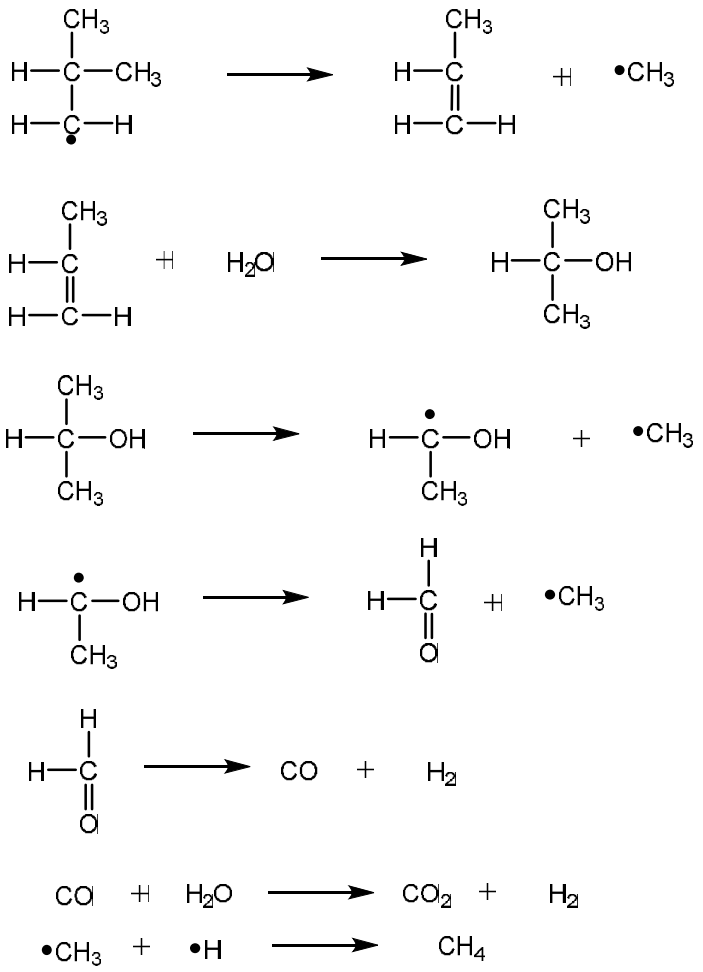

Figure 7.7 Reaction of isobutyl radical

7.4.2.1 Gas product

The composition of the obtained product gas, as shown in Figure 7.8, supports the reaction scheme which is shown in Figure 7.7. At low temperatures, the reaction does not proceed to completion and the product gas comprises mainly CO, CO_2, and H_2. These gases are likely produced during the initial decomposition stage, which is shown in

Figure 7. 3. At high temperatures, the yield of methane increases, but not as much as that of valine. Comparison of Figures 7.4 and 7.7 clearly shows that the main gaseous product in Figure 7.4 is CH_4, while that shown in Figure 7.7 also includes CO, CO_2, and H_2.

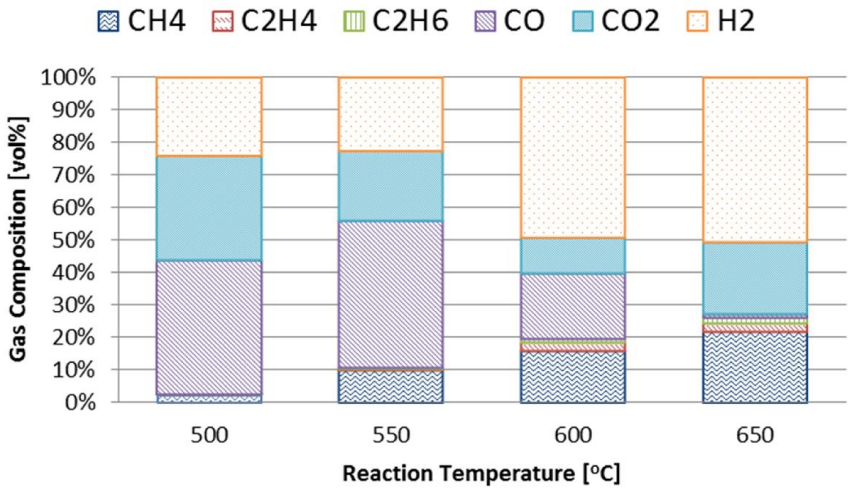

Figure 7.8 Effect of reaction temperature on leucine product gas composition of leuicne, concentration of 1.0 wt%, 25 MPa, and feedstock flow rate of 2 g/min.

7.5 Conclusion

The gasification characteristics of glycine, alanine, valine, and leucine in supercritical water were compared with the same feedstock concentration of 1.0 wt%, controlled reaction pressure of 25 MPa., and fixed feedstock flow rate at 2 g/min. It should be noted that the pre-exponential factors and activation energies for glycine, alanine, and leucine are similar, which indicates that they have the same rate-determining step, which is likely carboxyl radical production. The carbon gasification efficiency of valine is lower than those of glycine, alanine, and leucine. This is attributed to the relative stability of the secondary radical, which leads to a higher yield of the liquid-phase product.

CHAPTER 8

Effect of molecule structure on supercritical water gasification of amino acid

8.1 Introduction

As we have already determined gasification characteristics of amino acids of aliphatic classification, the results are shown in different from our expectation and they

are described in Chapter 7. Here again, if other amino acids also undergo gasification at the same rate, we will be able to safely apply this gasification rate to other amino acids and likely proteins as well. The difference of molecule structure may show some insight significant on gasification efficiency and it of interest to find out. Thus, the purpose of this study is to compare the gasification rates of five amino acids, i.e., glycine, alanine, valine, leucine, and proline. In addition, by gasifying proline, which has different at cyclic structures, as shown in Figure 8.1, the effects of its structural characteristics should be clarified.

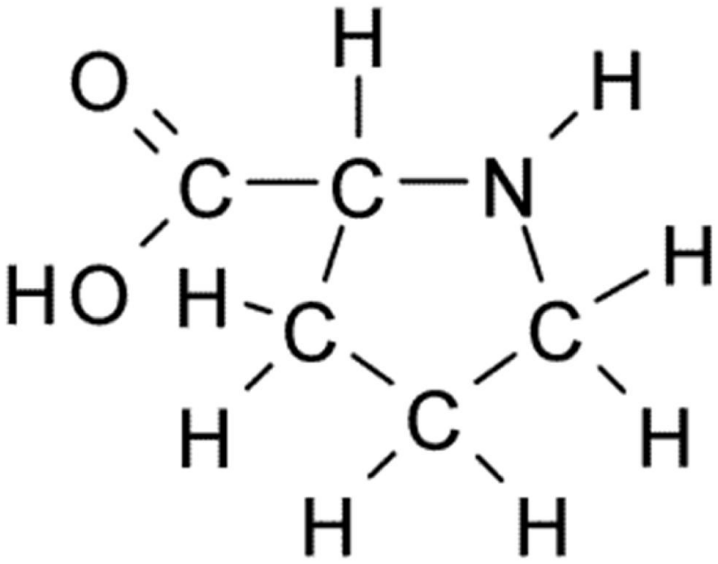

Figure 8.1 Molecule structure of proline

8.2 Experimental procedures

It can be seen that the description of the continuous flow reactor and procedures in previous, Chapter 4, this effect study also used practically the same experimental apparatus and procedures. In brief, proline aqueous solution was prepared to the desired concentration of 1.0 wt% by mixing with deionized water. The proline solution was fed into the reactor, a tubular SS316 steel reactor with inner diameter of 2.17 mm and length of 12 m., directly by high-pressure pump. After passed through the reactor, the effluent product came out and cooled-down by a heat exchanger, then depressurized by a back-pressure regulator, and then sampled. Note that the reaction temperature has been varied in a range of 500 – 650 ^{o}C as previous study in Chapter 7. The residence time in the reactor depending on the reaction temperature, it was ranged from 86 to 119 s. The proline feeding flow rate was controlled at 2 g/min.

The same as before, the gas product was collected under 0.1M HCL solution and measured the gas-generation rate which was determined using the time required for the effluent gas to fill a vial of known volume by water replacement. The gaseous product was qualified and quantified by a gas chromatography (GC) installed with TCD

and FID. GC-TCD, a thermal conductivity detector GC, will detect CO_2 and CO with He as the carrier gas. GC-FID, a flame ionization detector GC will detect CH_4, C_2H_4, and C_2H_6 with He as the carrier gas. GC-TCD with N_2 as the carrier gas will detect H_2.

Liquid product was quantified the amount of carbon which is containing in liquid product (NPOC) and in the dissolved gas product (IC). Dissolved gas product, IC value, that was detected by TOC refers to CO_2 which can be dissolved into liquid phase for a while. Then this IC value could be included with gas product which is measured by GC to calculate the carbon gasification efficiency.

Note that there is no particle observed and remained in filter and liquid-solid separator for all experimental runs in this study.

Carbon gasification efficiency is also defined as previous by using the ratio of the molar amount of carbon in the gas product to that carbon content in the feedstock solution as it has been described in Chapter 6, equation (6.1).

8.3 Experimental conditions

Proline gasification experimental runs were performed using the experimental conditions which are shown in Table 8.1.

Table 8.1. Experimental conditions for the proline gasification

Feedstock	Proline
Feedstock concentration	1.0 wt%
Reaction temperature	500 - 650 ^{o}C
Reaction pressure	25 MPa
Feedstock flow rate	2.0 g/min
Residence time	119, 108, 94, and 86 s
Catalyst	No catalyst
Reactor type	Tubing flow reactor
Reactor length	12 m

8.4 Results and discussion

The ranged of reaction temperature from 500 – 650 ^{o}C has been used to determine the gasification characteristics of proline in supercritical water conditions.

The others gasification parameters which are feedstock concentration, reaction pressure, and residence time (controlled by flow rate) have been used the same value as previous study that are 1.0 wt% of concentration, 25 MPa, and 2 g/min. of flow rate, representively.

As we have found decomposition of glycine and alanine in this reaction temperature region followed the first order reaction rate (Samanmulya and Matsumura, 2013 and Samanmulya et al., 2014), the same expectation apply here too. We assumed that the gasification reaction rate is first-order with respect to the amount of carbon feedstock here. Using the Arrhenius rate law for the reaction rate constant, the equation can be obtained as it has defined in Equations (7.1), (7.2), and (7.3). The resulting of proline would be shown in the next explanation.

8.4.1 Gasification characteristics of proline

Figure 8.2 shows the gasification characteristics of proline in supercritical water and also obtained the results of glycine and alanine in order to comparison purpose. It is clear that proline decomposes easily, unlike valine in Chapter 7, which is interesting because both proline and valine are C5 amino acids. Assuming the first-order-reaction rate equation, the parameters in Eq. (7.3) were determined by fitting the resulting carbon

gasification efficiencies to the experimental data of proline and also shown in Figure 8.2, and is in good agreement with the experimental data

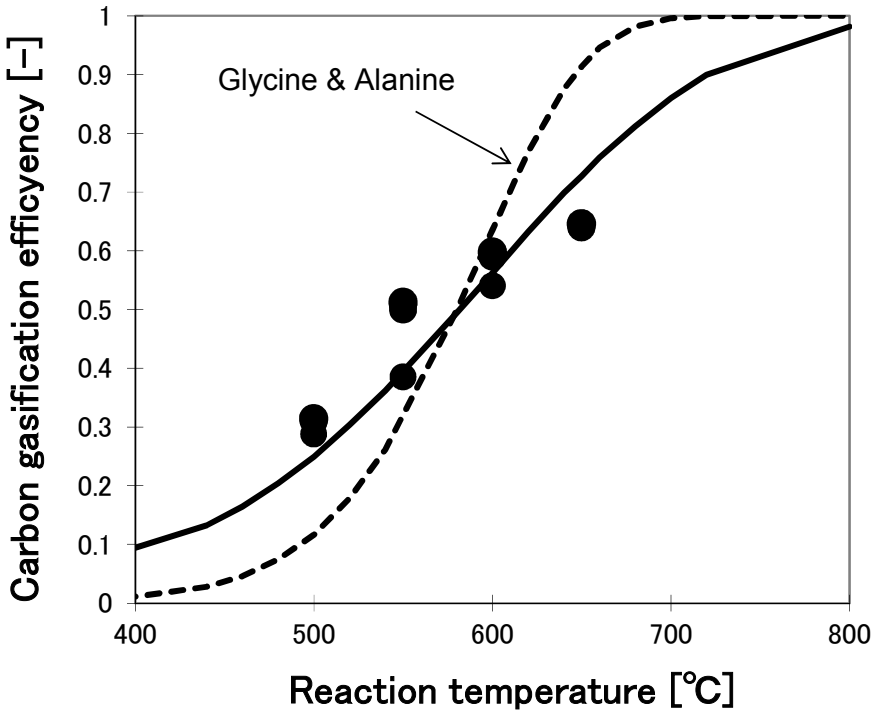

Figure 8.2 Gasification characteristics of proline

As proline is a ring compound, the reaction scheme of amino acids that is shown in Figure 7.3 must be modified to that shown in Figure 8.3. The radical produced from proline is primary and will decompose easily. These explanations would answer why its gasification rate is almost equal to those of glycine and alanine.

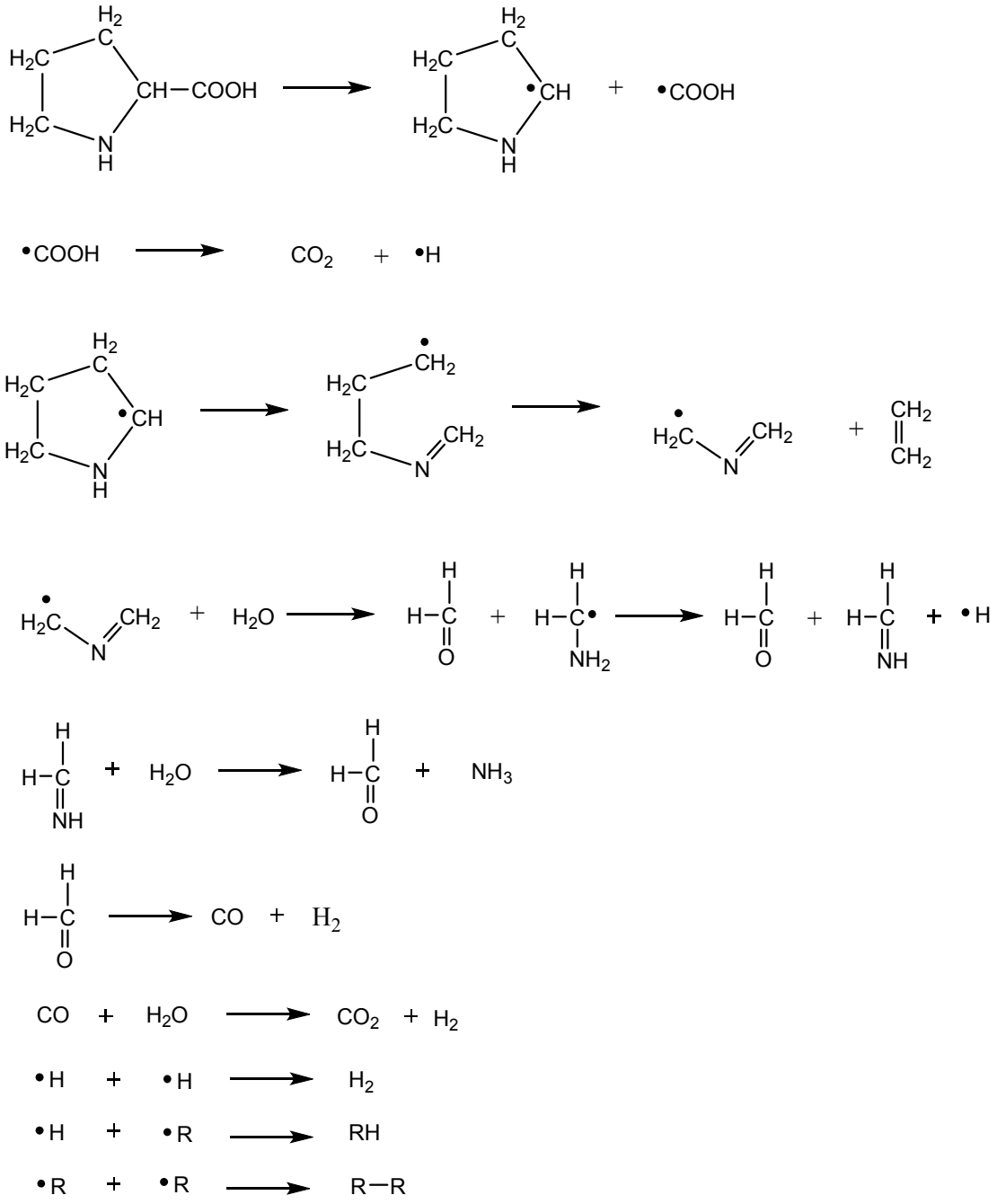

Figure 8.3 Reaction scheme of proline decomposition

However, gasification of proline is less sensitive to reaction temperature than that of glycine, alanine, and leucine. Even though, the radical, which is produced from proline, is determined to be a primary radical. This may be due to stabilization of the transition state of the carboxyl radical–producing reaction by the ring structure.

8.4.1.1 Gas Product

The composition of the gas which is produced from proline decomposition is shown in Figure 8.4. A higher fraction of ethylene is evident at low temperatures, i.e., 500 and 550 °C, which is explained by the production of ethylene in the reaction scheme shown in Figure 8.3. Because of its relatively high reactivity, ethylene is further consumed to produce other gases at later stages in the reaction scheme, which leads to a lower ethylene fraction at higher temperatures.

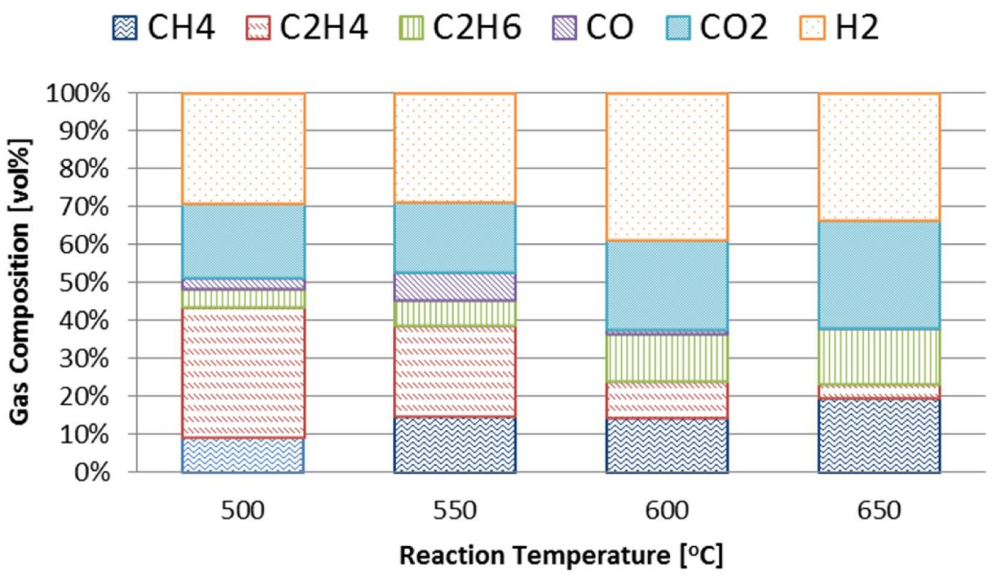

Figure 8.4 Effect of reaction temperature on proline product gas composition, concentration of 1.0 wt%, 25 MPa, and flow rate of 2 g/min.

8.5 Conclusion

The concentrations of the proline gasification experimental runs were all 1.0 wt%, the ranges of reaction temperatures and reaction pressure were equivalent as previous study, and the feedstock flow rate was fixed at 2.0 g/min. The carbon gasification efficiency increases with reaction temperature. It can be seen that the carbon gasification efficiency of proline look alike that of glycine and alanine, which is explained by the formation of a primary radical. During gasification of the other amino

acids, primary radicals are produced; accordingly, their gasification rates are similar. However, gasification of proline is less sensitive to reaction temperature than that of glycine, alanine, and leucine. This may be due to stabilization of the transition state of the carboxyl radical–producing reaction by the ring structure.

CHAPTER 9

Conclusions and Recommendations for Future Work

9.1 Introduction

This chapter has presented the conclusions of the present work, including of Chapter 5, Chapter 6, Chapter7, and Chapter 8, as discussed in Section 9.2. Subsequently, the recommendations for future work are proposed in Section 9.3.

9.2 Conclusions

Glycine, the smallest molecule of amino acid, has been chosen to be a model compound of protein to gasify and determined the gasification characteristics in supercritical water conditions. Gasification of glycine was conducted using a tubular flow reactor by varying supercritical water gasification parameters, reaction temperature in a range of 500 – 650 ^{o}C, glycine concentration of 1.0 – 5.0 wt%, residence time that is depended on feedstock flow rate from 1 to 3 g/min., and activated carbon catalyst addition. When the feedstock concentration was high, carbon gasification efficiency became lower. At a sufficiently low concentration of 1.0 wt%, the carbon gasification reaction followed the first order reaction rate. Its reaction rate constant was well expressed by the Arrhenius rate law. The gaseous product was constituted of Hydrogen, Methane, Carbon dioxide, Carbon monoxide, and a small amount of Ethene and Ethane. The effect of operation parameters on its composition agreed with the thermodynamic predictions. The activated carbon catalyst was found to be ineffective for glycine.

As glycine gasification characteristics had already clarified, the next task is alanine gasification that differs by one functional group, methyl. Gasification of alanine was conducted using the same tubular flow reactor. Gasification parameters that

was chose to determine are effect of alanine concentration (1.0, 2.0, and 3.0 wt%) and effect of reaction temperature (500 – 650 ^{o}C). The reaction pressure was controlled at 25 MPa and fixed alanine solution flow rate at 2 g/min. When the feedstock concentration was high, the carbon gasification efficiency does not much change. The carbon gasification reaction of alanine followed first order kinetics. Gasification rate is identical for both glycine and alanine, and the reaction rate parameters were determined. Its reaction rate constant was also well expressed by the Arrhenius equation. The product gas was composed of hydrogen, methane, carbon dioxide, carbon monoxide, methane, and a small amount of ethene and ethane. The effect of the methyl group in alanine is the production of methane, and the dilution of nitrogen so that the alkaline effect is suppressed. The former explains the higher methane yield, whereas the latter results in the high carbon monoxide yield.

When the gasification rate of glycine and alanine are determined to be identical, it is of interest if other amino acids also undergo gasification at the same rate, it could be possible to apply this gasification rate to other amino acids safely and likely proteins as well.

Valine and leucine were gasified in order to determine the gasification characteristics of amino acids in aliphatic classification that is the same class as glycine and alanine. Proline, an amino acid cyclic structure, had been chosen to determine the effect of molecule structure on gasification characteristics. Those three amino acids were performed in the same tubular flow reactor and fixed their concentration of 1.0 wt% but changing reaction temperature (500 – 650 ^{o}C) that corresponded to gasification rate. The gasification characteristics of glycine, alanine, valine, leucine, and proline in supercritical water were compared. The results show that the gasification rate parameters for glycine, alanine, and leucine are similar, while the activation energies of the gasification of valine and proline are lower than those of glycine, alanine, and leucine. This is attributed to stabilization of the transition state of the carboxyl radical–production step. Valine has a lower carbon gasification efficiency than proline, which could be explained by the relative stability of secondary radicals. The reaction networks scheme of amino acids decomposition have been proposed to show how amino acids decomposed and explain the product gas composition and also determined the type of reaction radicals, primary and secondary radical.

As we found decomposition of glycine and alanine in this temperature region followed the first order reaction rate (Samanmulya and Matsumura, 2013 and

Samanmulya et al., 2014), we assumed that the gasification reaction rate is first-order with respect to the amount of carbon feedstock here. Using the Arrhenius rate law for the reaction rate constant, the pre-exponential factors and activation energy are determine as shown in Table 9.1.

Table 9.1 : Reaction rate parameters of Supercritical Water Gasification for Five Amino Acids

Amino acids	Pre-exponential factor [s^{-1}], A	Activation Energy [kJ/mol], E_a
Glycine and Alanine	7.37×10^5	131
Valine	6.97×10^1	70
Leucine	7.37×10^5	135
Proline	1.96×10^2	73

A comparison of the carbon gasification efficiencies of the investigated amino acids is shown in Figure 9.1. Note that the concentrations of the amino acid were all 1.0 wt%, the ranges of reaction temperatures and reaction pressure were equivalent, and the

feedstock flow rate was fixed at 2.0 g/min. The carbon-gasification efficiency increases with reaction temperature. It is clearly evident that valine is the slowest to gasify, which is explained by the formation of a secondary radical. During gasification of the other amino acids, primary radicals are produced and their gasification rates are similar. Anyway, gasification of proline is less sensitive to reaction temperature than that of glycine, alanine, and leucine. This may be due to stabilization of the transition state of the carboxyl radical–producing reaction by the ring structure.

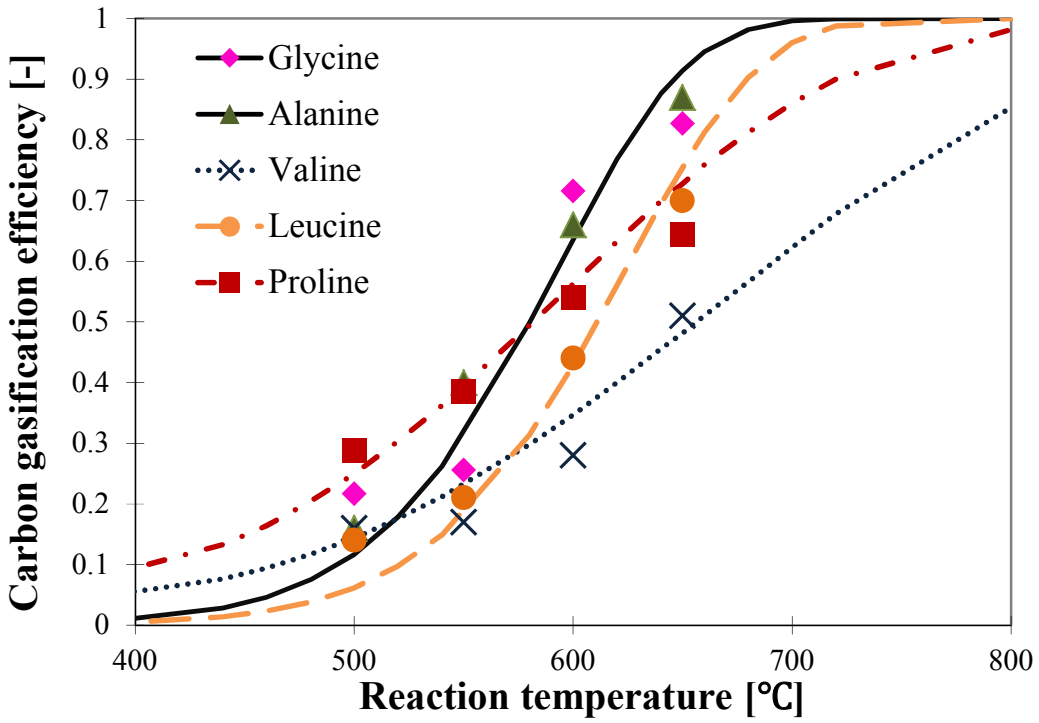

Figure 9.1 Comparison of carbon gasification efficiency for glycine, alanine, valine, leucine and proline

9.3 Recommendations for Future Work

The recommendations for future work on this particular study are as follows

1) As we had already determined gasification rate of five amino acids, the results show the same and different gasification rate and characteristics. To find out the gasification rate of the others amino acid that is also in the different classification which are hydroxyl or sulfer-containing, aromatic, basic, acidic and amine, it would be useful information to apply those of gasification rate to protein compound as well.

2) As TOC analyzer only quantified the amounts of carbon contained in liquid products. These values from TOC had been used to calculate the carbon balance and the results are closed to 1. However, TOC does not specify the unknown in liquid products. It would be good to qualify the liquid product composition because it may useful for reaction network hypothesis and define the radical reaction.

3) Amino acids contain nitrogen atom. It is interest to find where nitrogen gone. Although, it has been dissolved and form into ammonia in liquid phase as

previous work defined (Minowa et al., 2004 and Sato et al., 2004) but it may be better to quantify the amounts of ammonia that contained in liquid products.

REFERENCES

(1) Aida, T. M.; Sato, Y.; Watanabe, M.; Tajima, K.; Nonaka, T.; Hattori, H.; Arai, K. Dehydration of D-Glucose in High Temperature Water at Pressures up to 80 MPa. *J. Supercrit. Fluids.* **2007**, *40* (3), 381-388.

(2) Aida, T. M.; Tajima, K.; Watanabe, M.; Saito, Y.; Kuroda, K.; Nonaka, T.; Hattori, H.; Smith, R. L.; Arai, K. Reaction of D-fructose in water at temperatures up to 400 C and pressure up to 100 MPa. *J. Supercrit. Fluids.* **2007**, *42* (1), 110-119.

(3) Aida, T. M.; Tajima, K.; Watanabe, M.; Saito, Y.; Kuroda, K.; Nonaka, T.; Hattori, H.; Smith, R. L.; Arai, K. Reaction of D-fructose in water at temperatures up to 400 C and pressure up to 100 MPa. *J. Supercrit. Fluids.* **2007**, *42* (1), 110-119.

(4) Akhtar, J.; Kuang, S.K.; Amin, N.S. Liquefaction of empty palm fruit bunch (EPFB) in alkaline hot compressed water. *Renewable Energy* **2010**, *35*, 1220.

(5) Akiya, N.; Savage P.E. Roles of water for chemical reactions in high-temperature water. *Chem. Rev.* **2002**, *102*, 2725.

(6) Antal, M. J.; Mok, W. S.; Richards, G. N., Four-carbon model compounds for the reactions of sugar in water at high temperature. *Carbohydr. Res.* **1990**, *199,* 111-115.

(7) Antal, M. J.; Leesomboom, T.; Mok, W. S.; Richards, G. N., Mechanism of formation of 2-furaldehyde from D-xylose. *Carbohydr. Res.* **1991**, *217*, 71-85.

(8) Antal, M. J.; Allen, S. G.; Schulman, D.; Xu, X. D.; Divilio, R. J. Biomass gasification in supercritical water. *Ind. Eng. Chem. Res.* **2000**, *39*, 4040-4053.

(9) Asghari, F. S.; Yoshida, H. Acid-Catalyzed Production of 5-Hydroxymethyl Furfural from D-Fructose in Subcritical Water. *Ind. Eng. Chem. Res.* **2006**, *45*, 2163.

(10) Azadia, P.; Khodadadib, A. A.; Mortazavib, Y.; Farnood, R. Hydrothermal gasification of glucose using Raney nickel and homogeneous organometallic catalysts. *Fuel Processing Technology* **2009**, *90*, 145-151.

(11) Biller, P.; Ross, A.B. Potential yields and properties of oil from the hydrothermal liquefaction of microalgae with different biochemical content. *Bioresource Technology.* **2011**, *102,* 215-225.

(12) Blasi,C. D.; Branca, C.; Galgano, A. Biomass screening for the production of furfural via thermal decomposition. *Ind. Eng. Chem. Res.* **2010**, *49*, 2658.

(13) Brunner, G., Near critical and supercritical water Part I. Hydrolytic and hydrothermal processes. *J. Supercrit. Fluids.* **2009**, *47*, 373

(14) Bühler, W.; Dinjus, E.; Ederer, H.J.; Kruse, A.; Mas, C. Ionic reactions and pyrolysis of glycerol as competing reaction pathways in near- and supercritical water. *J. Supercrit. Fluids.* **2002**, *22,* 37-53.

(15) Byrd, A. J.; Pant, K. K.; Gupta, R. B. Hydrogen Production from Ethanol by Reforming in Supercritical Water Using Ru/Al2O3 Catalyst. *Energy & Fuels* **2007**, *21*, 3541-3547.

(16) Byrd, A. J.; Pant, K. K.; Gupta, R. B. Hydrogen Production from Glucose Using Ru/Al2O3 Catalyst in Supercritical Water. *Ind. Eng. Chem. Res.* **2007**, *46*, 3574-3579.

(17) Cantrell, K.; Ro, K.; Mahajan, D.; Anjom, M.; Hunt, P.G. Role of

thermochemical conversion in livestock waste-to-energy treatments: obstacles and opportunities. *Ind. Eng. Chem. Res.*, **2007**, *46*, 8918-8927.

(18) Cao, C.; Guo, L.; Chen, Y.; Guo, S.; Lu, Y. Hydrogen production from supercritical water gasification of alkaline wheat straw pulping black liquor in continuous flow system. *Int. J. Hydrogen Energy* **2011**, *3*6, 13528-13535.

(19) Chakinala, A.G.; Brilman, D.W.F.; Swaaij, W.P.N.van; Kersten, A.R.S. Catalytic and non-catalytic supercritical water gasification of microalgae and glycerol. *Ind. Eng. Chem. Res.* **2010**, *49*(3), 1113-1122.

(20) Cheng, L.; Ye, X. P.; He, R.; Liu, S. Investigation of rapid conversion of switchgrass in subcritical water. *Fuel processing technology* **2009**, 90, 301-311.

(21) Chuntanapum, A.; Formation mechanisms of gas and tarry materials in a supercritical water gasification process, Doctoral Thesis 2010, Hiroshima University,

(22) Chuntanapum, A.; Matsumura, Y. Char formation mechanism in supercritical water gasification process: A study of model compounds. *Ind. Eng. Chem. Res.* **2010**, *49,* 4055-4062.

(23) Chuntanapum, A.; Matsumura, Y. Role of 5-HMF in Supercritical Water Gasification of Glucose. *J. Chem. Eng. Jpn.,* **2011**, *44*, 91-97.

(24) Chuntanapum, A.; Shii, T.; Matsumura, Y. Acid-catalyzed char formation of 5-HMF in subcritical water. *J. Chem. Eng. Japan,* **2011**, *44,* 431-436.

(25) Demirbas, A. Hydrogen-rich gas from fruit shells via supercritical water extraction. *International Journal of Hydrogen Energy,* **2004**, *29,* 1237-1243.

(26) DiLeo, G. J.; Neff, M. E.; Kim, S.; Savage, P. E. Supercritical Water Gasification of Phenol and Glycine as Models for Plant and Protein Biomass. *Energy Fuels* **2008**, *22*, 871–877.

(27) D'Jesus, P.; Artiel, C.; Boukis, N.; Kraushaar-Czarnetzki, B.; Dinjus, E. Influence of Educt Preparation on Gasification of Corn Silage in Supercritical Water. *Ind. Eng. Chem. Res.* **2005**, *44*, 9071.

(28) D'Jesus, P.; Boukis, N.; Kraushaar-Czarnetzki, B.; Dinjus, E. Influence of Process Variables on Gasification of Corn Silage in Supercritical Water. *Ind. Eng. Chem. Res.* **2006**, *45*, 1622.

(29) Erkonak, H.; Sogut, O. O.; Akgun, M. Treatment of olive mill wastewater by supercritical water oxidation. *J. of Supercritical Fluids* **2008**, *46*, 142-148.

(30) Fang, Z.; Minowa, T.; Fang, C; Smith, R.L.Jr.; Inomata, H.; Kozinski, J.A. Catalytic hydrothermal gasification of cellulose and glucose. *Int. J. Hydrogen Energy* **2008**, *33*, 981.

(31) Fang, Z.; Minowa, T.; Fang, C; Smith, R.L.Jr.; Inomata, H.; Kozinski, J.A. Catalytic hydrothermal gasification of cellulose and glucose. *Int. J. Hydrogen Energy* **2008**, *33*, 981.

(32) Franco, C.; Pinto, F.; Gulyurtlu, I.; Cabrita, I. The study of reactions influencing the biomass steam gasification process. *Fuel* **2003**, *82*, 835–842.

(33) Furusawa, T.; Sato, T.; Sugito, H.; Miura, Y.; Ishiyama, Y.; Sato, M.; Itoh, N.; Suzuki, N. Hydrogen production from the gasification of lignin with nickel catalysts in supercritical water. *Int. J. Hydrogen Energy* **2007**, *32*, 699 – 704.

(34) Garcıa Jarana, M. B.; Sanchez-Oneto, J.; Portela, J. R.; Nebot Sanz, E.; Martınez de la Ossa, E. J. Supercritical water gasification of industrial organic wastes. *J. of supercritical fluids* **2008**, *46*, 329-334.

(35) Goodwin, A. K.; Rorrer, G. L. Conversion of glucose to hydrogen-rich gas by supercritical water in a microchannel reactor. *Ind. Eng. Chem. Res.* **2008**, *47*, 4106–4114.

(36) Guan, Q.; Wei, C.; Savage, P. E. Kinetic model for supercritical water gasification of algae. *Phys. Chem. Chem. Phys.* **2012**, *14,* 3140-3147.

(37) Guo, L.J.; Lu, Y.J.; Zhang, X.M.; Ji, C.M.; Guan, Y.; Pei, A.X. Hydrogen production by biomass gasification in supercritical water: A systematic experimental and analytical study. *Catalysis Today*. **2007**, *129*, 275-286.

(38) Hao, X. H.; Guo, L. J.; Mao, X.; Zhang, X. M.; Chen, X. J. Hydrogen production from glucose used as a model compound of biomass gasified in supercritical water. *Int. J. Hydrogen Energy* **2003**, *28*, 55 – 64.

(39) Hashaikeh, R.; Fang, Z.; Butler, I. S.; Hawari, J.; Kozinski, J. A. Hydrothermal dissolution of willow in hot compressed water as a model for biomass conversion. *Fuel* **2007**, *86*, 1614–1622.

(40) Herguido, J.; Corella, J.; Gonzalez, S.J. Steam gasification of lignocellulosic resideues in fluidized bed at a small pilot scale: Effect of the type of feedstock. *Ind. Eng. Chem. Res.*, **1992**, *3*, 1274-1282.

(41) *Ho, P.C.; Palmer, D.A.; Wood, R.H. J.Phys. Chem. B **2000**, 104, 12084-12089.*

(42) *Ho, P.C.; Palmer, D.A.; Gruszkiewicz, M.S. J.Phys. Chem. B **2001**, 105, 1260-1266.*

(43) Hui, J.; Youjun L.; Guo J.; Cao C.; Zhang, X. Hydrogen production by partial oxidative gasification of biomass and its model compounds in supercritical water. *Int J Hydrogen Energy*, **2010**, *35*. 3001–3010.

(44) *JSME Data Book: Thermophysical Properties of Fluids;* The Japan Society of Mechanical Engineers, 1983.

(45) *JSME steam tables;* The Japan Society of Mechanical Engineers, 1999.

(46) Kabyemela, B.M.; Adschiri, T,; Malaluan, R.; Arai, K., Degradation kinetics of dihydroxyacetone and glyceraldehyde in subcritical and supercritical water. *Ind. Eng. Chem. Res.* **1997**, *36,* 2025-2030.

(47) Kabyemela, B. M.; Adshiri, T.; Malaluan, R. M.; Arai, K. Kinetics of glucose epimerization and decomposition in subcritical and supercritical water. *Ind. Eng. Chem. Res.* **1997**, *36*, 1552-1558.

(48) Kabyemela, B. M.; Adschiri, T.; Malaluan, R. M.; Arai, K. Glucose and Fructose Decomposition in Subcritical and Supercritical Water: Detailed Reaction Pathway, Mechanism, and Kinetics. *Ind. Eng. Chem. Res.* **1999**, *38*, 2888-2895.

(49) Karayildirim, T.; Sinag, A.; Kruse, A. Char and coke formation as unwanted side reaction of the hydrothermal biomass gasification. *Chem. Eng. Technol.* **2008**, *31* (11), 1561-1568.

(50) Katritzky, A.R.; Nichols, D. A.; Siskin, M.; Murugan, R.; Balasubramanian, M. Reaction in high-temp aqueous media. *Chem. Rev.* **2001**, *101*, 837.

(51) Knežević, D.; Swaaij, W.P.M van; Kersten, S.R.A., Hydrothermal conversion of biomass: I, Glucose conversion in hot compressed water. *Ind. Eng. Chem. Res.* **2009**, *48,* 4731-4743.

(52) Kruse, A. Hydrothermal biomass gasification. *J. Supercrit. Fluids* **2009**, *47*, 391–399.

(53) Kruse, A.; Dinjus, E. Hot compressed water as reaction medium and reactant properties and synthesis reactions. *J. Supercrit. Fluids* **2007**, *39*, 362-380.

(54) Kruse, A; Faquir, M. Hydrothermal Biomass Gasification – Effects of Salts, Backmixing, and Their Interaction. *Chem. Eng. Technol.* **2007**, *30* (6), 749–754.

(55) Kruse, A.; Gawlik, A. Biomass Conversion in Water at 330-410 °C and 30-50 MPa. Identification of Key Compounds for Indicating Different Chemical Reaction Pathways. *Ind. Eng. Chem. Res.* **2003**, *42*, 267-279.

(56) Kruse, A.; Krupka, A.; Schwarzkopf, V.; Gamard, C.; Henningsen, T. Influence of proteins in the hydrothermal gasification and liquefaction of biomass 1. Comparison of different feedstocks. *Ind. Eng. Chem. Res.* **2005**, *44*, 3013-3020.

(57) Kruse, A.; Meier, D.; Rimbrecht, P.; Schacht, M. Gasification of pyrocatechol in supercritical water in the presence of potassium hydroxide. *Ind. Eng. Chem. Res.* **2000**, *39*, 4842-4848.

(58) Kruse, A.; Maniam, P.; Spieler, F. Influence of proteins in the hydrothermal gasification and liquefaction of biomass 2. Model copmpounds. *Ind. Eng. Chem. Res.* **2007**, *46*, 87-96.

(59) Lee, In-Gu; Ihm, Son-Ki. Gasification of Glucose in Supercritical Water. *Ind. Eng. Chem. Res.* **2002,** *41*, 1182–1188.

(60) Lee, In-Gu; Ihm, Son-Ki Catalytic Gasification of Glucose over Ni/Activated Charcoal in Supercritical Water. *Ind. Eng. Chem. Res.* **2009**, *48*, 1435–1442.

(61) Letellier, S.; Marias, F.; Cezac, P.; Serin, J.P. Gasification of aqueous biomass in supercritical water: A thermodynamic equilibrium analysis. *J. Supercrit. Fluids* **2010**, *51*, 353.

(62) Lu, Y.J.; Guo, L.J.; Ji,C.M.; Zhang, X.M.; Hao, X.H.; Yan, Q.H. Hydrogen production by biomass gasification in supercritical water: A parametric study. *Int. J. Hydrogen Energy* **2006**, *31*, 822-831.

(63) Luijkx, G. C. A.; Vanrantwijk, F.; Vanbekkum, H. Hydrothermal Formation of 1,2,4-Benzenetriol from 5-Hydroxymethyl-2-Furaldehyde and D-Fructose. *Carbohydrate Res.* **1993**, *242*, 131-139.

(64) Matsumura, Y. Evaluation of supercritical water gasification and biomethanation for wet biomass utilization in Japan. *Energy Conversion and Management* **2002**, *43*, 1301–1310.

(65) Matsumura, Y.; Hara, S.; Kaminaka, K.; Yamashita, Y.; Yoshida, T.; Inoue, S.; Kawai, Y.; Minowa, T.; Noguchi, T.; Shimizu, Y., Gasification Rate of Various Biomass Feedstocks in Supercritical Water. *J. Jpn. Petrol. Inst.* **2013**, *56*, 1-10.

(66) Matsumura, Y.; Xu, X.; Antal, M. J., Jr. Gasification characteristics of an activated carbon in supercritical water. *Carbon* **1997**, *35*, 819–824.

(67) Matsumura, Y.; Minowa, T.; Potic, B.; Kersten, S. R. A.; Prins, W.; Van Swaaij, W. P. M.; Van De Beld, B.; Elliott, D. C.; Neuenschwander, G. G.; Kruse, A.; Antal, M. J. Biomass gasification in near- and super-critical water: Status and prospects. *Biomass Bioenergy* **2005**, *29* (4), 269-292.

(68) Matsumura, Y.; Yanachi, S.; Yoshida, T. Glucose decomposition kinetics in water at 25 MPa in the temperature range of 448-673 K. *Ind. Eng. Chem. Res.* **2006**, *45*,

1875 – 1879.

(69) Matsumura, Y.; Harada, M.; Nagata, K.; Kikuchi, Y. Effect of Heating Rate of Biomass Feedstock on Carbon Gasification Efficiency in Supercritical Water Gasification. *Chem. Eng. Commun.* **2006**, *193* (5) 649-659.

(70) Ministry of Agriculture, Forestry and Fisheries of Japan ; Biomass Policies and Assistance Measures in Japan, http://www.maff.go.jp/e/pdf/reference6-8.pdf (2009)

(71) Minowa, T.; Fang, Z. Hydrogen Production from Cellulose in Hot Compressed Water Using Reduced Nickel Catalyst: Product Distribution at Different Reaction Temperatures. *J. Chem. Eng. Jpn.* **1998**, *31* (3), 488.

(72) Minowa, T.; Inoue, S. Hydrogen production from biomass by catalytic gasification in hot compressed water. *Renewable Energy* **1999**, *16*, 1114–1117.

(73) Mizan, T. I.; Savage, E.; Ziff, R. M. Temperature dependence of hydrogen bonding in supercritical water. *J. Phys. Chem.* **1996**, *100*, 403-408

(74) Modell, M., "Fundamentals of thermochemical biomass conversion,"eds. by Overend, R. P., Milne, T. A., Mudge, L. K.,Elsevier Applied Science Publishers, London (1985), p. 95.

(75) Nakamura, A.; Kiyonaga, E.; Yamamura, Y.; Shimizu, Y.; Minowa, T.; Noda, Y.; Matsumura, Y. Catalyst-suspended chicken manure gasification in supercritical water. *J. Chem. Eng. Jpn.* **2008**, *41*, 433–440.

(76) Nakamura, A.; Kiyonaga, E.; Yamamura, Y.; Shimizu, Y.; Minowa, T.; Noda, Y.; Matsumura, Y. Detailed Analysis of Heat and Mass Balance for Supercritical Water Gasification. *J. Chem. Eng. Jpn.* **2008**, *41* (8), 817-828.

(77) Okajima, I.; Shimoyama, D.; Sako, T. Gasification and hydrogen production from food wastes using high pressure superheated steam in the presence of alkali catalyst. *Journal of Chemical Engineering of Japan* **2007**, *40*, 356 – 364.

(78) Onwudili, J. A.; Williams, P. T. Hydrothermal Catalytic Gasification of Municipal Solid Waste. *Energy & Fuels* **2007**, *21*, 3676-3683.

(79) Onwudili, J. A.; Williams, P. T. Role of sodium hydroxide in the production of hydrogen gas from the hydrothermal gasification of biomass. *International journal of hydrogen energy* **2009**, *34*, 5645-5656.

(80) Onwudili, J. A.; Williams, P. T. Alkaline reforming of brominated fire-retardant plastics: fate of bromine and antimony. *Chemosphere* **2009**, *74*, 787-796.

(81) Picou, J.W.; Wenzel, J.E.; Lanterman, H.B.; Lee, S. Hydrogen production by noncatalytic autothermal reformation of aviation fuel using supercritical water. *Energy Fuels.* **2009**, *23*, 6089-6094.

(82) Peterson A. A.; Vogel, F.; Lachance, R. P.; Fröling, M.; Antal, M. J.; Tester, J. W. Thermochemical biofuel production in hydrothermal media: A review of sub- and supercritical water technologies. *Energy and Environmental Science* **2008**, *1*, 32-65.

(83) Promdej, C.; Chuntanapum, A.; Matsumura, Y. Effect of temperature on tarry material production of glucose in supercritical water gasification. *J. Jpn. Inst. Energy* **2010**, *89*, 1179-1184.

(84) Promdej, C; Matsumura, Y. Temperature effect on hydrothermal decomposition of glucose in sub- and supercritical water. *Ind. Eng. Chem. Res.* **2011**, *50(14)*, 8492-8497.

(85) Qi, J.; Xiuyang, L. Kinetics of non-catalyzed decomposition of glucose in high-temperature liquid water. *Chin. J. Chem. Eng.* **2008**, *16* (6), 890-894.

(86) Qi, X.; Watanabe, M.; Aida, T. M.; Smith, R. L., Jr. Catalytical conversion of fructose and glucose into 5-hydroxymethylfurfural in hot compressed water by microwave heating. *Catal. Commun.* **2008**, *9*, 2244–2249.

(87) Qian, Y.; Zuo, C.; Tan, J.; He, J. Structural analysis of bio-oils from sub-and supercritical water liquefaction of woody biomass. *Energy* **2007**, *32(3)*, 196-202.

(88) Resende, F. L. P.; Neff, M. E.; Savage, P. E. Noncatalytic Gasification of Cellulose in Supercritical Water. *Energy Fuels* **2007**, *21*, 3637–3643.

(89) Resende, F. L. P.; Fraley, S. A.; Berger, M. J.; Savage, P. E. Noncatalytic Gasification of Lignin in Supercritical Water. *Energy Fuels* **2008**, *22*, 1328–1334.

(90) Rodriguez, A.; Moral, A.; Sanchez, R.; Requejo, A.; Jimenez, L. Influence of variables in the hydrothermal treatment of rice straw on the composition of the resulting fractions. *Bioresource Technology* **2009**, *100*, 4863–4866.

(91) Ross, A.B.; Biller, P.; Kubacki, M.L.; Lim, H.; Lea-Langton, A.; Jones, J.M. Hydrothermal processing of microalgae using alkali and organic acids. *Fuel* **2010**, *89*, 2234-2243.

(92) Samanmulya, T.; Matsumura, Y., Effect of Activated Carbon Catalytic on Supercritical Water Gasification of Glycine as a Model Compound of Protein. *J. Jpn. Inst. Energy* **2013**, *92*, 894-899.

(93) Samanmulya, T.; Inoue, S.; Inoue, T.; Kawai, Y.; Kubota, H.; Munetsuna, H.; Noguchi, T.; Matsumura, Y., Gasification characteristics of alanine in supercritical water. *J. Jpn. Petrol. Inst.* **2014**, accepted. (In press)

(94) Sasaki, M.; Adschiri, T.; Arai, K. Kinetics of cellulose conversion at 25 MPa in sub- and supercritical water. Am. Inst. Chem. Eng.. **2004**, *50(1)*, 192-202.

(95) Sasaki, M.; Goto, K.; Tajima, M.; Adschiri, T.; Arai, K. Rapid and selective retro-aldol condensation glucose to glycolaldehyde in supercritical water. *Green Chem.* **2002**, *4*, 285-287.

(96) Sasaki, M.; Kabyemela, B.; Malaluan, R.; Hirose, S.; Takeda, N.; Adschiri, T, Arai, K. Cellulose hydrolysis in subcritical and supercritical water. *Journal of Supercritical Fluids*. **1998**, *13*, 261-268.

(97) Sato, T.; Kurosawa, S.; Smith, R. L., Jr.; Adschiri, T.; Arai, K. Water gas shift reaction kinetics under noncatalytic conditions in supercritical water. J. of Supercritical Fluids **2004**, *29*, 113–119.

(98) Savage, P. E. Organic Reactions in Supercritical Water. *Chem. Rev.*, **99**, *1999,* 603-621.

(99) Schmieder, H.; Abeln, J.; Boukis, N.; Dinjud, E.; Kruse, A.; Kluth, M.; Petrich, E.; Sadri, E.; Schacht, M. Hydrothermal gasification of biomass and organic wastes. *Journal of Supercritical Fluids.* **2000**, *17*, 145-153.

(100) Shaw, R.; Brill, T.; Clifford, A.; Eckert, C.; Frank, E. U. Supercritical water: a medium for chemistry. *Chem. Eng. News* **1991**, *69(51)*, 26-39.

(101) Sinag, A.; Kruse, A.; Schwarzkopf, V. Key Compounds of the Hydropyrolysis of glucose in Supercritical Water in the Presence of K_2CO_3. *Ind. Eng. Chem. Res.* **2003**, *42*, 3516.

(102) Sinag, A.; Kruse, A.; Rathert, J. Influence of the Heating Rate and the Type of Catalyst on the Formation of Key Intermediates and on the Generation of Gases

During Hydropyrolysis of Glucose in Supercritical Water in a Batch Reactor. *Ind. Eng. Chem. Res.* **2004**, *43*, 502.

(103) Sınag, A.; Gulbay, S.; Uskan, B.; Gullu, M. Comparative Studies of Intermediates Produced from Hydrothermal Treatments of Sawdust and Cellulose. *J. of Supercritical Fluids* **2009**, *50*, 121–127.

(104) Sricharoenchaikul, V. Assessment of black liquor gasification in supercritical water. *Bioresource Technology* **2009**, *100*, 638-643.

(105) Stucki, S.; Vogel, F.; Ludwig, C.; Haiduc, A. G.; Brandenberger, M. Catalytic gasification of algae in supercritical water for biofuel production and carbon capture *Energy Environ. Sci.* **2009**, *2*, 535–541.

(106) Subramanlam, B.; McHugh, M. A. Reactions in supercritical fluids-A review. *Ind. Eng. Chem. Process Des. Dev.* **1986**, *25,* 1-12.

(107) Sun, X.; Li, Y. Colloidal Carbon Spheres and Their Core/ShellStructures with Noble-Metal Nanoparticles. *Angew. Chem. Int. Ed.* **2004**, *43*, 597-601.

(108) Toor, S. S.; Rosendahl, L.; Rudolf, A. Hydrothermal liquefaction of biomass' A review of subcritical water technologis. *Energy*. **2011**, *36*, 2328-2342.

(109) van Rossum, G.; Potic, B.; Kersten, S.R.A.; van Swaaij, W.P.M. Catalytic gasification of dry and wet biomass. *Catalysis Today* **2009**, *145*, 10–18.

(110) Voll, F.A.P.; Rossi, C.C.R.S.; Silva, C.; Guiradello, R.; Souza, R.O.M.A.; Cabral, V.F.; Cardozo-Filho, L. Thermodynamic analysis of supercritical water gasification of methanol,ethanol, glycerol, glucose and cellulose. *Int. J. Hydrogen Energ.* **2009**, *34*, 9737.

(111) Wada, Y.; Oyama, K.; Yamasaki, T.; Uchiyama, I.; Yamamura, Y.; Kubota, H.; Matsumura, Y.; Minowa, T.; Noguchi, T.; Kawai, Y. The Effect of Catalyst Content on Supercritical Water Gasification Process with Shochu (Japanese Popular Distilled Liquor) Residue and the Result of Long-time Continuous Operation. J. Jpn. Inst. Energy **2013**, *92*, 1159-1166.

(112) Wahyudiono, M.; Sasaki, M.; Goto, M. Conversion of biomass model compound under hydrothermal conditions using batch reactor. *Fuel.* **2009**, *88*, 1656-1664.

(113) Wahyudiono, M.; Sasaki, M.; Goto, M. Thermal decomposition of guaiacal in sub- and supercritical water and its kinetic analysis. *J. Mater Cycles Waste Manage.* **2011**, *13*, 68-79.

(114) Watanabe, M.; Aizawa, Y.; Iida, T.; Levy, C.; Aida, T. M.; Inomata, H. Glucose reactions within the heating period and the effect of heating rate on the reactions in hot compressed water. *Carbohydr. Res.* **2005**, *340*, 1931–1939.

(115) Watanabe, M.; Sato, T; Inomata, H.; Smith, R.L. Jr.; Arai, K.; Kruse, A.; Dinjus, E. Chemical reactions of C1 Compounds in near-critical and supercritical water. *Chem. Rev.* **2004**, *104,* 5803.

(116) Williams, P. T.; Onwudili, J. Subcritical and Supercritical Water Gasification of Cellulose, Starch, Glucose, and Biomass Waste. *Energy Fuels* **2006**, *20*, 1259-1265.

(117) Xu, X.; Antal, M. J., Jr. Gasification of sewage sludge and other biomass for hydrogen production in supercritical water. *Environmental Progress* **1998**, *17,* 216-220.

(118) Xu, X.; Matsumura, Y.; Stenberg, J.; Antal, M. J., Jr., Carbon-catalyzed gasification of organic feedstocks in supercritical Water. *Ind. Eng. Chem. Res.* **1996**, *35*, 2522-2530.

(119) Yamaguchi, D.; Sanderson, P. J.; Lim, S.; Aye, L. Supercritical water gasification of Victorian brown coal: Experimental characterization. *International journal of hydrogen energy* **2009**, *34*, 3342-3350.

(120) Yanagida, T.; Minowa, T.; Shimizu, Y.; Matsumura, Y.; Noda, Y. Recovery of activated carbon catalyst, calcium, nitrogen and phosphate from effluent following supercritical water gasification of poultry manure. *Bioresource Technology* **2009**, 100, 4884-4886.

(121) Yanik, J.; Ebale, S.; Kruse, A.; Saglam, M.; Yüksel, M. Biomass gasification in supercritical water: Part I. Effect of the nature of biomass. *Fuel.* **2007**, *86* (15), 2410.

(122) Yanik, J.; Ebale, S.; Kruse, A.; Saglam, M.; Yüksel, M., Biomass gasification in supercritical water: II. Effect of catalyst. *Int. J. Hydrogen Energy.* **2008**, *33*, 4520-4526.

(123) Yasaka, Y.; Yoshida, K.; Wakai, C.; Matubayasi, N.; Nakahara, M. Kinetic and Equilibrium Study on Formic Acid Decomposition in Relation to the Water-Gas-Shift Reaction. *J. Phys. Chem. A* 2006, *110* (38), 11082 -11090.

(124) Yong, T. L.-K.; Matsumura, Y., Kinetic Analysis of Lignin Hydrothermal Conversion in Sub- and Supercritical Water. *Ind. Eng. Chem. Res.* **2013**, *52*, 5626-5639.

(125) Yong, T. L.-K.; Matsumura, Y., Reaction Pathways of Phenol and Benzene

Decomposition in Supercritical Water Gasification. *J. Jpn. Petrol. Inst.* **2013**, *56*, 331-343

(126) Yong, T. L.-K.; Matsumura, Y., Kinetic Analysis of Guaiacol Conversion in Sub- and Supercritical Water. *Ind. Eng. Chem. Res.* **2013**, *52*, 9048-9059.

(127) Yoshida, T.; Matsumura, Y. Gasification of cellulose, xylan and lignin mixtures in supercritical water. *Ind. Eng. Chem. Res.* **2001**, *40*, 5469-5474.

(128) Yoshida, T.; Oshima, Y.; Matsumura Y. Gasification of biomass model compounds and real biomass in supercritical water. *Biomass Bioenergy* **2004**, *26*, 71 – 78.

(129) Yoshida, T.; Oshima, Y. Partial Oxidative and Catalytic Biomass Gasification in Supercritical Water: A Promising Flow Reactor System. *Ind. Eng. Chem. Res.* **2004**, *43* (15), 4097-4104.

(130) Yoshida, T; Yanachi, S; Matsumura, Y. Glucose decomposition in water under supercritical pressure at 448-498 K. J. Jpn. Inst. Energy **2007**, *86*, 700-706.

(131) Youssef, E. A.;Elbeshbishy, E.; Hafez, H.; Nakhla, G.; Charpentier, P. Sequential supercritical water gasification and partial oxidation of hog manure. International Journal of Hydrogen Energy **2010**, *35,* 11756-11767.

(132) Youssef, E. A.; Nakhla, G.; Charpentier, P. A. Co-gasification of catechol and starch in supercritical water for hydrogen production. International Journal of Hydrogen Energy **2012**, *37,* 8288-8297.

(133) Yu, D.; Aihara, M.; Antal, M. J. Hydrogen production by steam reforming glucose in supercritical water. *Energy Fuels* **1993**, *7*, 574.

(134) Yuan, Z.; Cheng, S; Leitch, M; Xu, C. Hydrolytic degradation of alkaline lignin in hot-compress-watered and ethanol. *Bioresource Technology* **2010**, *101,* 9308-9313.